2014

# Redox Triggering of Podocyte NLRP3 Inflammasomes and Glomerular Injury in Hyperhomocysteinemia

Justine M. Abais
*Virginia Commonwealth University*

# Redox Triggering of Podocyte NLRP3 Inflammasomes and Glomerular Injury in Hyperhomocysteinemia

A dissertation submitted in partial fulfillment of the requirements for the degree of Doctor of Philosophy at Virginia Commonwealth University

by

Justine M. Abais
Bachelor of Science in Chemistry
Virginia Commonwealth University, 2009

Director: Pin-Lan Li, MD, PhD
Professor, Pharmacology and Toxicology

Virginia Commonwealth University
Richmond, Virginia
April 2014

## ACKNOWLEDGMENTS

There are no words to fully express the deep gratitude I feel towards everyone who has supported me throughout this incredible journey. Attaining this degree is the product of the hard work of many, and I have been extremely fortunate to come across so many people willing to help me achieve this milestone. First and foremost, my sincerest thanks to Dr. Pin-Lan Li for going above and beyond what is expected of a mentor. She humbly leads by example and her amazing work ethic is fueled by her desire to offer her students the best possible training, resources, and environment to achieve their career and life goals. As my 'scientific mother', her high energy and love for science is contagious, and with her compassionate nature, Dr. Li has gone beyond caring for me solely as a scientist, but wholly as a person. I cannot imagine what my life would have been like had she not recognized my potential and given me the guidance and encouragement to lead me to where I am today, and for that I am eternally grateful.

My training and this study could not have been made possible without the help from many past and present members of the lab, especially Dr. Fan Yi for his early guidance when I was an undergraduate summer student, and to Drs. Krishna Boini and Yang Zhang for sharing with me their expertise and being prime examples of honest, hardworking scientists. Thank you to Mark, Vicky, Mike, Sarah, Rex, Mia, Lisa, Emma, Joe C, Peter, George, Ashley, and Sabena, for their help scientifically, but just as importantly, for making the lab such a wonderful and happy place to work every day.

My sincere thanks to my committee members, Dr. Todd Gehr, Dr. Ningjun Li, Dr. Richard Moran, and Dr. Scott Walsh, who I have gotten the pleasure of knowing over the past five years. Their insightful expertise, constructive criticism, and advice on my research proposal have been invaluable throughout the course of these studies and in the preparation of this

dissertation. Thank you to Dr. Qinglian Liu, who patiently helped me as I learned how to use the FPLC and size-exclusion chromatography system. I would also like to thank Dr. William Dewey, Dr. Stephen Sawyer, and Dr. Hamid Akbarali, for giving me this wonderful opportunity in the first place and to all the staff of the Department of Pharmacology and Toxicology, especially Mrs. Sheryol Cox, for being so kind and helpful over the years.

Finally, I am the person as I am today because of my parents, Peter and Mildred Abais, my sisters, Lauren and Kelsey Abais, and my fiancé, Francis Battad. Their unconditional love has always been a constant source of drive and motivation for me. My greatest thanks go to them for their tireless support and understanding, which is beyond what anyone could ever ask for.

## TABLE OF CONTENTS

## LIST OF FIGURES

## LIST OF ABBREVIATIONS

| | |
|---|---|
| $^{\bullet}OH$ | hydroxyl radical |
| 5-methyl-THF | N5-methylenetetrahydrofolate |
| ASC | apoptosis-associated speck-like protein containing a CARD |
| CBS | cystathionine-β-synthase |
| CGD | chronic granulomatous disease |
| CKD | chronic kidney disease |
| CVD | cardiovascular disease |
| DAMPs | damage-associated molecular patterns |
| DPI | diphenylene iodonium |
| ECM | extracellular matrix |
| ENaC | epithelial sodium channel |
| ER | endoplasmic reticulum |
| ESR | electron spin resonance |
| ESRD | end-stage renal disease |
| FF | folate-free |
| FPLC | fast-protein liquid chromatography |
| GAP | GTPase-activating protein |
| GDI | glomerular damage index |
| GEF | guanine nucleotide exchange factor |
| $H_2O_2$ | hydrogen peroxide |
| Hcys | homocysteine |
| hHcys | hyperhomocysteinemia |
| ICE | interleukin converting enzyme |
| IL-1β | interleukin-1β |
| LRR | leucine-rich repeats |
| MDP | muramyl dipeptide |
| MnTMPyP | manganese (III) tetrakis (1-methyl-4-pyridyl) porphyrin |
| MS | methionine synthase |
| MSU | monosodium urate |
| MTHFR | methylenetetrahydrofolate reductase |
| mtROS | mitochondrial ROS |
| NAC | N-acetyl-cysteine |
| NADPH | nicotinamide adenine dinucleotide phosphate |
| ND | normal diet |
| NLRP3 | NOD-like receptor protein 3 |
| NMDA | N-methyl-D-aspartate |
| NO | nitric oxide |
| Nox2 | NADPH oxidase containing $gp91^{phox}$ |
| $O_2^{\bullet -}$ | superoxide |
| $ONOO^-$ | peroxynitrite |
| PAMPs | pathogen-associated molecular patterns |

| | |
|---|---|
| PAN | puromycin aminonucleoside |
| PEG-SOD | polyethylene glycol-superoxide dismutase |
| ROS | reactive oxygen species |
| SAH | S-adenosyl-homocysteine |
| SAM | S-adenosyl-methionine |
| SDS-PAGE | sodium dodecyl sulfate-polyacrylamide gel electrophoresis |
| SEC | size-exclusion chromatography |
| shRNA | short hairpin RNA |
| siRNA | small interfering RNA |
| TBP-2 | thioredoxin-binding protein-2 |
| TEMPOL | 4-Hydroxy-2,2,6,6-tetramethylpiperidine-1-oxyl |
| TMTU | tetramethylthiourea |
| TRX | thioredoxin |
| TXNIP | thioredoxin-interacting protein |
| VDUP-1 | vitamin D3 upregulated protein 1 |
| VEGF | vascular endothelial growth factor |

## ABSTRACT

REDOX TRIGGERING OF PODOCYTE NLRP3 INFLAMMASOMES AND GLOMERULAR INJURY IN HYPERHOMOCYSTEINEMIA

By Justine M. Abais

A dissertation submitted in partial fulfillment of the requirements for the degree of Doctor of Philosophy at Virginia Commonwealth University

Virginia Commonwealth University, 2014

Major Director: Pin-Lan Li, MD, PhD, Professor, Pharmacology and Toxicology

Hyperhomocysteinemia (hHcys), an important pathogenic factor contributing to the progression of end-stage renal disease (ESRD), has been shown to activate NOD-like receptor protein 3 (NLRP3) inflammasomes and cause podocyte dysfunction and glomerular sclerosis. hHcys induces aggregation of the three inflammasome components – NLRP3, apoptosis-associated speck-like protein (ASC), and caspase-1 – and its activation is indicated by increased caspase-1 activity and secretion of interleukin-1β (IL-1β). The aims of the present study sought to elucidate the role of nicotinamide adenine dinucleotide phosphate (NADPH) oxidase-mediated redox signaling in hHcys-induced NLRP3 inflammasome activation, to dissect the contribution of common endogenous reactive oxygen species (ROS) including superoxide ($O_2^{\bullet-}$), hydrogen peroxide ($H_2O_2$), peroxynitrite ($ONOO^-$), and hydroxyl radical ($^{\bullet}OH$), and to explore the molecular mechanisms by which the NLRP3 inflammasome senses changes in oxidative stress through thioredoxin-interacting protein (TXNIP). Specific inhibition of the gp91$^{phox}$ subunit of NADPH oxidase markedly reduced Hcys-induced caspase-1 activity and IL-1β production in cultured podocytes. Concurrently, gp91$^{phox-/-}$ or administration of a gp91*ds-tat* peptide also exhibited diminished glomerular inflammasome formation and activation in mice fed a folate-free (FF) diet to induce hyperhomocysteinemia and displayed glomerular protection as shown by

prevention of hHcys-induced proteinuria, albuminuria and glomerular sclerosis. Interestingly, dismutation of $O_2^{\bullet-}$ by 4-Hydroxy-2,2,6,6-tetramethylpiperidine-1-oxyl and administration of $H_2O_2$ decomposer catalase either in cultured podocytes or hyperhomocysteinemic mice inhibited hHcys-induced NLRP3 inflammasome aggregation and activation. Hyperhomocysteinemic mice also demonstrated a significant increase in glomerular TXNIP binding to NLRP3, confirmed by confocal microscopy, size-exclusion chromatography, and co-immunoprecipitation studies. Blockade of TXNIP by genetic interference or by the calcium channel blocker verapamil prevented this hHcys-induced TXNIP-NLRP3 binding, NLRP3 inflammasome formation and activation, as well as protected hyperhomocysteinemic mice from glomerular dysfunction and damaged morphology. In conclusion, hHcys-induced NADPH oxidase activation is importantly involved in the switching on of NLRP3 inflammasomes in podocytes, where NADPH oxidase-derived $O_2^{\bullet-}$ and $H_2O_2$ primarily contribute to NLRP3 inflammasome activation. TXNIP binding to NLRP3 is a key signaling mechanism allowing NLRP3 inflammasome to sense these changes in oxidative stress. These findings greatly enhance our understanding of the early pathogenesis of hHcys-induced glomerular sclerosis, which may identify new therapeutic targets for prevention or treatment of ESRD.

# CHAPTER ONE

## INTRODUCTION

Hyperhomocysteinemia (hHcys) has been reported to be an important pathogenic factor leading to the progression of end-stage renal disease (ESRD) and related cardiovascular complications associated with aging and different diseases [1-6]. Despite extensive studies, the mechanisms mediating the pathogenic actions of hHcys are not yet fully understood. Recent studies in our laboratory provided evidence that hHcys may generate its detrimental effects by activation of a NOD-like receptor protein (NLRP3)-centered inflammasome in podocytes. The activation of NLRP3 inflammasomes in podocytes turns on the inflammatory response, causing chronic inflammation in glomeruli and ultimately leading to glomerular dysfunction and sclerosis. It has been proposed that the activation of podocyte NLRP3 inflammasomes during hHcys is a critical mechanism inducing kidney senescence and progressive degenerative glomerular dysfunction and sclerosis [7]. However, it remains to be determined how the NLRP3 inflammasomes are formed and activated during hHcys and how activated NLRP3 inflammasomes induce glomerular degenerative pathology ultimately leading to end-stage renal disease (ESRD). The current project provided convincing evidence suggesting that elevated extracellular Hcys concentrations activate NADPH oxidase to produce reactive oxygen species (ROS) and thereby activate NLRP3 inflammasomes in podocytes and increase the downstream recruitment of inflammatory cells in glomeruli, resulting in local inflammation and ultimate glomerular sclerosis. This redox activation of podocyte inflammasomes associated with hHcys may represent an early mechanism switching on local inflammatory responses in glomeruli. The following section will review our current understanding of hyperhomocysteinemia, NADPH

oxidase in the kidney, and the regulation of NLRP3 inflammasomes and their interactions as it pertains to the development of hHcys-induced glomerular injury and ESRD.

## 1.1 Hyperhomocysteinemia

A considerable amount of evidence indicates that plasma homocysteine (Hcys) levels are elevated in patients with ESRD, where hyperhomocysteinemia (hHcys) occurs in about 85% of chronic kidney disease patients due to impairments in Hcys metabolism and excretion [8-10]. These complications associated with hHcys have also been reported in a wide range of chronic pathological conditions, including vascular dysfunction, neurological diseases, metabolic disorders, the development of cancer, and many complications associated with aging [11-17]. In the kidney, hHcys has been known to directly cause deleterious effects, promoting a vicious cycle responsible for chronic kidney disease, where hHcys decreases renal function and leads to further increased plasma Hcys levels due to decreases in Hcys excretion in the kidney [18]. In humans, a plasma Hcys concentration <10μM is considered to be within the normal range, 10-16 μM is clinically defined as mild hHcys, 16-30 μM as moderate hHcys, 30-100 μM as intermediate hHcys, and >100μM as severe hHcys [18].

### 1.1.1 Homocysteine metabolism

Homocysteine is a thiol-containing, nonessential amino acid derived from the metabolism of the essential amino acid methionine. Upon activation of methionine by ATP, S-adenosyl-methionine (SAM) undergoes demethylation to form S-adenosyl-homocysteine (SAH). This reaction makes SAM a major methyl group donor for many reactions including the methylation

of DNA. SAH is then subsequently hydrolyzed to form Hcys and adenosine by SAH hydrolase [9].

As depicted in **Figure 1**, the remethylation of Hcys back to methionine or its transsulfuration to cysteine are the two major catabolic pathways metabolizing Hcys. The remethylation pathway involves the enzyme methionine synthase (MS) using $N^5$-methyltetrahydrofolate (5-MTHF) as the methyl donor that requires cobalamin (vitamin $B_{12}$), as well as the enzyme methylenetetrahydrofolate reductase (MTHFR) that requires folates as an essential cofactor for the reduction and formation of 5-MTHF. The transsulfuration of Hcys is carried out via two enzymes, cystathionine-β-synthase (CBS) and γ-cystathionase. Together with serine, Hcys first undergoes irreversible condensation by CBS using pyridoxal-5′-phosphate (vitamin $B_6$) as a cofactor. Cystathionine is then further broken down by γ-cystathionase into cysteine, and converted into sulfates that are then excreted in the urine. The liver and kidney are two major sites of Hcys metabolism, with an estimated ~70% of Hcys clearance occurring in the kidneys [19-21].

There are multiple ways by which Hcys can become elevated [22]. First, an overwhelming intake of methionine-rich animal protein not only overwhelms the transsulfuration pathway, but can also lead to inhibition of the remethylation pathway due to the existing overload of methionine. Second, nutritional deficiencies in the cofactors required for these reactions may result in enzymatic dysfunction, thus impairing either pathway of Hcys clearance. This was substantiated in the Framingham Heart Study, where elderly patients deficient in vitamin $B_6$ and folates exhibited hHcys and arteriosclerosis [23]. Finally, genetic polymorphisms in the enzymes

themselves have been identified in ESRD patients, where mutations in the MTHFR enzyme are correlated with increased plasma level of Hcys [24-25] and are also indicative of the patients' response to Hcys-lowering therapies.

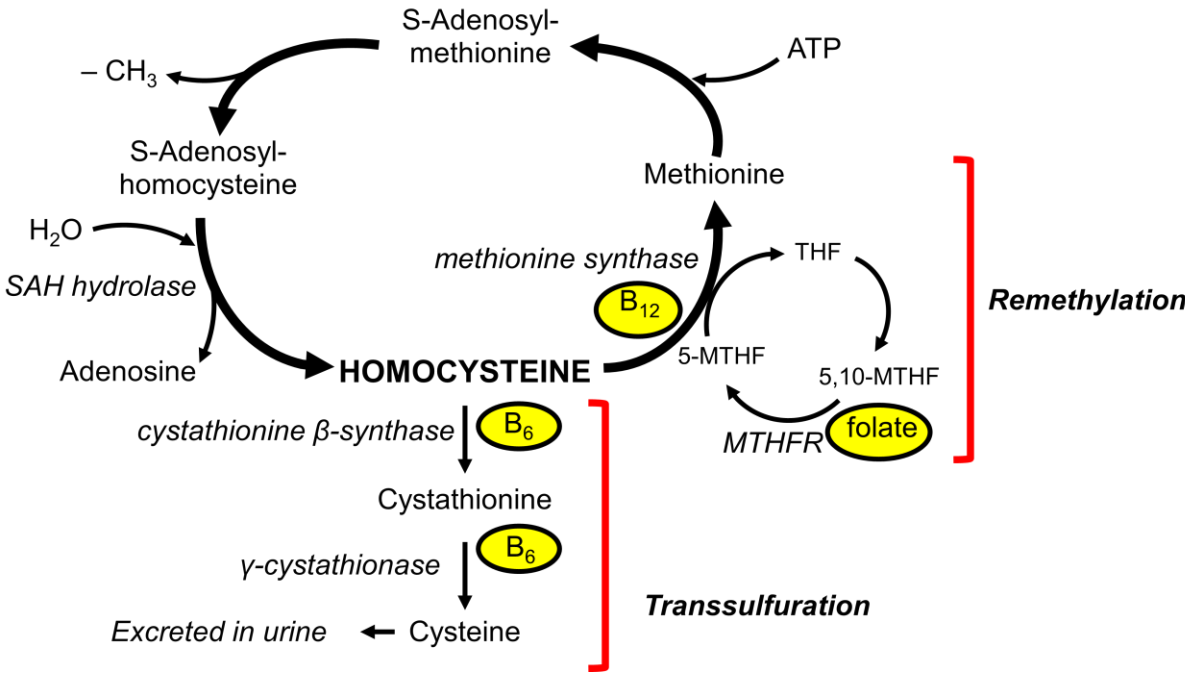


**Figure 1. Homocysteine metabolism.** When methionine is activated by ATP, S-adenosyl-methionine (SAM) undergoes demethylation to form S-adenosyl-homocysteine (SAH). SAH is then subsequently hydrolyzed to form Hcys and adenosine by SAH hydrolase. Homocysteine levels are regulated through its remethylation back to methionine by methionine synthase (MS) or its transsulfuration to cysteine by cystathionine β-synthase.

### 1.1.2 Pathogenic role of hHcys in ESRD

Recognition of hHcys as a detrimental risk factor came from the early pioneer work carried out by Dr. Kilmer S. McCully in the 1960s on the role of deficient Hcys-metabolizing enzymes in childhood arteriosclerosis, and was the first to propose that elevated Hcys directly causes arterial damage [3]. This seminal work has since expanded from arteriosclerosis and cardiovascular disease to include many other degenerative diseases and pathological processes.

Numerous clinical and epidemiological studies demonstrated positive correlations between elevated plasma Hcys with ESRD and its related cardiovascular complications [26-30]. In nearly every clinical study where plasma Hcys levels were measured in patients with renal complications, there was a strong positive correlation between plasma levels of Hcys and serum creatinine, a marker for declining renal function [31]. Additionally, these patients exhibited plasma Hcys concentrations three to five times higher than healthy controls [32-34].

Despite the strong associations made between ESRD and the prevalence of hHcys, the mechanisms underlying Hcys-induced pathogenesis of glomerular injury and dysfunction are still poorly understood. The detrimental or sclerotic actions of hHcys have been attributed to altered extracellular matrix metabolism, reduced protection from nitric oxide (NO), and increased production of ROS. With a diminished capacity to maintain the extracellular matrix (ECM) [7, 35-38], hyperhomocysteinemic conditions cause a serious imbalance in matrix synthesis and degradation, resulting in vascular remodeling. Besides alterations in ECM metabolism, Hcys has been shown to alter the local oxidative state and elevate levels of superoxide ($O_2^{\bullet -}$) by uncoupling NO synthase, directly trapping NO itself, and activating NADPH oxidase, the dominant source of $O_2^{\bullet -}$ in many non-phagocytic cells, especially in the kidney [39-43]. Together, these effects of inhibiting extracellular matrix degradation and the production of local oxidative stress all contribute to the sclerotic process that eventually leads to the loss of renal function [37-38].

Studies from our laboratory and by others have demonstrated that hHcys directly induces glomerular injury, affecting glomerular endothelial cells, mesangial cells, and podocytes [44-46].

Mechanistically, our laboratory has shown that hHcys-induced glomerular sclerosis and ultimate ESRD involve N-methyl-D-aspartate (NMDA) receptor activation and occur in an nicotinamide adenine dinucleotide phosphate (NADPH) oxidase-dependent manner, which is associated with the activation of small GTPase Rac1 and guanine nucleotide exchange factor Vav2 [7, 38, 44]. Additionally, our laboratory has provided substantial evidence that increases in ROS production are a result from activation of NADPH oxidase by Hcys [7-8, 47]. It has been shown that knockout of the gp91$^{phox}$ gene, a catalytic subunit of NADPH oxidase, is protective towards Hcys-induced glomerular injury in mice [48], preventing the accumulation of $O_2^{\bullet -}$ and consequent podocyte damage, attenuating proteinuria, and preserving glomerular filtration rate when compared to hyperhomocysteinemic wild-type mice. These results suggest a crucial role for functioning NADPH oxidase in the sclerotic mechanism of hHcys during the progression of glomerular injury. Most recently, Nod-like receptor protein 3 (NLRP3) inflammasome-mediated caspase-1 activation and IL-1β production were found to be necessary for hHcys-induced podocyte and glomerular dysfunction, where inhibition of NLRP3 inflammasomes either by apoptosis-associated speck-like protein (ASC) gene silencing or pharmacological inhibition of caspase-1 attenuated hHcys-induced injury [49]. However, further studies are warranted to fully understand the mechanisms mediating Hcys-induced NLRP3 inflammasome activation and its contribution to glomerular injury.

### 1.1.3 Murine models of hHcys

hHcys can be experimentally modeled in animals through dietary and genetic manipulations, modifications, or a combination of the two. In order to hereditarily model hHcys, the mouse genes for the enzymes CBS, MTHFR, and MS have been genetically modified.

$CBS^{-/-}$ mice exhibit severely elevated levels of plasma Hcys (>200 μM), but rarely survive beyond 3-5 weeks of age due to the severity of hHcys [50]. Therefore, the use of heterozygous CBS mice, which develop mild hHcys, is much more common [50-52]. $MTHFR^{-/-}$ mice, developed in 2001, only exhibit moderate hHcys but also undergo difficulties in survival after just 5 weeks of age [53-54]. Finally, homozygous knockout of the *Mtr* gene, which encodes the enzyme MS, is embryonic lethal, but heterozygous mutation only produces mild hHcys (5-10 μM) [55]. The advantage of these genetic models is the avoidance of potential side effects that may arise from the global deficiency of essential cofactors, thereby making these genetic approaches commonly used.

In regards to dietary approaches used to elevate plasma Hcys, these interventions include directly adding Hcys to the drinking water, overwhelming the metabolic pathway depicted in **Figure 1** through administration of a high-methionine diet, limiting Hcys transsulfuration by restricting dietary intake of vitamin $B_6$, or limiting Hcys remethylation back to methionine through a folate or vitamin $B_{12}$-deficient deficient diet. However, excessive plasma methionine is not a clinically observed phenomenon in patients with hHcys, thereby limiting the translational validity of the high-methionine diet. Generally, human patients with hHcys display deficiencies in folate, vitamin $B_6$, or vitamin $B_{12}$, making these particular diet-induced experimental models of hHcys directly relevant to the human condition [56]. Therefore, a model of folate-free (FF) diet-induced hHcys was selected for the current study.

## 1.2 NADPH oxidase in the kidney

Nicotinamide adenine dinucleotide phosphate (NADPH) oxidase, an enzyme generating $O_2^{\bullet-}$ from oxygen and NADPH, can primarily be found in phagocytic cells, where its primary role is to generate large amounts of reactive oxygen to carry out traditional immune functions [57]. However, this enzyme and its isoforms are also found spread throughout various organs, where its primary function is not for defense and to kill non-host organisms, but instead to produce small amounts of $O_2^{\bullet-}$ to act a signaling messengers [58]. In the kidney, there are many enzymatic systems that contribute to the production of ROS, including mitochondrial oxidases, xanthine/xanthine oxidase, lipoxygenases, cyclooxygenases, and cytochrome P450s. However, unlike these other systems where the production of $O_2^{\bullet-}$ is a secondary process, NADPH oxidase is the only enzyme identified to produce $O_2^{\bullet-}$ as its principal function. NADPH oxidase has been considered as the major source of $O_2^{\bullet-}$ in the kidney, specifically in the renal cortex [39]. Its action relies on an enzymatic complex with five subunits including two membrane-associated flavocytochrome components ($gp91^{phox}$ and $p22^{phox}$), three cytosolic components ($p40^{phox}$, $p47^{phox}$, $p67^{phox}$), and a GTPase, Rac1, all being reported to be expressed in the kidney [39]. When stimulated, the translocation of its cytosolic components to the subunits in the membrane results in the transfer of electrons from NADPH to form $O_2^{\bullet-}$ from oxygen. The generation of $O_2^{\bullet-}$ by NADPH oxidase is the precursor for other species of reactive oxygen, including hydrogen peroxide, hydroxyl radical, peroxynitrite, hypochlorous acid, and singlet oxygen [58-61]. Interestingly, our laboratory and others have found increased local oxidative stress, for the most part mediated through NADPH oxidase, to be strongly associated with the cardiovascular complications related to ESRD as well as with the damaging effects of hHcys [47, 62-65].

### 1.2.1 Regulation of NADPH oxidase by Rac1 GTPase and GEF Vav2

The activation of NADPH oxidase is dependent on the aggregation of its membrane and cytosolic components to the plasma membrane, which requires phosphorylation of the $p47^{phox}$ subunit, its translocation to the membrane along with the remaining cytosolic subunits, protein-protein interactions between all components, and Rac GTPase activation [66-68]. Rac1 is a member of the Rho-family of GTPases which are binary switches important for the regulation of many cellular functions including cell cycle progression, apoptosis, differentiation, adhesion, and migration and vesicle trafficking through control of actin polymerization [69-71]. In 1991, Abo et al identified phagocytic NADPH oxidase to be the first Rac effector [72]. Since then, a central role for Rac, in particular, Rac1, has been established in the regulation and activation of NADPH oxidase.

NADPH oxidase activation and production of $O_2^{\bullet -}$ are dependent on the switching of Rac1 between two conformations – the active GTP-bound and inactive GDP-bound states. The cycling of Rac1 between these two states is highly and mainly regulated by GTPase-activating proteins (GAPs) and guanine nucleotide exchange factors (GEFs). GAPs promote GTP hydrolysis and push GTPases to the inactive GDP-bound state, while GEFs facilitate the exchange of GDP for GTP to promote the active GTP-bound state [73]. With over 30 GEFs identified, the Vav subfamily of GEFs has been shown to exhibit high specificity to and importantly regulate Rac GTPase and NADPH oxidase [74-77].

With substantial evidence our laboratory has demonstrated these NADPH oxidase-activating pathways to be involved in Hcys-induced glomerular injury. These previous studies

have shown that through *de novo* ceramide synthesis, Hcys stimulated NADPH oxidase activation by enhancing Rac GTPase activity in rat mesangial cells [65]. Furthermore, inhibition of GEF Vav2, the predominant isoform was found to be expressed in these cells, prevented Hcys-induced increase in Rac1 activity and consequent activation of NADPH oxidase [38, 44]. Together, these results signify the importance of Rac1 and its regulation by Vav2 in the development of hHcys-induced production of oxidative stress and glomerular injury. However, how ROS from NADPH oxidase activation produces glomerular injury remains unclear, which will be a major focus of the present study.

### 1.2.2 Physiological and pathological role of NADPH oxidase in the kidney

ROS play a very critical role in normal physiology in a variety of renal activities. It has been reported that in the kidney the major source of ROS production is through NADPH oxidase [78-79]. Many homeostatic processes of the kidney are affected by the activation of NADPH oxidase, including renal glucogenesis and transport, tubuloglomerular feedback, hemodynamics, and electrolyte transport [80]. Especially in the diabetic kidney, NADPH oxidase regulates proximal tubular cell glucose balance as well as the transport of glucose through sodium/glucose cotransporters [81-82]. $O_2^{\bullet-}$ increases tubuloglomerular feedback and, therefore, NADPH oxidase also helps control the hemodynamic response in situations of high salt [83]. Along the nephron, NADPH oxidase has been demonstrated to be important for control of proximal tubular $Na^+/K^+$-ATPase activity, $Na^+/K^+/2Cl^-$ cotransporters, and epithelial sodium channel (ENaC) activity [84-86], all suggesting regulation of tubular ion transport by NADPH oxidase.

However, as with any organ, the kidney is vulnerable when exposed to continuous, excessive levels of oxidative stress [87-88]. Diabetic mice have increased $gp91^{phox}$/Nox2 expression in the renal cortex, where Nox2 downregulation proved protective from diabetes-induced oxidative stress, glucose intolerance, and renal fibrosis [89]. $O_2^{\bullet-}$ production has been demonstrated to impair endothelial function and perhaps lead to increased arterial responsiveness to vasoconstricting stimuli [90-91]. Previous studies have demonstrated NADPH oxidase-derived $O_2^{\bullet-}$ production to also regulate renal medullary blood flow, where persistently increased oxidative stress may contribute to the development of hypertension [92]. During hHcys, our laboratory has demonstrated the importance of NADPH oxidase in the pathogenesis of hHcys-induced glomerular sclerosis by showing that inhibition or deletion of NADPH oxidase and its subunits, in particular, $gp91^{phox}$, can attenuate glomerular damage and restore normal renal function [48]. Similarly, antioxidants have been shown to ameliorate Hcys-induced toxicity [64]. The current study seeks to further explore the mechanisms by which elevated Hcys and its activation of NADPH oxidase lead to glomerular dysfunction and the pathological progression to ESRD via NLRP3 inflammasomes, an intracellular inflammatory machinery.

### 1.3 The NLRP3 inflammasome

The Nod-like receptor protein 3 (NLRP3) inflammasome, found to be a key mediator of the innate immune system in response to a host of initiating factors, has been extensively demonstrated to be activated in response to a wide range of danger signals derived from disease and infection [93-97]. Oligomerization of the NLRP3 protein, the adaptor molecule apoptosis-associated speck-like protein containing a CARD (caspase recruitment domain) (ASC), and the cysteine protease caspase-1 forms this cytosolic multiprotein complex, causing the maturation of

pro-inflammatory cytokines IL-1β and IL-18. It is assumed that this inflammasome activation and extracellular secretion of inflammatory cytokines sense diverse danger signals and instigate the innate inflammatory response, in particular, the sterile inflammatory response during chronic degenerative diseases [98-99]. More recently, NLRP3 inflammasome activation has been reported to trigger many other cell injury responses far beyond inflammation [100]. It has been assumed that the inflammatory and non-inflammatory actions produced by activation of NLRP3 inflammasomes together induce cell or tissue degenerative injuries during many chronic diseases such as atherosclerosis, Alzheimer's diseases, cancer, metabolic disorders and gout [101]. Recent studies in our laboratory have found that the activation of these inflammasomes during hHcys turns on local inflammatory response in glomeruli, inducing kidney senescence and progressive degenerative glomerular dysfunction and sclerosis, where active caspase-1 promotes maturation of IL-1β to induce decreases in nephrin expression in podocytes [49].

### 1.3.1 Types of inflammasomes

The pro-inflammatory cytokine IL-1β, one of most powerful inflammatory mediators, is the most studied cytokine due to its key role in the inflammatory process. Jurg Tschopp and his research group identified the inflammasome as the molecular platform required for the activation of caspase-1, previously known as interleukin converting enzyme (ICE), which is responsible for the maturation of IL-1β from its precursor form [102]. There are various types of inflammasomes centered around different members of the Nod-like receptor (NLR) family, and although 23 NLR genes have been identified to date, only a few form oligomeric complexes and result in posttranslational activation of caspases [103]. Although caspases are generally thought to be pro-

apoptotic, a subclass of inflammatory caspases is responsible for the maturation of inactive cytokine precursors like IL-1β and IL-18 [104].

The major caspase-processing inflammasomes currently found throughout the literature include the NLRP1, NLRC4, AIM2, and NLRP3 inflammasomes. The NLRP1 inflammasome, shown to minimally require only NLRP1 and caspase-1 for its activation, has been demonstrated to be sensitive to bacterial cell wall component muramyl dipeptide (MDP) as well as *Bacillus anthracis* lethal toxin [105-106]. However, it was also shown that the addition of the adaptor protein ASC resulted in a more robust activation of the NLRP1 inflammasome. The NLRC4 inflammasome is most associated with caspase-1 activation and IL-1β in response to various gram-negative bacteria. As with the NLRP1 inflammasome, NLRC4 can also directly interact with the CARD domain of caspase-1, and it has been hypothesized that NLRC4 activates caspase-1 upon sensing the presence of bacteria-specific and conserved proteins: flagellin, rod, and needle [107-109]. AIM2 inflammasomes become activated by preferentially binding to cytosolic double-stranded DNA, where ASC then becomes recruited to AIM2, leading to the proteolytic cleavage of caspase-1 [110].

However, because of its important role in sterile inflammation, the most widely studied member of the NLR family is the NLRP3 inflammasome. The NLRP3 inflammasome responds to a very diverse range of activators, including those of microbial origin, endogenous danger signals, and exogenous non-microbial stimuli. It has become of great scientific interest in not only trying to identify activators of the NLRP3 inflammasome, but also importantly trying to understand how such a broad range of stimuli can activate the same molecular platform [111].

### 1.3.2 Exogenous and endogenous NLRP3 inflammasome activators

Many studies have provided evidence of NLRP3 inflammasome activation in response to a whole host of various exogenous danger signals and microbes, including the influenza virus, adenoviruses, *Staphylococcus aureus*, *E. coli*, *Neisseria gonorrhoe*, and *Candida albicans* [112-117]. Although the ability of the toxins from many of these microbes to form membrane pores is linked to an ability to activate NLRP3, it still remains unknown whether a single or a combination of pathogen-associated molecular patterns (PAMPs) is directly responsible for inflammasome activation. Another group of NLRP3 stimulators are the non-microbial phagocytosed materials, where monosodium urate crystal accumulation associated with gout was one of the first inflammatory diseases linked to the activation of NLRP3 [118]. In a similar manner, silica, asbestos, and aluminum salts have also been shown to trigger caspase-1 cleavage and IL-1β production via NLRP3 activation [119-120].

The activation of NLRP3 inflammasomes to a very wide range of endogenous danger signals is what makes NLRP3 unique among all other inflammasomes. Excessive levels of ATP was described as one of the first endogenous damage-associated molecular patterns (DAMPs) to induce NLRP3 inflammasome formation and activation, a mechanism involving high concentrations of extracellular ATP binding to the purinergic P2X7 receptor [121]. The aggregation of endogenous peptides like amyloid-β are also sensed by NLRP3 [122], leading to the production of pro-inflammatory cytokines, which explains the elevation of IL-1β detected in the brains of patients with Alzheimer's disease [123]. Cholesterol crystals are known to cause phagolysosomal damage, and have been recently shown to lead to the early activation of NLRP3 and the promotion of a pro-atherosclerotic phenotype [124], while endogenous danger signal of

trauma, hyaluronan, also triggers chemokine release in affected tissues through NLRP3 [125]. Finally, damage to pancreatic islet cells by hyperglycemia caused NLRP3 inflammasome activation, ultimately developing to glucose intolerance and insulin resistance in a murine model of diabetes [126]. We have since demonstrated that the elevated levels of the amino acid Hcys also cause NLRP3 inflammasome formation and activation, leading to podocyte injury and eventually glomerular sclerosis [49]. Inhibition of NLRP3 via ASC shRNA or the caspase-1 inhibitor, WEHD, prevented Hcys-induced detrimental effects on glomerular structure and dysfunction, signifying a critical role for NLRP3 in the pathogenesis of ESRD related to hHcys [49].

### 1.3.3 NLRP3 inflammasomes in disease

Deficiencies in this multiprotein complex have been associated with autoimmune disorders such as familial Mediterranean fever and Muckle-Wells syndrome, but aberrant NLRP3 inflammasome activation has extended to many traditionally considered non-inflammatory disorders including diabetes, obesity, silicosis, liver toxicity, and kidney diseases [118, 120, 127-130]. Here we will focus on the role of NLRP3 in metabolic disorders.

Demonstrated in clinical trials, levels of circulating IL-1β are predictive of type 2 diabetes [131], and treatment with IL-1β antagonist anakinra demonstrated protective effects in these diabetic patients [132]. NLRP3$^{-/-}$ mice as well as adipocytes isolated from NLRP3$^{-/-}$ mice exhibited marked improvement in glucose tolerance and insulin, with reduced IL-1β production [133]. Most interestingly, weight loss in obese patients with type 2 diabetes resulted in a reduction of NLRP3 expression and activity in adipose tissue and improved glucose handling

[134], altogether suggesting an important role for NLRP3 in the pathogenesis of type 2 diabetes associated with obesity. Highly associated with obesity and diabetes, these patients are also at risk for cardiovascular disease (CVD). Recent studies have defined the potential benefit of caspase-1 inhibition as an intervention for myocardial infarction and ischemia [135-136]. NLRP3 inflammasome activation occurs mainly in cardiac fibroblasts after myocardial ischemia/reperfusion injury, where $ASC^{-/-}$ protects mice from phagocytic infiltration, myocardial fibrosis and dysfunction, and enlarged infarct size [137].

$NLRP3^{-/-}$ has also been shown to protect mice from both renal ischemic acute tubular necrosis as well as the progression of chronic kidney disease (CKD) in the unilateral ureteral obstruction model [138-139]. NLRP3 mRNA levels correlated with renal function in CKD patients, and IL-1β and IL-18 levels are increased in both animal models and patients with CKD [139-140]. Thus, these studies strongly support a crucial role for NLRP3 inflammasome involvement in the progression of acute kidney injury and CKD. Glomerular IL-1β mRNA is enhanced after the first day of the mouse model of streptozotocin-induced diabetic glomerulosclerosis [141]. With podocytes being a major site of IL-1β synthesis [142], we further demonstrated that hHcys-induced glomerular injury and IL-1β production occurs in an NLRP3-dependent mechanism [49].

### 1.4 Regulation of NLRP3 inflammasome activation

Despite rapid and extensive efforts in identifying various agents that stimulate the NLRP3 inflammasome, the underlying mechanisms by which these diverse danger signals activate the

same molecular machinery remain poorly understood. This next section will review the current status of this controversial area.

### 1.4.1 Primary models of NLRP3 inflammasome activation

The activation of NLRP3 inflammasomes has been implicated in a growing number of diverse pathological conditions, ranging from bacterial infections to cardiovascular dysfunction and metabolic syndrome [124, 143-145]. Despite the plethora of studies demonstrating the widespread prevalence of NLRP3 activation in disease, it remains poorly understood how this unique molecular machinery is activated in response to a very diverse range of stimuli. Particularly in phagocytes such as macrophages, it is known that NLRP3 inflammasome activation requires two signals – a 'priming' transcriptional step that involves TLR/NF-κB signaling, followed by post-translational regulation responsible for the oligomerization of the inflammasome components and the maturation of pro-inflammatory cytokine IL-1β [146-147]. In some other cells like endothelial cells and podocytes, such a two signal pattern may not be needed, where a constitutive or basal expression of pro-IL-1 and other associated molecules may be adequate to form and activate NLRP3 inflammasomes, albeit to a lesser extent than those in phagocytes, but sufficient enough to produce pathological changes, in particular, in chronic degenerative disease [142]. Whether or not its activation needs priming, NLRP3 inflammasomes are usually triggered through three major signaling pathways, stimulated either separately or in combination. In this regard, $K^+$ efflux and low intracellular $K^+$ concentration caused by activation of the P2X7 purinergic receptor in response to ATP is considered as an important signaling pathway to activate NLRP3 inflammasomes [115, 148]. ATP has also been demonstrated to cause transient pore formation through pannexin-1, allowing NLRP3 stimulators

to cross the plasma membrane and directly activate inflammasome assembly [121]. Another activating mechanism of NLRP3 inflammasomes is related to the actions of lysosomal enzymes in response to asbestos, silica, monosodium urate (MSU) crystals, and other stimulations that are too large to cross the membrane and instead are taken up into the cell via phagocytosis. When frustrated or incomplete phagocytosis occurs, lysosomal rupture or permeability changes release cathepsin B, a lysosomal enzyme that activates NLRP3 inflammasomes [120]. In addition, reactive oxygen species (ROS) produced by many known activators of NLRP3 inflammasomes are also shown to be an critical mechanism triggering NLRP3 inflammasome formation and activation in response to many exogenous stimuli as well as endogenously produced or secreted molecules from damaged cells such as DAMPs [149]. It has been demonstrated that the crystal structure of NLRP3 has a highly conserved disulfide bond connecting the PYD domain and the nucleotide-binding site domain, which is highly sensitive to or regulated by altered redox states [150].

### 1.4.2 ROS and its role in NLRP3 inflammasome activation

Due to the leucine-rich repeats (LRR) found in the C-terminus of NLRP3, it was originally hypothesized to act as a cytosolic receptor and directly bind to a ligand. However, this hypothesis was neglected after the discovery of many diverse stimuli that were all found to activate NLRP3, and it became much more accepted that NLRP3 sensed some molecular intermediate generated by these broad activators. The generation of ROS was one of the first intermediates discovered to be common to ATP, MSU, asbestos, and silica-induced NLRP3 activation [120]. Since then, there have been many conflicting reports regarding the role of ROS

in this process, creating much controversy in trying to understand the regulation of NLRP3 inflammasome activation.

Some of the first studies reported the importance of NADPH oxidase-derived ROS in activating NLRP3 in response to ATP, asbestos, and silica [120, 151-152]. This has since been extended to more recent reports, where NADPH oxidase inhibition via diphenylene iodonium (DPI) or more specifically through $gp91^{phox}$ blockade, can prevent free fatty acid, TNFα, and atheroprone oscillatory flow-induced NLRP3 inflammasome activation [153-155]. It has been disputed, however, that ROS are not involved in the activation of NLRP3 inflammasomes, but instead are derived from Toll-like receptors (TLRs) and contribute to the priming mechanism responsible for the transcriptional upregulation of NLRP3 and pro-IL-1β [156]. Additionally, macrophages isolated from $gp91^{phox-/-}$ mice or patients with chronic granulomatous disease (CGD) and deficient NADPH oxidase display normal inflammasome function when challenged with NLRP3 agonists [119, 157]. Caspase-1 activation and IL-1β secretion in response to cyclic stretch was undisturbed in murine alveolar macrophages, even in those isolated from $gp91^{phox-/-}$ mice, demonstrating the dispensability of NADPH oxidase to NLRP3 activation in this particular mechanism [158]. Alternatively, there is an emerging role for mitochondrial ROS (mtROS) in the mechanism of NLRP3 inflammasome activation [159-160]. The same study by Wu et al revealed that mtROS inhibition by mitochondrial antioxidant SS-13 prevented cyclic stretch-induced IL-1β. These greatly varying effects between ROS of NADPH oxidase or mitochondrial origin suggest that the mechanism of NLRP3 activation may be a very cell and stimuli-specific phenomenon.

While there is a plethora of evidence supporting ROS activation of NLRP3 inflammasomes, the exact mechanisms by which NLRP3 senses these changes in oxidative stress are still largely unknown. In this regard, the canonical work done by Zhou et al provided strong evidence of thioredoxin-interacting protein (TXNIP) as a binding partner to NLRP3, where association between these two proteins was necessary for downstream inflammasome activation [126]. TXNIP, the negative regulator of the antioxidant thioredoxin (TRX), may time-dependently dissociate from TRX to bind with NLRP3 leading to inflammasome formation and activation. This study also seeks to determine the involvement of TXNIP as a potential mediator between hHcys-induced oxidative stress and consequent NLRP3 inflammasome activation.

### 1.5 Aims of the study

The hypothesis to be tested in the present study states that: NADPH oxidase redox signaling mediates inflammasome activation in podocytes and glomerular injury during hHcys, ultimately resulting in glomerular sclerosis and ESRD.

The specific aims are:

1. To determine whether the *in vitro* formation and activation of NLRP3 inflammasomes by Hcys are associated with NADPH oxidase-mediated redox signaling in mouse podocytes and to explore the mechanisms mediating the action of NADPH oxidase-derived ROS on this inflammasome activation, including the potential involvement of specific ROS and TXNIP.

2. To determine whether *in vivo* hHcys-induced activation of NLRP3 inflammasomes and associated glomerular injury are blocked by selective inhibition of local NADPH oxidase activity or by knocking out the gp91$^{phox}$ gene in mice.
3. To determine whether *in vivo* activation of NADPH oxidase by overexpression of Vav2 gene, an endogenous NADPH oxidase activator, enhances the inflammasome formation and glomerular injury in glomeruli of hyperhomocysteinemic mice.

The overall hypothesis and the specific aims of this project are schematically represented in **Figure 2**.

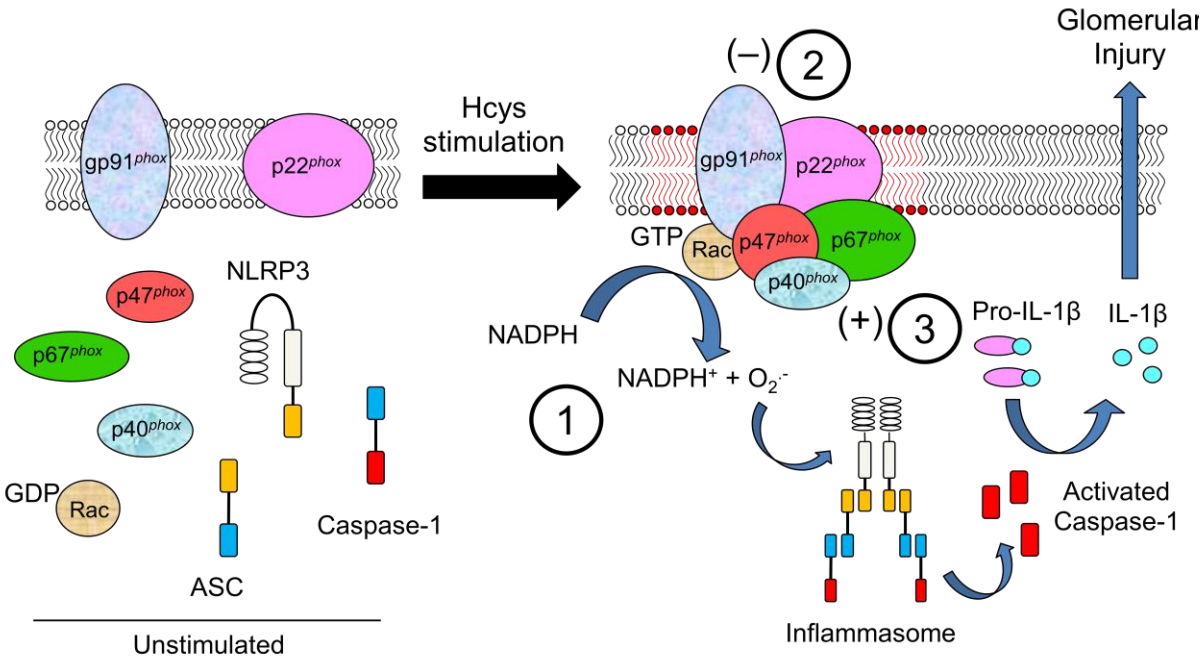


**Figure 2. The working hypothesis.** Through its inhibition both *in vitro* and *in vivo*, Aim 1 and 2 will explore the role of NADPH oxidase in Hcys-induced NLRP3 inflammasome activation. These aims will include further understanding which ROS are responsible for NLRP3 activation as well as determine the potential role of TXNIP in this mechanism. Aim 3 will further substantiate the role of NADPH oxidase by observing the effects of its overexpression of its endogenous activator and determining if that is sufficient to activate NLRP3 inflammasomes.

# CHAPTER TWO

# GENERAL METHODS

## 2.1 Culture of mouse podocytes

A conditionally immortalized mouse podocyte cell line, graciously provided by Dr. Paul E. Klotman (Division of Nephrology, Department of Medicine, Mount Sinai School of Medicine, New York, USA), was constructed with a temperature-sensitive variant of the simian virus (SV40) containing a large T antigen (tsA58) inducible by interferon-γ at 33°C, allowing for cellular proliferation. These cells were cultured and maintained on collagen-coated flasks in RPMI 1640 medium supplemented with 10% fetal bovine serum, 10 U/ml recombinant mouse interferon-γ, 100 U/ml penicillin and 100 mg/ml streptomycin. The podocytes were then passaged and allowed to differentiate to a mature cell type at 37°C for two weeks without interferon-γ before use in experiments.

### 2.1.1 *In vitro* podocyte treatments

Podocytes were treated with L-Hcys, which is considered to be the pathogenic form of Hcys, at a concentration of 40 μM for 24 hours, a dose and treatment time chosen based on previous studies [49]. Pharmacological NADPH oxidase inhibitors apocynin (100 μM), diphenylene iodonium (10 μM), and gp91*ds-tat* peptide (5 μM) were added to the cells 1 hour prior to Hcys treatment. ROS scavengers were used at the following doses: TEMPOL (100 μM), catalase (50 U/ml), tetramethylthiourea (TMTU, 100 μM), manganese (III) tetrakis (1-methyl-4-pyridyl) porphyrin (MnTMPyP, 25 μM), polyethylene glycol-superoxide dismutase (PEG-SOD,

50 U/ml), and ebselen (10 μM). The calcium channel blocker verapamil, which has been demonstrated to be a potent inhibitor of TXNIP, was used at a dose of 50 μM.

### 2.1.2 siRNA transfection

ASC and gp91$^{phox}$ small interfering RNAs (siRNA) were purchased from Qiagen (Valencia, CA), while TXNIP siRNA was purchased from Life Technologies (Grand Island, NY). A nonsilencing, double-stranded RNA (Qiagen) was used as a negative control. Briefly, podocytes were incubated with the serum-free medium for 15 minutes prior to ASC, gp91$^{phox}$, TXNIP, or scrambled siRNA transfection using the siLentFect Lipid Reagent (Bio-Rad, Hercules, CA) according to the manufacturer's instructions. After 18 hours of incubation at 37°C, the medium was changed, and cells were treated with 40 μM Hcys for 24 hours.

### 2.1.3 Nucleofection

Podocytes were transfected with a scrambled or Vav2 shRNA, or a constitutively active form of Vav2 (oncoVav2) plasmid directly to the nucleus via nucleofector technology developed by Lonza (Basel, Switzerland). This dominant active oncoVav2 plasmid containing an N-terminal truncation was a generous gift from Dr. Keith Burridge from the University of North Carolina at Chapel Hill [161]. The nucleofector technology involves the temporary creation of small pores in the membrane through electrical impulses together with cell-specific solutions to deliver substrates through the cytoplasm and into the nuclear membrane. Podocytes were trypsinized, counted, and 1 x $10^6$ cells were gently centrifuged at 90xg for 10 min at RT. Cells were resuspended in SF Cell Line nucleofector solution containing 2 μg plasmid DNA and then transferred into a certified cuvette. The cuvette was placed into the nucleofector system and

subject to cell-type specific program CM-137, chosen based on optimization experiments. Nucleofected cells were resuspended with pre-warmed medium and transferred to culture plates for use in experiments.

## 2.2 Mouse model of hyperhomocysteinemia

For all animal studies, eight-week old male C57BL/6J mice (Jackson Laboratories, Bar Harbor, ME, USA) were uninephrectomized to accelerate renal injury, as described previously [162]. After allowing a week for recovery after surgery, mice were fed either a normal diet or a folate-free (FF) diet for 4 weeks to induce hHcys [48]. Folates are a cofactor required for the breakdown of Hcys, and restricting folate consumption in the diet prevents the remethylation of Hcys back to methionine, causing elevated levels of plasma Hcys [38, 163]. After 4 weeks of treatment, all mice were placed in metabolic cages and urine samples were collected for 24 hours before collecting blood samples, sacrificing, and harvesting tissues for analysis. The Institutional Animal Care and Use Committee of Virginia Commonwealth University approved all protocols.

### 2.2.1 *In vivo* mouse treatments

For *in vivo* NADPH oxidase inhibition studies, gp91$^{phox-/-}$ mice (Jackson Laboratories, Bar Harbor, ME, USA) as well as gp91$^{phox+/+}$ mice that were injected intraperitoneally with gp91*ds-tat* or scrambled gp91*ds-tat* at a dose of 5 mg/kg every day were used [164]. Developed by Pagano and his research group, this custom gp91*ds-tat* peptide constructed with a *tat* sequence (first 9 amino acids) to enable cell membrane penetration and inhibition of NADPH oxidase, was synthesized by RS Synthesis (Louisville, KY) with the following amino acid sequence: YGRKKRRQRRR-CSTRIRRQL [165].

For *in vivo* ROS scavenging studies, mice received vehicle, 4-Hydroxy-2,2,6,6-tetramethylpiperidine-1-oxyl (TEMPOL), or catalase treatment and were fed either a normal diet or a FF diet for 4 weeks to induce hHcys. 3 mM TEMPOL (~100 mg/kg/day, Sigma, St. Louis, MO) was administered to the mice through the drinking water, while catalase (Sigma) was injected intraperitoneally at a dose of 5 kU/kg/day [166-167].

For *in vivo* TXNIP inhibition studies, one group of mice received plasmids encoding either the reporter gene luciferase or TXNIP short hairpin RNA (shRNA) by ultrasound-microbubble transfection. Another group of mice received verapamil in the drinking water (1 mg/ml), equating to a dose of approximately 100 mg/kg/day [168].

For *in vivo* Vav2 overexpression and inhibition studies, mice received either Vav2 shRNA or constitutively active variant oncoVav2 via ultrasound-microbubble transfection. Following transfection, mice were maintained on either the normal or FF diet for 4 weeks. All of these treatment paradigms can be found in **Figure 3**.

| Treatment Group A | 1 | 2 | 3 | 4 | 5 | 6 |
|---|---|---|---|---|---|---|
| ND | + | – | + | – | + | – |
| FF | – | + | – | + | – | + |
| gp91$^{phox-/-}$ | – | – | + | + | – | – |
| gp91*ds-tat* (5 /mg/kg/day) | – | – | – | – | + | + |

| Treatment Group B | 1 | 2 | 3 | 4 | 5 | 6 |
|---|---|---|---|---|---|---|
| ND | + | – | + | – | + | – |
| FF | – | + | – | + | – | + |
| TEMPOL (100 mg/kg/day) | – | – | + | + | – | – |
| Catalase (5000 U/kg/day) | – | – | – | – | + | + |

| Treatment Group C | 1 | 2 | 3 | 4 | 5 | 6 |
|---|---|---|---|---|---|---|
| ND | + | – | + | – | + | – |
| FF | – | + | – | + | – | + |
| TXNIP shRNA | – | – | + | + | – | – |
| Verapamil (100 mg/kg/day) | – | – | – | – | + | + |

| Treatment Group D | 1 | 2 | 3 | 4 | 5 | 6 |
|---|---|---|---|---|---|---|
| ND | + | – | + | – | + | – |
| FF | – | + | – | + | – | + |
| Vav2 shRNA | – | – | + | + | – | – |
| OncoVav2 | – | – | – | – | + | + |

**Figure 3. Different mouse treatment groups used in the present study.**

### 2.2.2 Mouse genotyping

Each mouse used in the *in vivo* NADPH oxidase inhibition studies was genotyped for the gp91$^{phox}$ gene to confirm its deletion prior to use in experiments. Briefly, genomic DNA extracted from the tail was subjected to PCR amplification using *taq* DNA polymerase (Invitrogen, Inc., Grand Island, NY). Using a Bio-Rad iCycler, PCR was performed using a validated protocol provided by Jackson Laboratories: denaturing the DNA at 94°C for 3 min, followed by a first round of 12 cycles: 94°C for 20 sec, 64°C for 30 sec (-0.5°C per cycle), 72°C for 35 sec, and then a second round of 25 cycles: 94°C for 20 sec, 58°C for 30 sec, 72°C for 35 sec, and a final extension step at 72° C for 2 min. The following gp91$^{phox}$-specific primers were provided by Jackson Laboratory and used for genotyping: oIMR0517 (AAG AGA AAC TCC TCT GCT GTG AA), oIMR0518 (CGC ACT GGA ACC CCT GAG AAA GG), and oIMR0519 (GTT CTA ATT CCA TCA GAA GCT TAT CG). The PCR products were separated by gel electrophoresis on a 3% agarose gel, visualized by ethidium bromide fluorescence, and compared to a 100 bp DNA ladder (New England Biosystems, Ipswich, MA).

### 2.2.3 Ultrasound-microbubble transfection and *in vivo* imaging

After allowing one week for recovery from uninephrectomy surgery, a preparation of plasmid encoding either TXNIP shRNA, oncoVav2, Vav2 shRNA or the reporter gene luciferase was mixed with cationically charged Optison microbubbles (GE Healthcare, Piscataway, NJ), then injected into the femoral artery and locally transfected to the kidney by sonoporation with a continuous wave output of 1 MHz at 10% power output at 30 sec intervals for a total of 6 min. To daily monitor the efficiency of gene expression, mice were anesthetized with ketamine (100 mg/kg IP) and xylazine (10 mg/kg IP), and an aqueous solution of luciferin (150 mg/kg IP) was

injected 5 minutes before imaging, as described previously [49]. The anesthetized mice were imaged using the Xenogen IVIS200 *in vivo* imaging system (Perkin Elmer, Waltham, MA). Photons emitted from luciferase-expressing cells and transmitted through tissue layers were quantified over a defined period of time ranging up to 5 minutes using the software program Living Image (Xenogen) as an overlay on an Igor program (Wavemetrics). If transfection was not detected by *in vivo* imaging, the mice were sacrificed and experiments terminated due to unsuccessful transgene expression.

### 2.3 Preparation of cell and tissue homogenates

Cell homogenates were freshly prepared by washing cultured cells three times with ice-cold PBS, followed by scraping the cells in ice-cold sucrose buffer (20 mM Tris-Hcl, 250 mM sucrose, pH 7.2) and transferring to a microcentrifuge tube pre-chilled on ice. Renal cortical tissue lysate was prepared by homogenizing the tissue in ice-cold sucrose buffer using a motorized microcentrifuge conical pestle. These homogenates from cells and tissues then underwent sonication using a handheld sonicator for 10 pulses on ice. This was repeated until all samples underwent sonication for a total of 3 times. Samples were incubated on ice for 30 minutes prior to centrifugation at 7,500 x g for 15 minutes at 4° C to remove cellular debris, and the supernatant was transferred to a new, pre-chilled microcentrifuge tube for use in downstream assays.

### 2.4 Microsome preparation

Podocyte lysate was subject to centrifugation at 1,000g for 10 minutes at 4° to remove the nuclear fraction. The collected supernatant was then centrifuged at 10,000g for 20 minutes at 4°

to remove the granular fraction. The resulting supernatant was assayed for protein concentration to normalize protein loading across all samples, and subject to a final centrifugation at 100,000g for 90 minutes at 4° to separate the microsomes (pellet) and cytosolic fraction (supernatant). The isolated pellet was then immediately assayed for $O_2^{\bullet -}$ production using electromagnetic spin resonance analysis as described in the following sections.

### 2.5 Western blot analysis

Cell or tissue homogenates were loaded in equal protein concentration (10-20 μg) and run at 120V for 1.5 hrs using sodium dodecyl sulfate-polyacrylamide gel electrophoresis (SDS-PAGE). The proteins were transferred from the gel onto polyvinylidene fluoride nitrocellulose membranes for 1 hr at 100V. After blocking the membranes for 1 hr with 5% non-fat dry milk in Tris-buffered saline with 0.1% Tween 20 (TBS-T), the membrane was probed with rabbit anti-ASC (1:1000, Enzo, Farmingdale, NY), rabbit anti-NLRP3 (1:500, Abcam, Cambridge, MA) or mouse anti-TXNIP (1:1000, MBL, Woburn, MA) overnight at 4°C, followed by incubation with the appropriate horseradish peroxidase-labeled IgG (1:5000) at RT for 1 hr. The bands were detected by chemiluminescence and visualized on Kodak Omat X-ray films, and band density was analyzed by ImageJ software (NIH, Bethesda, MD).

### 2.6 Confocal microscopy and immunofluorescence of frozen tissue and cell slides

Indirect immunofluorescent staining was used to observe the colocalization of inflammasome and podocyte marker proteins in both cultured cells as well as frozen mouse kidney sections. Podocytes seeded in 8-well chambers were fixed in 4% paraformaldehyde (PFA), washed with phosphate-buffered saline (PBS), and blocked with 1% bovine serum

albumin (BSA) in PBS before being incubated in primary antibodies (1:100) overnight at 4°C. The primary goat anti-NLRP3 (Abcam, Cambridge, MA) antibody was used in combination with the following: rabbit anti-ASC (Santa Cruz, Dallas, TX), rabbit anti-caspase (Santa Cruz), or mouse anti-TXNIP (MBL, Woburn, MA). Frozen mouse kidney tissue slides were fixed in acetone, blocked with 3% donkey serum, then incubated with the same aforementioned primary antibodies (1:50) overnight at 4°C. Some coverslips with podocytes and frozen kidney sections were only stained for podocyte markers podocin (1:50; Sigma, St. Louis, MO) or desmin (1:50; BD Biosciences, San Jose, CA), or also in combination with goat anti-NLRP3 antibody. Double immunofluorescent staining was performed by Alexa-488 or Alexa-555-labeled secondary antibody (1:200 podocytes, 1:50 frozen kidney slides; Life Technologies, Grand Island, NY) incubation for 1 hr at room temperature. Slides were then washed, mounted, and observed using a confocal laser scanning microscope (Fluoview FV1000, Olympus, Japan) and tools in Image Pro Plus 6.0 software (Media Cybernetics, Bethesda, MD) was used to analyze colocalization, or the degree of overlap between the two wavelengths, which was expressed as the Pearson Correlation Coefficient.

### 2.7 Size-exclusion chromatography

As described in our previous studies [169-170], homogenates from either treated podocytes or renal cortical tissue was prepared using the following protein extraction buffer: 20 mM 4-(2-hydroxyethyl)-1-piperazineethanesulfonic acid-KOH (pH 7.5), 10 mM KCl, 1.5 mM Na-EDTA, 1 mM Na-EGTA, and 1x protease inhibitor cocktail (Roche Applied Science, Indianapolis, IN). Samples were centrifuged at 16,000g for 10 minutes at 4°C, the supernatant filtered through a 0.45 μm centrifuge tube filter, and the protein concentration was measured. Samples were

normalized by loading 1 mg protein in less than 500 µl total volume onto a Superose 6 10/300 GL Column using an ÄKTAprime plus fast-protein liquid chromatography (FPLC) system (GE Healthscience, Uppsala, Sweden). Fractions were collected (600 µl), protein precipitated using tricholoroacetic acid, and analyzed by Western blot as described above.

### 2.8 Co-immunoprecipitation

Renal cortical tissue was homogenized on ice in IP lysis buffer (30 mM Tris-HCl, 150 mM NaCl, 2 mM EDTA, 1% Triton X-100, 10% glycerol, 1x Protease Inhibitor) followed by brief pulses of hand sonication. After a 30 minute incubation on ice, the lysate was centrifuged and the supernatant precleared by incubation with Protein A/G PLUS-Agarose Beads (Santa Cruz, sc-2003) in 4°. The precleared supernatant was incubated with 2 µg antibody against NLRP3 (Abcam) for 4 hours on a rocker in 4°. Beads were added for an additional 1 hr, and then immunoprecipitates collected by centrifugation at 1,000g for 5 minutes and washed three times with IP lysis buffer with centrifugation after each wash. The pellet was resuspended in 2x sample buffer, boiled, and analyzed for NLRP3 and TXNIP protein expression by Western blot.

### 2.9 Caspase-1 activity, IL-1β production, and VEGF measurements

Caspase-1 activity was measured by a commercially available colorimetric assay (Biovision, Mountain View, CA), while IL-1β production and vascular endothelial growth factor-A (VEGF-A) secretion was measured in the supernatant of cultured podocytes using an enzyme-linked immunosorbent assay (R&D System, Minneapolis, MN) according to manufacturer's instructions.

### 2.10 Electron spin resonance spectrophotometry of $O_2^{\bullet-}$ production

Protein from cultured podocytes or renal cortical tissue was extracted using a sucrose buffer, and then prepared for analysis by resuspension in a modified Krebs-Hepes buffer containing deferoximine (100 μM; Sigma, St. Louis, MO, USA) and diethyldithiocarbamate (5 μM; Sigma). To measure NADPH oxidase-dependent superoxide production, 1 mM NADPH substrate was added to 50 μg protein, and each sample was read twice on an ESR spectrometer and examined in the presence or absence of superoxide dismutase (SOD, 200 U/ml; Sigma). 1-hydroxy-3-methoxycarbonyl-2,2,5,5-tetramethylpyrrolidine (CMH, 1mM), a superoxide specific spin trapping compound, was added to the sample before being loaded into a glass capillary, and analyzed in an ESR spectrometer for 10 minutes [171]. Results were obtained by taking the difference between the total CMH signal without SOD and the SOD-specific signal, and all values were expressed as the fold change from the control.

### 2.11 RNA isolation and real time RT-PCR

Total RNA was isolated from both podocytes and renal cortical tissue using the TRIzol reagent (Grand Island, NY), reverse transcribed to cDNA, and subject to PCR amplification according to the procedures described previously [172]. All primers were synthesized by Operon (Huntsville, AL) with the following sequences: Nox1, sense 5′-AATGCCCAGGATCGAGGT, antisense 5′-GATGGAAGCAAAGGGAGTGA-3′; Nox2, sense 5′-TGGCACATCGATCCCTCACTGAAA-3′, antisense 5′-GGTCACTGCATCTAAGGCAACCT-3′; Nox4, sense 5′-GAAGGGGTTAAACACCTCTGC-3′, antisense 5′-ATGCTCTGCTTAAACACAATCCT-3′; TXNIP, sense 5′-CAGCCTACAGCAGGTGAGAAC-3′, antisense 5′-CTCATCTCAGAGCTCGTCCG-3′.

### 2.12 F-actin staining of podocytes

To determine the role of NADPH oxidase and inflammasome activation in Hcys-induced cytoskeleton changes, podocytes were cultured in 8-well chambers. After washing with PBS, the cells were fixed in 4% PFA for 15 min at room temperature, permeabilized with 0.1% Triton X-100, and blocked with 3% bovine serum albumin. F-actin was stained with rhodamine–phalloidin (Invitrogen, Carlsbad, CA) for 15 min at room temperature. After mounting, the slides were examined by a confocal laser scanning microscope (Fluoview FV1000, Olympus, Japan). Cells with distinct F-actin fibers were counted as described previously [173]. Scoring was obtained from 100 podocytes from each group on each slide.

### 2.13 Immunohistochemistry

Kidneys were embedded with paraffin and 5 μm sections were cut from the embedded blocks. After heat-induced antigen retrieval, CD43 staining of T cells and WT-1 staining of podocytes required citrate buffer antigen retrieval, while F4/80 staining of macrophages required Proteinase K antigen retrieval. After a 20 min wash with 3% $H_2O_2$ and 30 min blocking with serum, slides were incubated with primary antibodies diluted in phosphate-buffered saline (PBS) with 4% serum. Anti-CD43 (1:50; Santa Cruz Biotechnology, Santa Cruz, CA), anti-F4/80 (1:50; AbD Serotec, Raleigh, NC), and anti-WT-1 (1:50; Abcam, Cambridge, MA) antibodies were used in this study for detection of macrophages and T-cells. After incubation with each of these primary antibodies overnight, the sections were washed in PBS and incubated with biotinylated IgG (1:200) for 1 h and then with streptavidin-HRP for 30 min at room temperature. 50 μl of DAB was added to each kidney section and stained for 1 min. After washing, the slides were counterstained with hematoxylin for 5 min. The slides were then mounted and observed under a

microscope, and photographs were taken at 100x magnification. All of the glomeruli in the cortical fields were counted and blindly used for analysis of each slide [174].

### 2.14 Chronic catheterization and arterial blood pressure measurement

Mean arterial pressure (MAP) was measured for 3 days in mice involved with the TXNIP inhibition studies, including luciferase-transfected, TXNIPsh-transfected, or verapamil-administered mice, to make sure there were no effects of diet or treatment on blood pressure. As we described previously [175-176], mice were anaesthetized by isoflurane inhalation, and a telemetry transmitter catheter implanted into the carotid artery. The transmitter was placed subcutaneously, allowing mice to be housed unrestrained, with the arterial blood pressure signal transmitted to a remote receiver (Data Sciences International, St. Paul, MN, USA).

### 2.15 Urinary protein and albumin measurements

Total urinary protein excretion was determined spectrophotometrically using the Bradford assay (Sigma) using a standard curve of BSA, and urinary albumin excretion was measured using a commercially available mouse albumin ELISA kit (Bethyl Laboratories, Montgomery, TX).

### 2.16 Glomerular morphological examination

Renal tissues were fixed with a 10% formalin solution, paraffin-embedded, and stained with periodic acid–Schiff (PAS). Renal morphology was observed using a light microscope, and glomerular sclerosis was assessed semiquantitatively and expressed as glomerular damage index (GDI) [177]. Fifty glomeruli per slide were counted and blindly scored as 0, 1, 2, 3, or 4,

according to 0, <25, 25–50, 51–75, or >75% sclerotic changes, respectively, across a longitudinal kidney section. The GDI for each mouse was calculated by the formula ((N1 ×1) + (N2 ×2) + (N3 ×3) + (N4 ×4))/n, where N1, N2, N3, and N4 represent the numbers of glomeruli exhibiting grades 1, 2, 3, and 4, respectively, and n is the total number of glomeruli scored.

### 2.17 HPLC analysis of plasma Hcys

Total plasma Hcys levels were measured by HPLC as previously described [178-179]. A 100 µL plasma or standard solution mixed together with 10 µL of the internal standard thioglycolic acid (2.0 mmol/L) solution, was treated with 10 µL of 10% tri-n-butylphosphine (TBP) solution in dimethylformamide at 4°C for 30 minutes. In order to precipitate and remove proteins in the sample, 80 µL of ice-cold 10% trichloroacetic acid (TCA) in 1 mmol/L EDTA was added and followed with centrifugation. 100 µL of the resulting supernatant was transferred into the mixture of 20 µL of 1.55 mol/L sodium hydroxide, 250 µL of 0.125 mol/L borate buffer (pH 9.5), and 100 µL of 1.0 mg/mL 7-fluoro-2,1,3-benzoxadiazole-4-sulfonamide (ABD-F) solution, then incubated at 60°C for 30 minutes to achieve derivatization of thiols. HPLC was performed with a HP 1100 series instrument equipped with a binary pump, a vacuum degasser, a thermo stated column compartment, and an auto sampler (Agilent Technologies, Waldbronn, Germany). Separation was carried out at ambient temperature on a Supelco LC-18-DB (Supelco; 150×4.6 mm i.d., 5 µm particle size) analytical column with a Supelcosil LC-18 guard column (Supelco; 20×4.6 mm i.d., 5 µm particle size). Fluorescence intensities were measured with a Hewlett-Packard Model 1046A fluorescence detector (excitation: 386 nm, emission: 515 nm), with a Hewlett-Packard 3392 integrator quantifying the peak area of the chromatographs. The

analytical column was eluted with 0.1 mol/L potassium dihydrogen phosphate buffer (pH 2.1) containing 6% acetonitrile (v/v) as the mobile phase with a flow rate of 2.0 mL/min.

### 2.18 Statistical analysis

All results were expressed as the arithmetic mean ± SEM; n represents the number of independent experiments. Data obtained from multiple animal or experimental groups were tested for significance using one- or two-way ANOVA, and a paired and unpaired Student's t-test was used for two animal or experimental groups. A $\chi^2$ test was used to determine the significance of ratio and percentage data. Results with $p<0.05$ were considered statistically significant.

# CHAPTER THREE

## NADPH oxidase-mediated triggering of inflammasome activation in mouse podocytes and glomeruli during hyperhomocysteinemia

### 3.1 Rationale and Hypothesis

As depicted in **Figure 4** the present study hypothesized that NADPH oxidase-mediated redox signaling play an essential role in triggering hHcys-induced inflammasome activation within podocytes, thereby inducing glomerular inflammatory injury such as immune cell infiltration and consequently leading to glomerular sclerosis. To test this hypothesis, we first used cultured murine podocytes to examine whether inhibition of NADPH oxidase attenuates Hcys-induced NLRP3 inflammasome formation and activation and also addressed the functional relevance of this early inflammatory event. Using pharmacological inhibitors or mice lacking the $gp91^{phox}$ gene, we also tested the *in vivo* role of NADPH oxidase activation in hHcys-induced NLRP3 inflammasome formation and activation, glomerular inflammatory pathology and glomerular sclerosis compared with wild-type littermates.

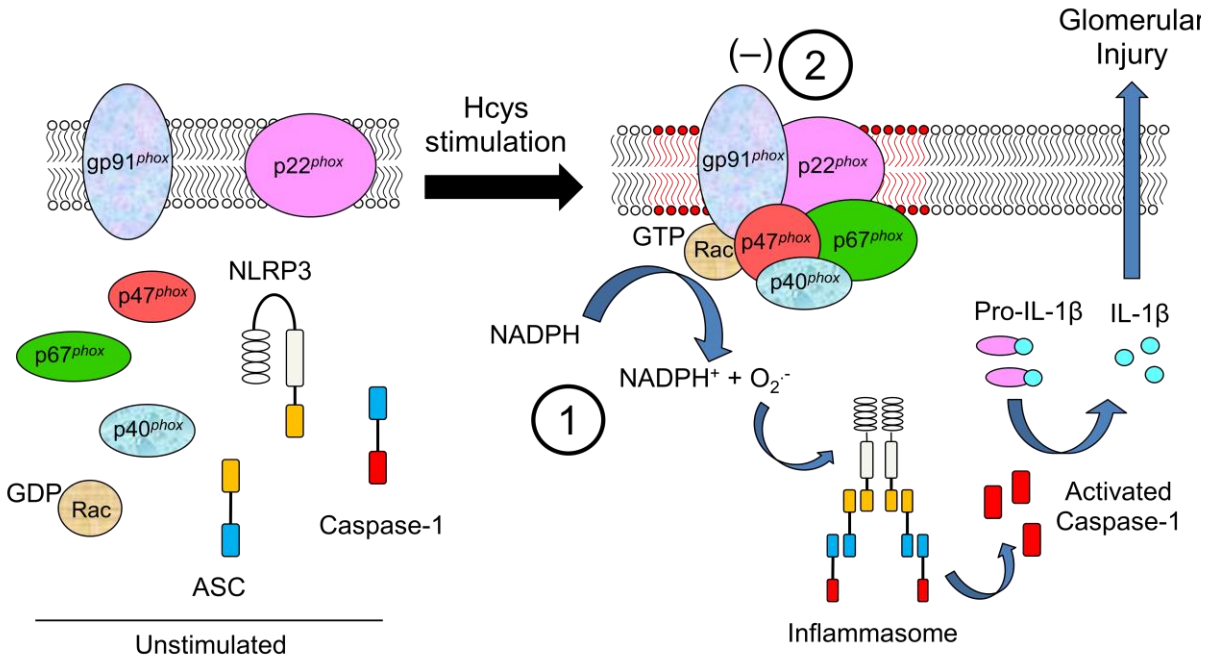


**Figure 4. Representative schematic for Aims 1 and 2.** Through the specific inhibition of gp91$^{phox}$ both *in vitro* and *in vivo*, Aim 1 and 2 will explore the role of NADPH oxidase in Hcys-induced NLRP3 inflammasome activation.

## 3.2 Results

### 3.2.1 Attenuation of Hcys-induced NLRP3 inflammasome formation through inhibition of NADPH oxidase

As shown in **Figure 5A**, confocal microscopic analysis demonstrated that Hcys induced the colocalization of inflammasome markers (NLRP3 with ASC and NLRP3 with caspase-1) in podocytes compared to untreated control cells. Pretreatment of podocytes with NADPH oxidase inhibitors DPI or gp91*ds-tat* peptide significantly abolished the Hcys-induced aggregation of NLRP3 with ASC and NLRP3 with caspase-1, suggesting blockade of inflammasome formation in these cells. Furthermore, small interfering RNA against ASC and gp91$^{phox}$ also blocked Hcys-

induced inflammasome formation. The Pearson correlation coefficient was calculated for each of the groups using the colocalization analysis program in the Image Pro Plus 6.0 software and summarized in **Figure 5B**. In addition, co-immunoprecipitation experiments demonstrated that Hcys significantly increased the binding of NLRP3 and caspase-1 together with ASC compared to control cells, which is attenuated in the presence of apocynin and gp91*ds-tat* peptide (data not shown). Together, these results suggest that inhibition of NADPH oxidase or silencing ASC gene attenuates Hcys-induced inflammasome formation in podocytes.

Size-exclusion chromatography (SEC) was employed to further determine the role of NADPH oxidase in the process of Hcys-induced inflammasome complex formation. A representative chromatogram is shown in **Figure 6A**, illustrating the peaks produced from both a standard and typical protein sample when run and separated by the Sepharose 6 column. As depicted in **Figure 6B**, under control conditions the specific bands for NLRP3 and ASC were located in the low molecular weight fractions (18-22). Upon stimulation with Hcys for 24 hours, the NLRP3 and ASC bands markedly shifted to high molecular weight fractions (3-7), termed the inflammasome fractions due to complex formation. However, when NADPH oxidase was inhibited in podocytes by treatment with gp91*ds-tat* or DPI prior to the addition of Hcys, a clear decrease in inflammasome protein complex aggregation was observed in the high-molecular weight fractions. The intensity of these bands were quantified by ImageJ software and summarized in **Figure 6C**.

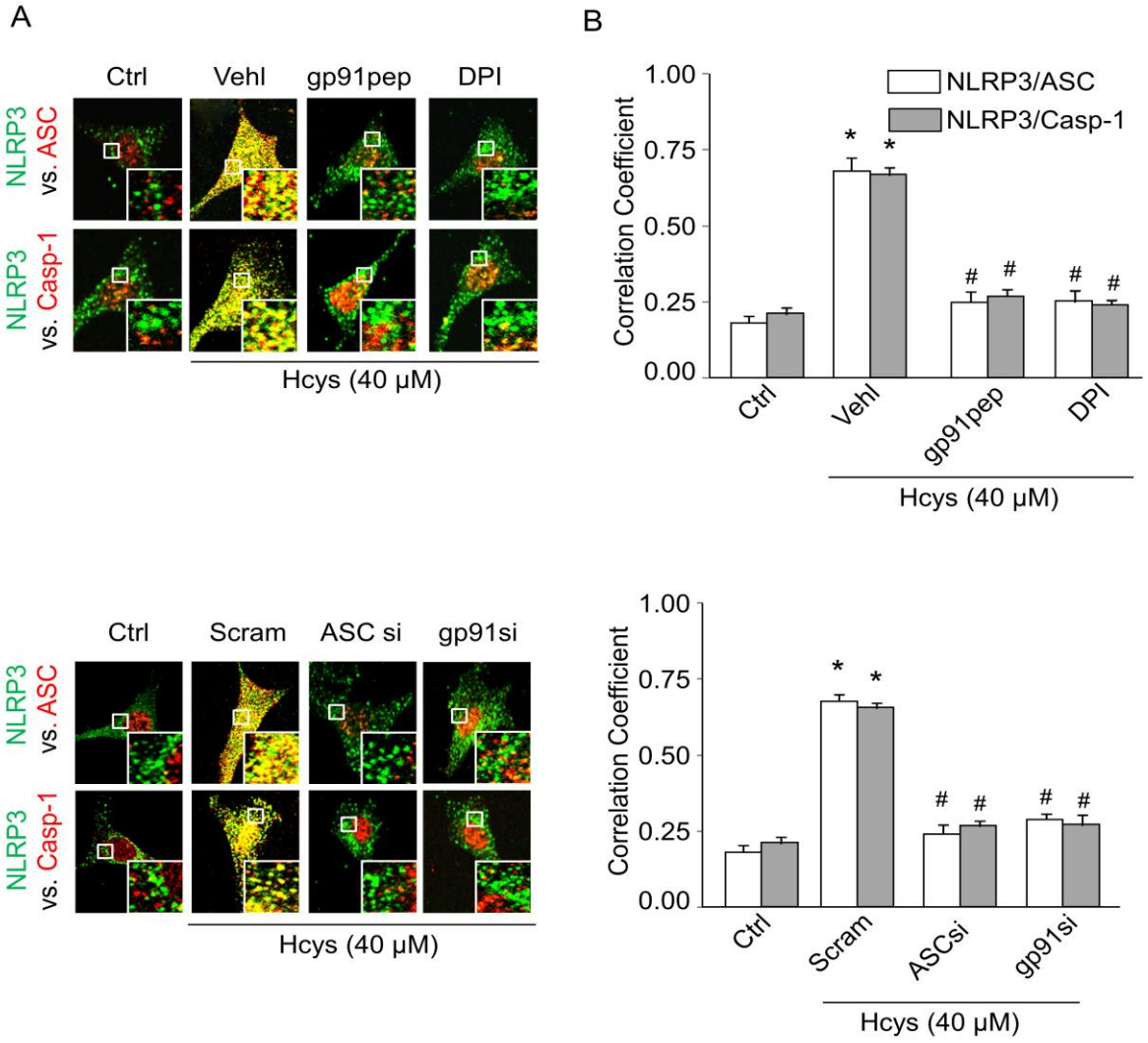


**Figure 5. NADPH oxidase inhibition attenuated inflammasome formation induced by hHcys in podocytes.** A. Confocal images representing the colocalization of NLRP3 (green) with ASC (red) and NLRP3 (green) with caspase-1 (red) in podocytes. B. Summarized data showing the fold change of PCC for the colocalization of NLRP3 with ASC and NLRP3 with caspase-1. (n=6-7). Ctrl: Control; Vehl: Vehicle; gp91pep: gp91*ds-tat*; DPI: diphenylene iodonium; Scram: Scramble siRNA; ASCsi: ASC siRNA; gp91si: $gp91^{phox}$ siRNA. * $P$<0.05 vs. Control; # $P$<0.05 vs. Hcys.

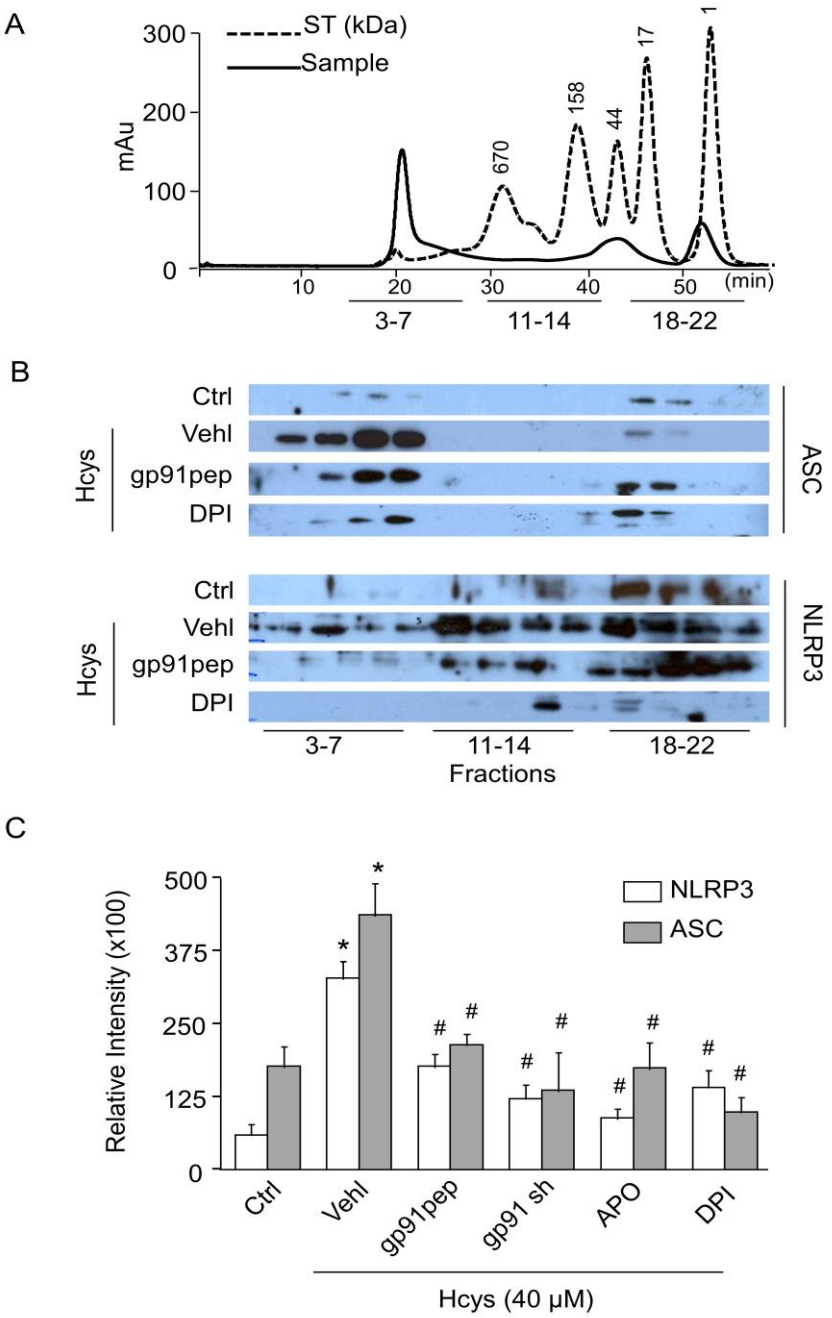


**Figure 6. Distribution of inflammasome components after size-exclusion chromatography of podocytes.** A. Elution profile of proteins from both a standard and podocyte samples at an absorbance of 280 nm. Molecular mass of the samples were determined by comparison to a gel filtration standard. B. Western blot analysis of FPLC protein fractions obtained from untreated, Hcys-treated, and gp91*ds-tat*-treated podocytes probed with anti-NLRP3 and ASC antibodies. C. Summarized data showing the band intensities measured from the inflammasome complex fractions (fractions 3-7) of NLRP3 and ASC (n=4-6). Ctrl: Control; Vehl: Vehicle; gp91pep: gp91*ds-tat*; DPI: diphenylene iodonium; gp91sh: $gp91^{phox}$ shRNA, APO: apocynin. * $P<0.05$ vs. Control; # $P<0.05$ vs. Hcys.

### 3.2.2 Inhibition of NADPH oxidase blocked NLRP3 inflammasome functionality by suppressing caspase-1 activity and IL-1b secretion

We further tested whether inhibition of NADPH oxidase also attenuates Hcys-induced caspase-1 activity and IL-1β production in podocytes. As shown in **Figure 7A**, the increase in caspase-1 activity caused by Hcys was markedly inhibited by the NADPH oxidase inhibitors apocynin, DPI, gp91*ds-tat*, and gp91$^{phox}$ siRNA, implicating an important role for NADPH oxidase in inflammasome activation. ASC siRNA also produced a similar significant decrease in caspase-1 activity. **Figure 7B** demonstrated that these decreases in caspase-1 activity also resulted in less IL-1β being converted from the pro-inflammatory cytokine form to the active form during the simultaneous treatment of Hcys with either NADPH oxidase or inflammasome inhibitors.

### 3.2.3 Effect of NLRP3 inflammasome inhibition on Hcys-induced $O_2^{\bullet-}$ production

To determine whether NADPH oxidase-derived $O_2^{\bullet-}$ plays a role in inflammasome activation, $O_2^{\bullet-}$ levels were measured in podocytes pretreated with NADPH oxidase or inflammasome inhibitors in the presence of Hcys. As expected, treatment of podocytes with DPI, gp91*ds-tat*, or gp91$^{phox}$ siRNA produced a distinct decrease in $O_2^{\bullet-}$ production when compared to Hcys alone (**Figure 7C**). Additionally apocynin or gp91*ds-tat* peptide also significantly attenuated the Hcys-induced $O_2^{\bullet-}$ production in the plasma membranes of podocytes (**Figure 7D**). However, ASC siRNA or caspase-1 inhibition could not prevent the Hcys-induced increase in $O_2^{\bullet-}$. This suggests that NADPH oxidase activation by Hcys and subsequent production of $O_2^{\bullet-}$ is upstream of inflammasome activation, given that inhibition of the inflammasome did not affect the levels of NADPH oxidase-derived $O_2^{\bullet-}$.

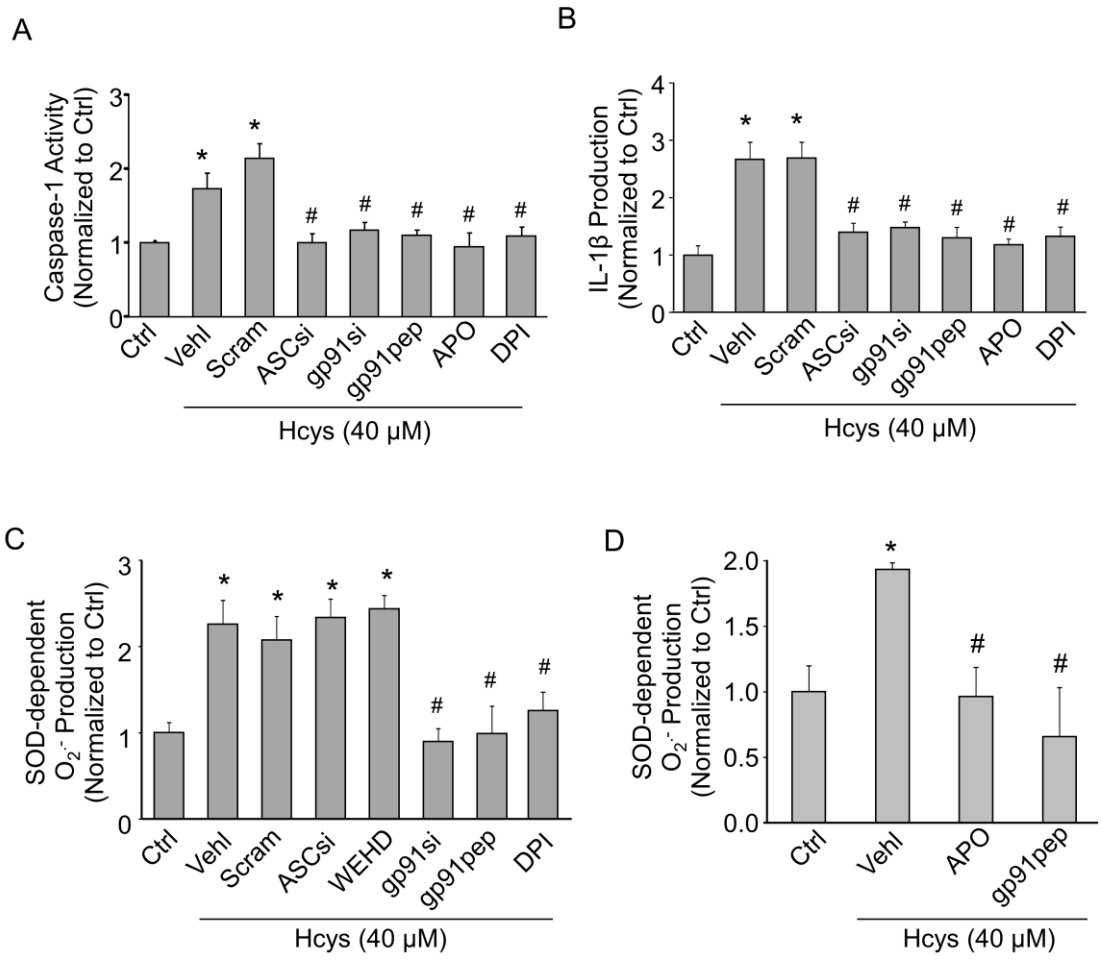


**Figure 7. Effects of NADPH oxidase inhibition and ASC silencing on Hcys-induced caspase-1 activity, IL-1β secretion, and $O_2^{\bullet-}$ production in podocytes.** A. Caspase-1 activity in groups treated with Hcys in the presence of various genetic and pharmacologic inhibitors of NADPH oxidase and the inflammasome (n=6). B. IL-1β production in podocytes treated with Hcys in the presence of various genetic and pharmacologic inhibitors of NADPH oxidase and the inflammasome (n=6). C. Hcys-induced $O_2^{\bullet-}$ production decreased with treatment of NADPH oxidase inhibitors, but not genetic or pharmacologic inhibitors of the inflammasome (n=5). D. Hcys induced superoxide production in microsomes isolated from cultured podocytes, which was prevented by pharmacological NADPH oxidase inhibitors APO and gp91pep (n=4-5). Ctrl: Control; Vehl: Vehicle; gp91pep: gp91*ds-tat*; DPI: diphenylene iodonium; Scram: Scramble siRNA; ASCsi: ASC siRNA; gp91si: $gp91^{phox}$ siRNA; APO: apocynin. * $P<0.05$ vs. Control; # $P<0.05$ vs. Hcys.

### 3.2.4 Inhibition of NADPH oxidase or NLRP3 inflammasomes attenuated Hcys-induced podocyte injury

As shown in **Figure 8A**, immunofluorescent analysis demonstrated that Hcys stimulation increased desmin expression in podocytes compared to untreated cells. Prior treatment with gp91$^{phox}$ siRNA, ASC siRNA, gp91*ds-tat*, apocynin, DPI, or caspase-1 inhibitor WEHD decreased this Hcys-induced desmin expression in podocytes. Another podocyte marker, podocin, was markedly reduced upon Hcys stimulation in podocytes, and prior treatment with the same inhibitors almost completely attenuated the decrease in podocin expression. Positive cells were counted and summarized in **Figure 8B**. These results signify the importance of both NADPH oxidase and inflammasome functionality in this injurious process of podocytes when exposed to Hcys. Using rhodamine-phalloidin to stain F-actin, the control condition exhibited well-defined F-actin fibers which run along the longitudinal axis of these podocytes, and as demonstrated by the obvious lack of distinct fibers, Hcys resulted in a significant loss of these longitudinal fibers as they reorganize to the cell border. Puromycin aminonucleoside (PAN), a classic and specific inducer typical used to cause podocyte injury [180], served as a positive control (**Figure 8C**). However, inhibition of NADPH oxidase or inflammasomes hindered the Hcys-induced decrease and rearrangement of F-actin. These changes in F-actin staining were summarized in **Figure 8D**.

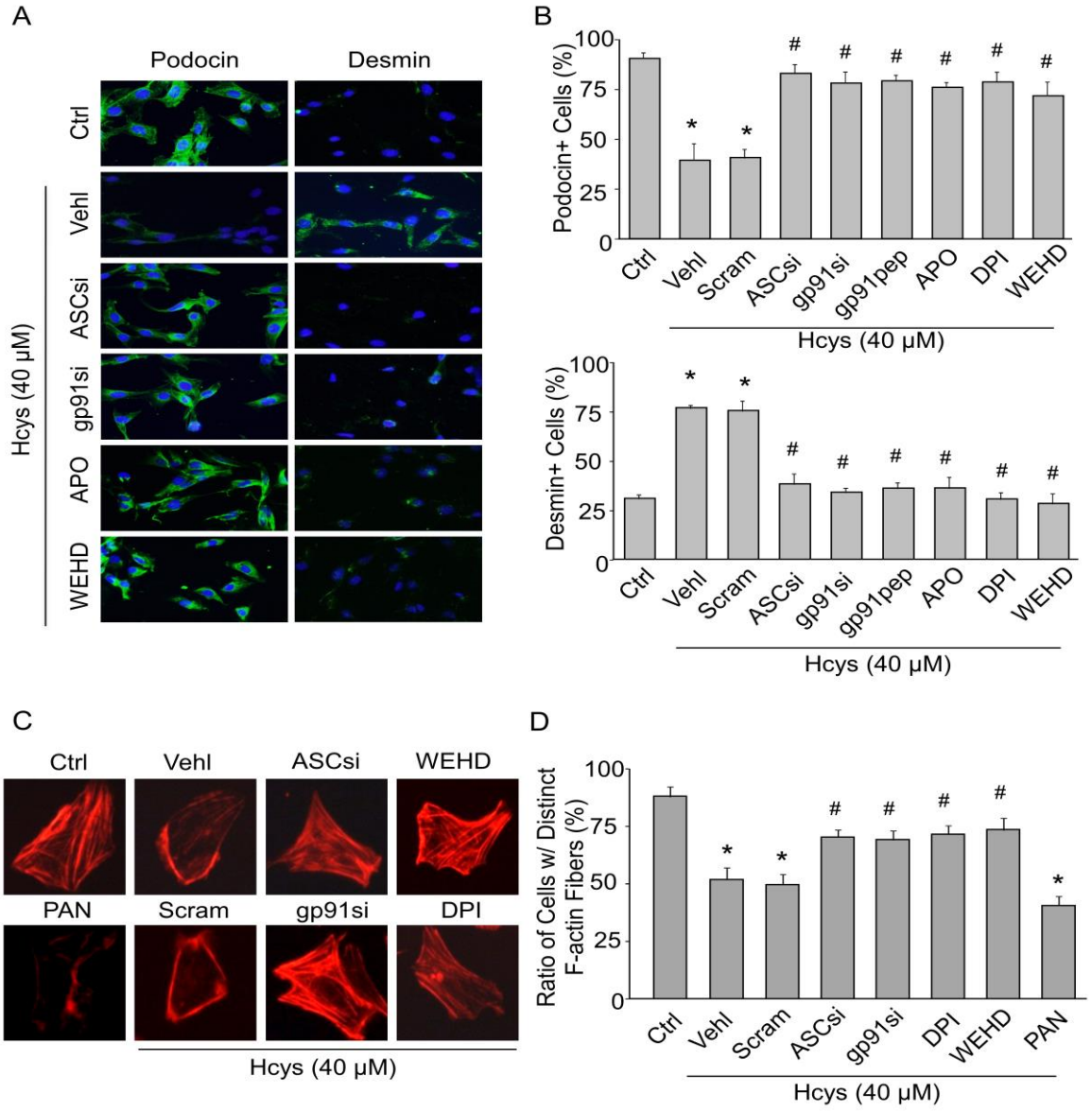


**Figure 8. Amelioration of Hcys-induced podocyte dysfunction by NADPH oxidase and inflammasome inhibitors.** A. Immunofluorescence staining showed that inhibition of NADPH oxidase activation by gp91$^{phox}$ siRNA, gp91*ds-tat*, apocynin and DPI, or inflammasome inhibition by ASC siRNA or WEHD rescued Hcys-induced expression of podocyte marker podocin (original magnification, x400). Inhibition of NADPH oxidase or inflammasome activation also resulted in suppressed expression of podocyte injury marker desmin. B. Summarized data shows the percentage of podocyte cells positive for podocin and desmin. C. Microscopic images of F-actin by rhodamine-phalloidin staining (original magnification, x400). PAN treatment served as a positive control. D. Summarized data from counting the cells with distinct, longitudinal F-actin fibers. Scoring was determined from 100 podocyte cells on each slide (n=5-6). Ctrl: Control; Vehl: Vehicle; gp91pep: gp91*ds-tat*; DPI: diphenylene iodonium; Scram: Scramble siRNA; ASCsi: ASC siRNA; gp91si: gp91$^{phox}$ siRNA. * $P$<0.05 vs. Control; # $P$<0.05 vs. Hcys.

### 3.2.5 gp91$^{phox-/-}$ and gp91*ds-tat*-treated mice had no hHcys-induced glomerular NLRP3 inflammasome formation and activation

To further confirm the role of NADPH activation *in vivo* in experimental hHcys mice, double fluorescent-immunostaining of kidney slides was performed. As shown in **Figure 9A**, under control condition NLRP3, ASC and caspase-1 were expressed at low levels within the glomeruli, and very few colocalizations of these inflammasome molecules could be detected by confocal microscopy. In gp91$^{phox+/+}$ mice, the colocalization of NLRP3 with ASC or caspase-1 markedly increased in glomeruli of FF diet-fed hHcys mice. However, the increased colocalization of NLRP3 with ASC or caspase-1 was suppressed in glomeruli of hyperhomocysteinemic gp91$^{phox-/-}$ and gp91*ds-tat*-treated mice. The summarized data were shown in **Figures 9B and 9C**. In addition, using podocin and desmin as podocyte markers we showed that hHcys-induced inflammasome activation in glomeruli was mostly located in podocytes, as demonstrated by the colocalization of podocin with NLRP3 or caspase-1 and desmin with NLRP3 or caspase-1. This colocalization was substantially blocked in hyperhomocysteinemic gp91$^{phox-/-}$ mice and gp91*ds-tat*-treated mice (**Figure 9A**). The summarized data were shown in **Figures 9D and 9E**.

Consistent with decreased aggregation of inflammasome components in the glomeruli, hHcys-enhanced caspase-1 activity and IL-1β production were markedly attenuated in glomeruli of gp91$^{phox-/-}$ and gp91*ds-tat*-treated mice (**Figures 10A and 10B**). In addition, hHcys-induced glomerular superoxide production was significantly attenuated in gp91*ds-tat*-treated and gp91$^{phox-/-}$ mice compared to their wild-type littermates (**Figure 10C**). The plasma Hcys concentration was similar in gp91$^{phox+/+}$, gp91$^{phox-/-}$ and gp91*ds-tat*-treated mice on the normal diet. However, the FF diet significantly increased the plasma Hcys concentration in all three

groups compared to normal diet fed mice (gp91$^{phox+/+}$ mice: 12.6 ± 2.0 versus 4.1 ± 0.41 μM for control; gp91$^{phox-/-}$ mice: 13.0 ± 1.6 versus 4.0 ± 0.8 μM for control; gp91*ds-tat* mice: 11.6 ± 1.0 versus 5.1 ± 0.41 μM for control).

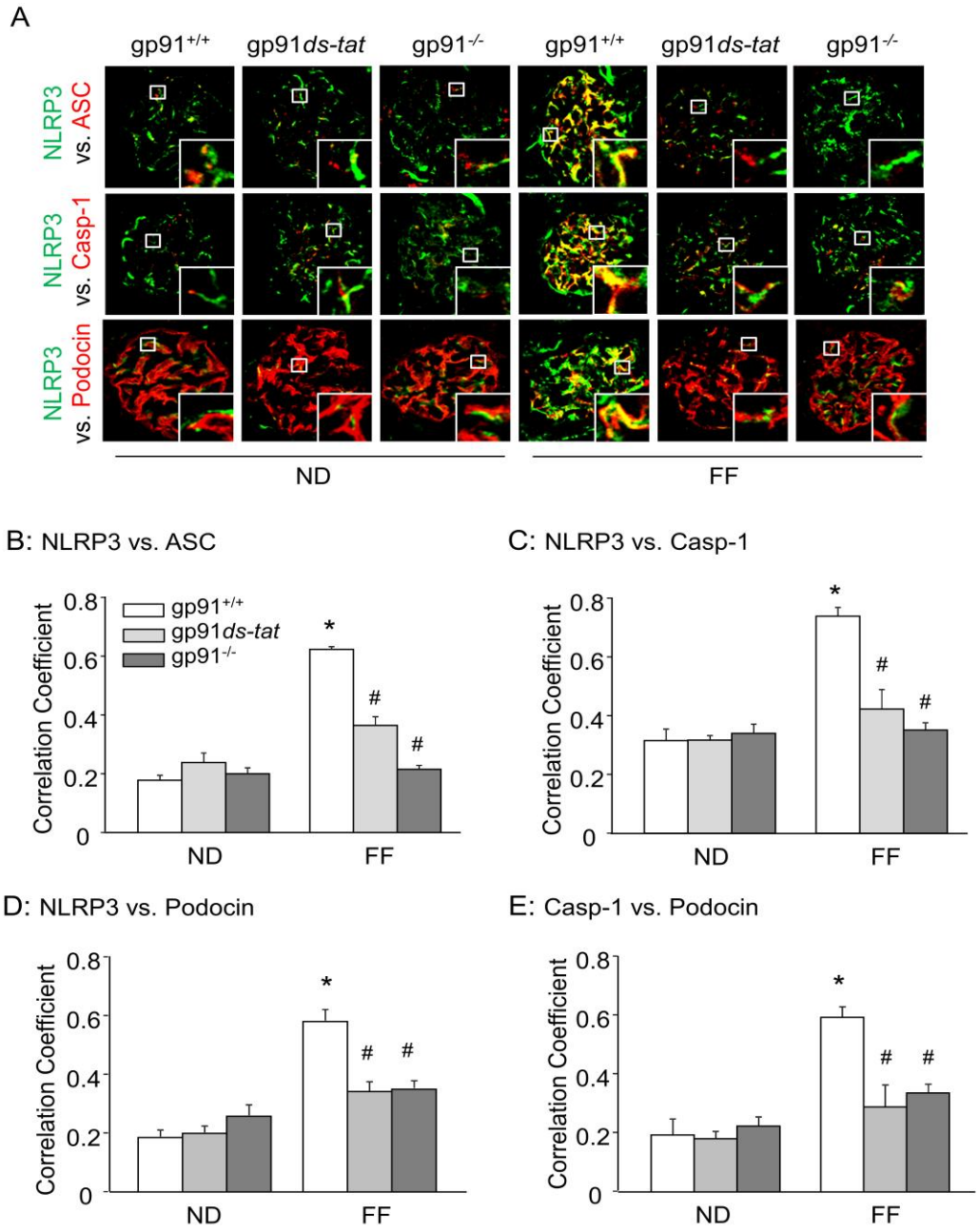


**Figure 9. Attenuation of Hcys-induced inflammasome activation in the glomeruli of gp91$^{phox-/-}$ and gp91*ds-tat*-treated mice on a FF diet.** A. Colocalization of NLRP3 (green) with ASC (red), NLRP3 (green) with caspase-1 (red), and NLRP3 (green) with podocyte marker podocin (red) in the mouse glomeruli of gp91$^{phox+/+}$, gp91*ds-tat*, and gp91$^{phox-/-}$ mice fed a normal or FF diet. B and C. Summarized data showing the correlation coefficient between NLRP3 with ASC and NLRP3 with caspase-1 (n=7). D and E. Summarized data showing the correlation coefficient between NLRP3 with podocin and caspase-1 with podocin (n=4-5). *$P$<0.05 vs. gp91$^{phox+/+}$ on Normal Diet; # $P$<0.05 vs. gp91$^{phox+/+}$ on FF Diet.

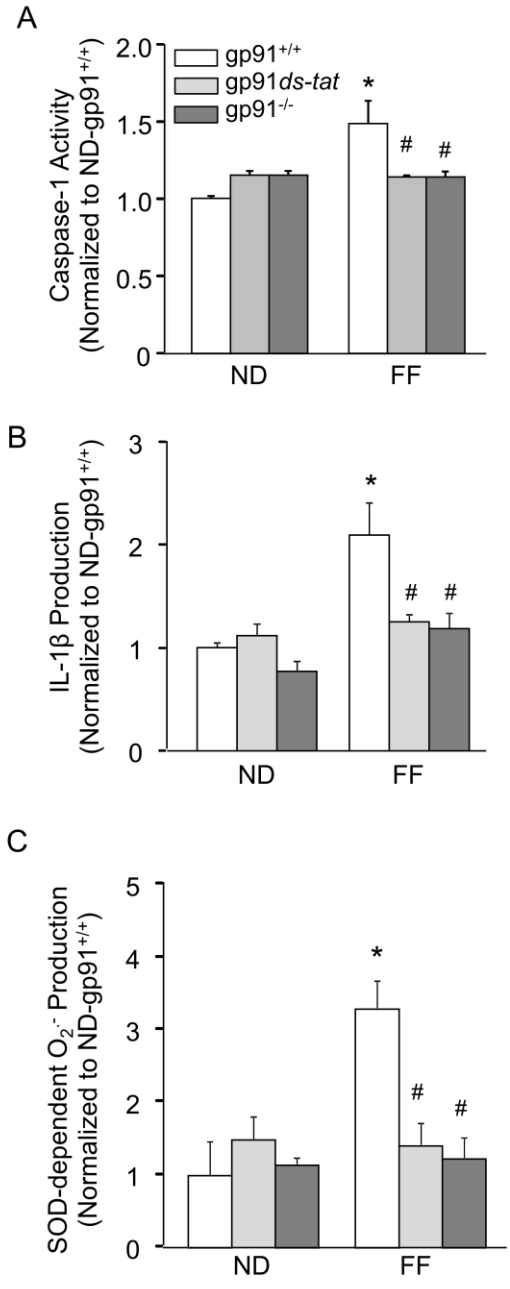


**Figure 10. *In vivo* effect of NADPH oxidase inhibition on Hcys-induced caspase-1 activity, IL-1β secretion, and $O_2^{\bullet-}$ production.** A. Caspase-1 activity in gp91$^{phox+/+}$, gp91*ds-tat*, and gp91$^{phox-/-}$ mice with hHcys induced by the FF diet (n=6). B. IL-1β production induced by hHcys was inhibited in both the mice treated with gp91*ds-tat* and in gp91$^{phox-/-}$ mice (n=6). C. Hcys-induced superoxide production was attenuated in the gp91*ds-tat* and gp91$^{phox-/-}$ groups (n=5). * $P$<0.05 vs. gp91$^{phox+/+}$ on Normal Diet; # $P$<0.05 vs. gp91$^{phox+/+}$ on FF Diet.

### 3.2.6 *In vivo* inhibition of NADPH oxidase prevented hHcys-induced glomerular inflammation and injury

As shown in **Figures 11A and 11C**, immunohistochemical analysis demonstrated that Hcys stimulation induced macrophage (F4/80+) and T-cell (CD43+) infiltration in the glomeruli of hHcys gp91$^{phox+/+}$ mice. However, the glomeruli of gp91$^{phox-/-}$ and gp91*ds-tat*-treated mice had significantly less macrophage and T-cell recruitment when compared to gp91$^{phox+/+}$ mice on the FF diet. The summarized data were shown in **Figures 11B and 11D**. These results suggest that normal NADPH oxidase gene expression and activity are required for inflammasome activation and consequent inflammatory response, which includes macrophage and T-cell recruitment and aggregation in glomeruli of mice during hHcys.

Next, we tested whether gp91$^{phox}$ contributes to hHcys-induced glomerular injury. As shown in Figure 12, hHcys significantly increased the urinary protein and albumin in gp91$^{phox+/+}$ mice compared to normal diet-fed mice. Mice treated with gp91*ds-tat* and gp91$^{phox-/-}$ mice had significantly attenuated hHcys-enhanced urinary protein and albumin excretion in FF diet-fed mice, but had no effect in normal diet-fed mice (**Figures 12A and 12B**). Morphological examinations revealed a typical pathological change in glomerular sclerotic damage indicated by capillary collapse, fibrosis, cellular proliferation and mesangial cell expansion in glomeruli of hHcys gp91$^{phox+/+}$ mice (**Figure 12C**). The average glomerular damage index was significantly higher in glomeruli of hHcys gp91$^{phox+/+}$ mice compared to normal diet-fed mice. However, in gp91$^{phox-/-}$ or gp91*ds-tat*-treated mice, hHcys-induced glomerular injuries were significantly inhibited (**Figure 12D**).

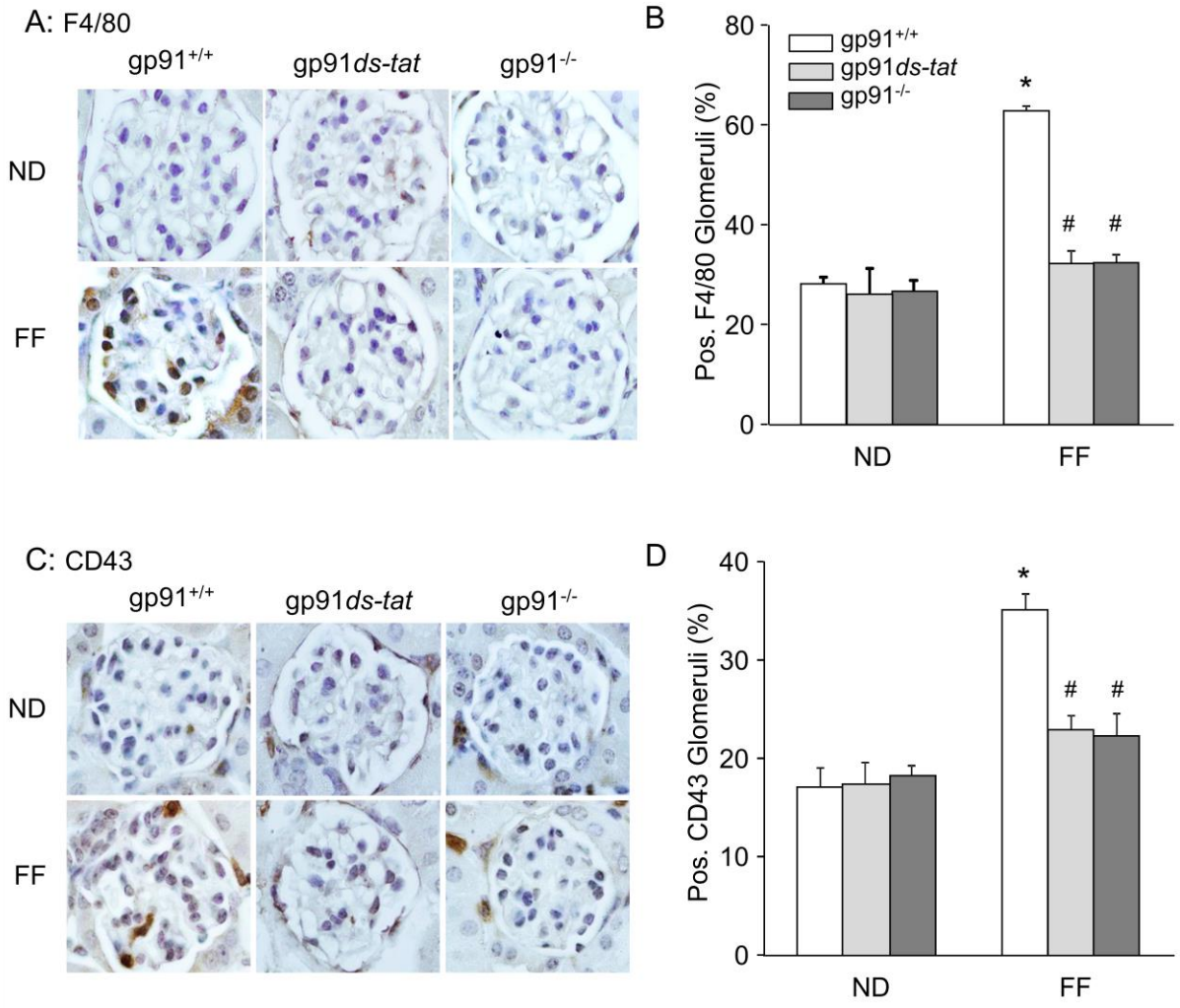


**Figure 11. Inhibition of NADPH oxidase expression and activity prevented hHcys-induced infiltration of macrophages and T-cells into the glomeruli.** A. gp91*ds-tat* and gp91$^{phox-/-}$ mice prevented the increased expression and staining of macrophage marker F4/80 that is seen in gp91$^{phox+/+}$ on FF Diet. B. Summarized counts of F4/80 positive glomeruli (n=6). C. gp91*ds-tat* and gp91$^{phox-/-}$ mice prevented the increased expression and staining of T-cell marker CD43 that is seen in gp91$^{phox+/+}$ on FF Diet. D. Summarized counts of CD43 positive glomeruli (n=6). * $P$<0.05 vs. gp91$^{phox+/+}$ on Normal Diet; # $P$<0.05 vs. gp91$^{phox+/+}$ on FF Diet.

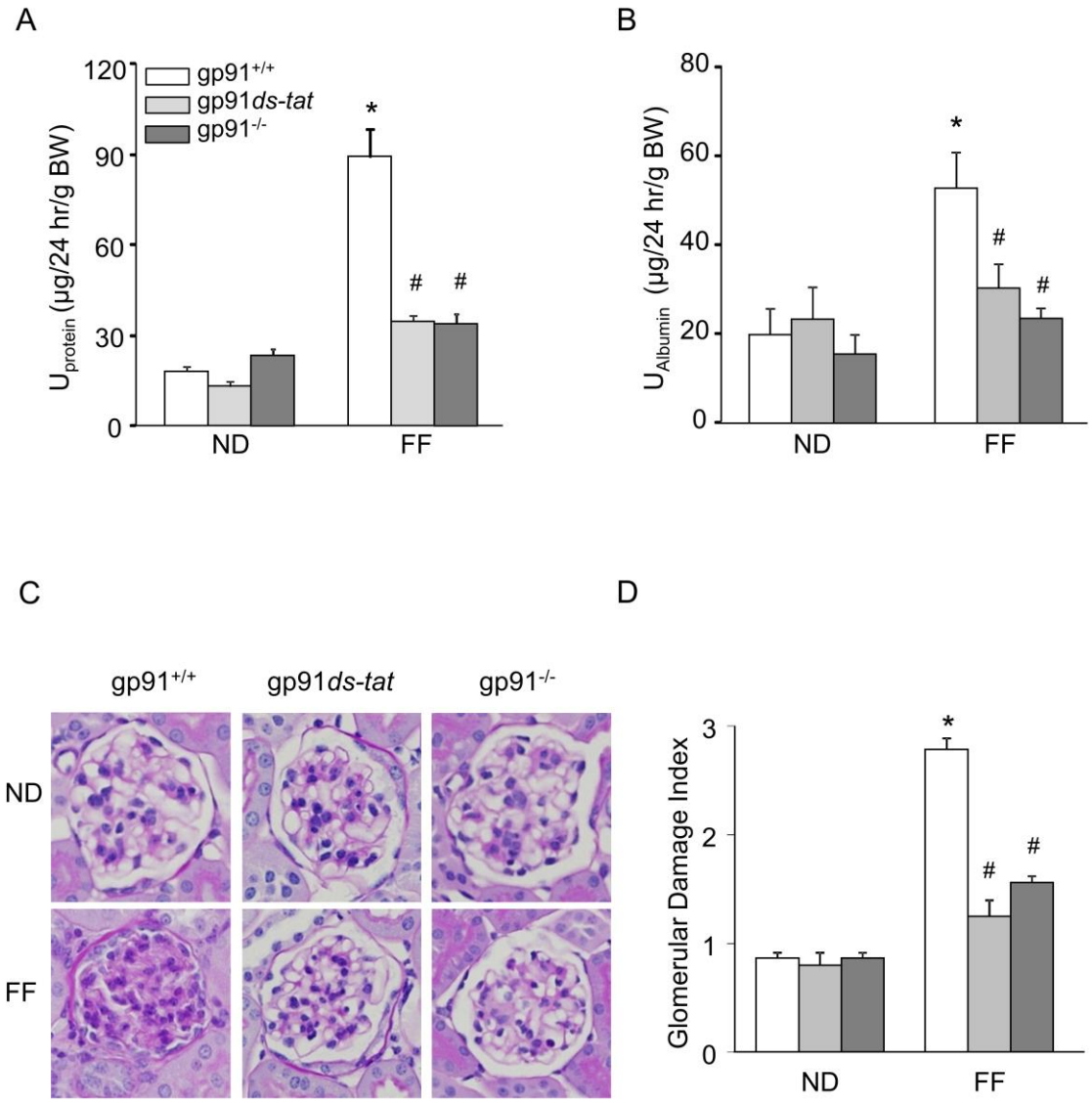


**Figure 12. Inhibition of NADPH oxidase expression and activity protected glomerular function from hHcys-induced injury.** A. Hyperhomocysteinemic gp91$^{phox+/+}$ mice produced proteinuria, which was alleviated in the gp91$^{phox-/-}$ or in the gp91*ds-tat*-treated mice (n=6). B. Hyperhomocysteinemic gp91$^{phox+/+}$ mice produced albuminuria, where blockade of NADPH oxidase in gp91$^{phox-/-}$ mice or in gp91*ds-tat*-treated mice prevented this glomerular damage (n=6). C. Glomerular morphological examination by PAS staining demonstrated that gp91*ds-tat* administration or gp91$^{phox-/-}$ mice prevented capillary collapse, fibrosis, cellular proliferation and expansion induced by hHcys (n=4-6). D. Glomerular damage index (GDI) was assessed by a standard semiquantitative analysis to determine severity of glomerular sclerosis. * $P$<0.05 vs. gp91$^{phox+/+}$ on Normal Diet; # $P$<0.05 vs. gp91$^{phox+/+}$ on FF Diet.

### 3.3 Summary

In summary, these studies demonstrated that at the very early stages of glomerular damage, Hcys *in vitro* or hHcys *in vivo* stimulated the formation and activation of the NLRP3 inflammasome, which initiated early injurious events in podocytes and glomeruli, leading to more serious glomerular injury and ultimate sclerosis. This NLRP3 inflammasome activation, podocyte injury, and the glomerular pathology induced by hHcys could be substantially suppressed by inhibition of NADPH oxidase. These results may establish a new concept that NADPH oxidase-derived ROS upon Hcys stimulation trigger the formation and activation of NLRP3 inflammasomes and thereby produce IL-1β and other factors, leading to podocyte and glomerular injury, potentially progressing into glomerular sclerosis.

# CHAPTER FOUR

## Contribution of endogenously produced reactive oxygen species to the activation of podocyte NLRP3 inflammasomes in hyperhomocysteinemia

### 4.1 Rationale and Hypothesis

Much evidence demonstrates that many inflammasome stimulators are also known to produce ROS, and the ROS model of inflammasome activation proposes NLRP3 to be a general sensor for changes in local and intracellular oxidative stress, allowing it to become activated in response to a diverse range of stimuli [126, 149, 181-182]. Although homocysteine (Hcys)-induced ROS production in podocytes has been documented, it remains unknown how this Hcys-induced ROS production is involved in the activation of NLRP3 inflammasomes in podocytes and ultimate glomerular injury. We have previously reported, and also shown above in Chapter 3, that inhibition of NADPH oxidase prevented Hcys-induced podocyte dysfunction, and more recently confirmed that inhibition of NADPH oxidase and the downstream production of $O_2^{\bullet-}$ abrogates NLRP3 inflammasome formation and activation [48, 169]. However, it is still poorly understood which species of ROS is responsible for NLRP3 inflammasome activation and how ROS lead to the formation or activation of this inflammasome. In this regard, recent studies have indicated that ROS may serve as important signaling messengers and that $O_2^{\bullet-}$ and hydrogen peroxide ($H_2O_2$) are common ROS that may act as second messengers to activate inflammasomes within podocytes. Hence, the present study, as depicted in **Figure 13**, sought to dissect the potential role of these endogenously produced ROS in Hcys-induced NLRP3 inflammasome activation and to determine which ROS are required for glomerular injury associated with such activation of NLRP3 inflammasomes.

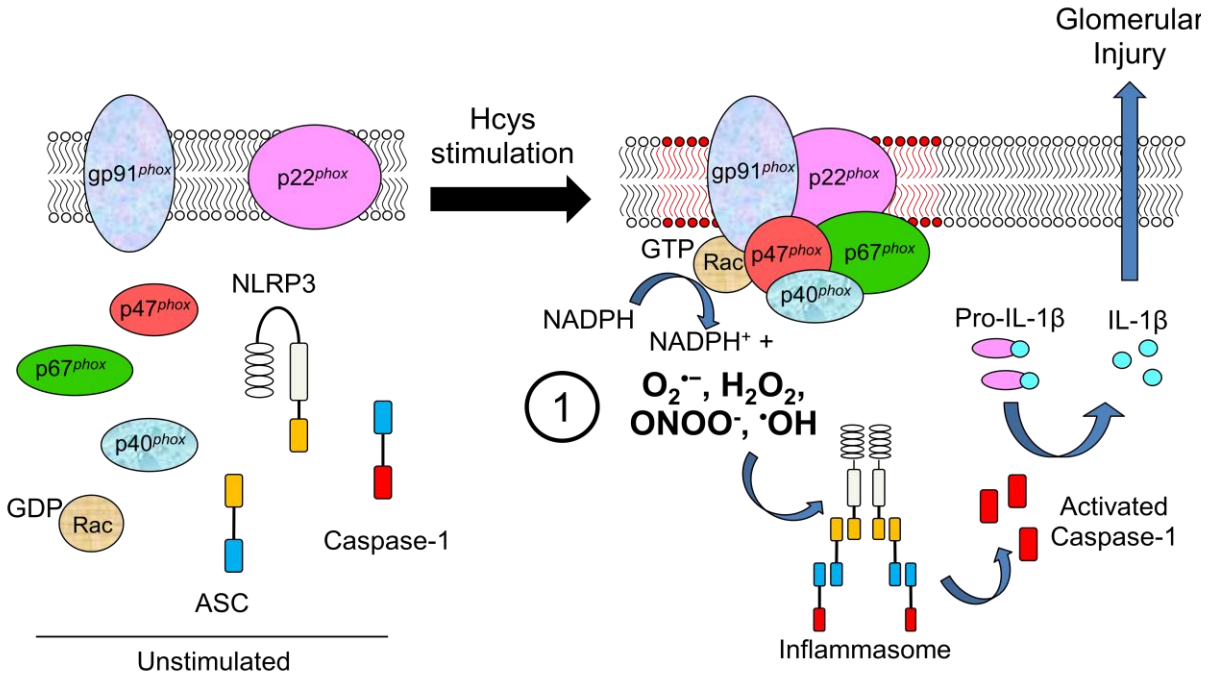


**Figure 13. Representative schematic for ROS dissection in Aim 1.** Deeper investigation in Aim 1 sought to understand which specific ROS are responsible for hHcys-induced NLRP3 inflammasomes activation.

## 4.2 Results

### 4.2.1 Reduction of intracellular $O_2^{\bullet-}$ and $H_2O_2$ levels prevented Hcys-induced NLRP3 inflammasome formation in podocytes

Using the $O_2^{\bullet-}$ dismutase mimetic TEMPOL, the $H_2O_2$ destroying enzyme catalase, or the $^{\bullet}OH$ scavenger TMTU, we tested whether Hcys-induced inflammasome formation and activation can be altered. By confocal microscopy analysis, we demonstrated that Hcys induced colocalization (yellow spots) of inflammasome molecules (NLRP3 (green) vs. ASC or caspase-1 (red)) in podocytes compared to control cells, suggesting increased formation of NLRP3

inflammasomes (**Figure 14A**). However, prior treatment of podocytes with TEMPOL or catalase blocked Hcys-induced colocalization of NLRP3 with ASC or caspase-1. In contrast, TMTU did not block Hcys-induced inflammasome formation, suggesting that $O_2^{\bullet-}$ and $H_2O_2$, but not $^{\bullet}OH$, is involved in Hcys-induced inflammasome formation in podocytes. The colocalization coefficient analyses were summarized and shown in **Figure 14B**. These effects are thought to originate from ROS derived by specific Nox2, and not Nox1 or Nox4, activation (**Figure 15**). Furthermore, this Hcys-induced Nox2 mRNA upregulation was unaffected by $O_2^{\bullet-}$ scavenging, suggesting that the subsequent effects of scavenging these ROS are due to events occurring downstream of NADPH oxidase activation (**Figure 15**).

To further confirm inflammasome formation in response to elevated Hcys, size exclusion chromatography was employed and further provided evidence that TEMPOL or catalase treatment prevented Hcys-induced inflammasome formation, as shown by the inhibited shift of ASC proteins into higher-molecular weight fractions (**Figure 16B**). These fractions are compared to a standard protein size marker in **Figure 16A**, a representative chromatogram where proteins that are part of the inflammasome complex elute within fractions 3-7 and are analyzed by SDS-PAGE. The intensity of bands were quantified and summarized in **Figure 16C**, showing that scavenging of $O_2^{\bullet-}$ and $H_2O_2$, but not $^{\bullet}OH$, was able to inhibit inflammasome formation in podocytes treated with Hcys.

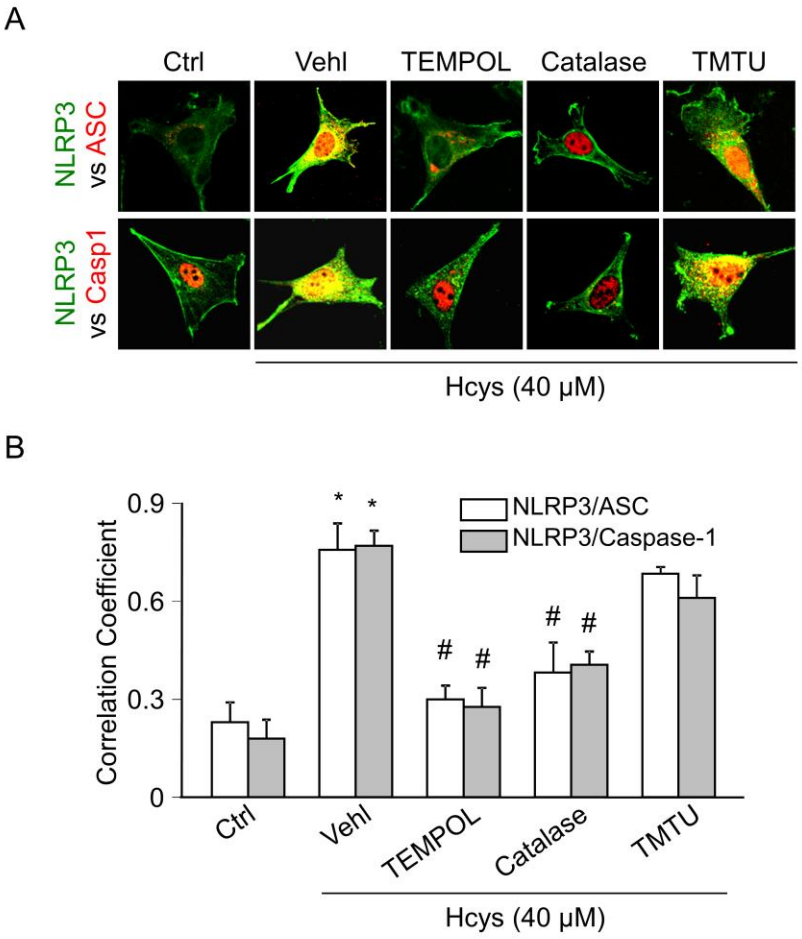


**Figure 14. TEMPOL and catalase attenuated Hcys-induced inflammasome formation in podocytes.** A. Confocal images representing the colocalization of NLRP3 (green) with ASC or caspase-1 (red) in cultured podocytes. B. Summarized data showing the fold change of PCC for the colocalization of NLRP3 with ASC and NLRP3 with caspase-1 (n=4). Ctrl: Control; Vehl: Vehicle; TMTU: tetramethylthiourea, PCC: Pearson coefficient correlation. * $P<0.05$ vs. Control; # $P<0.05$ vs. Hcys.

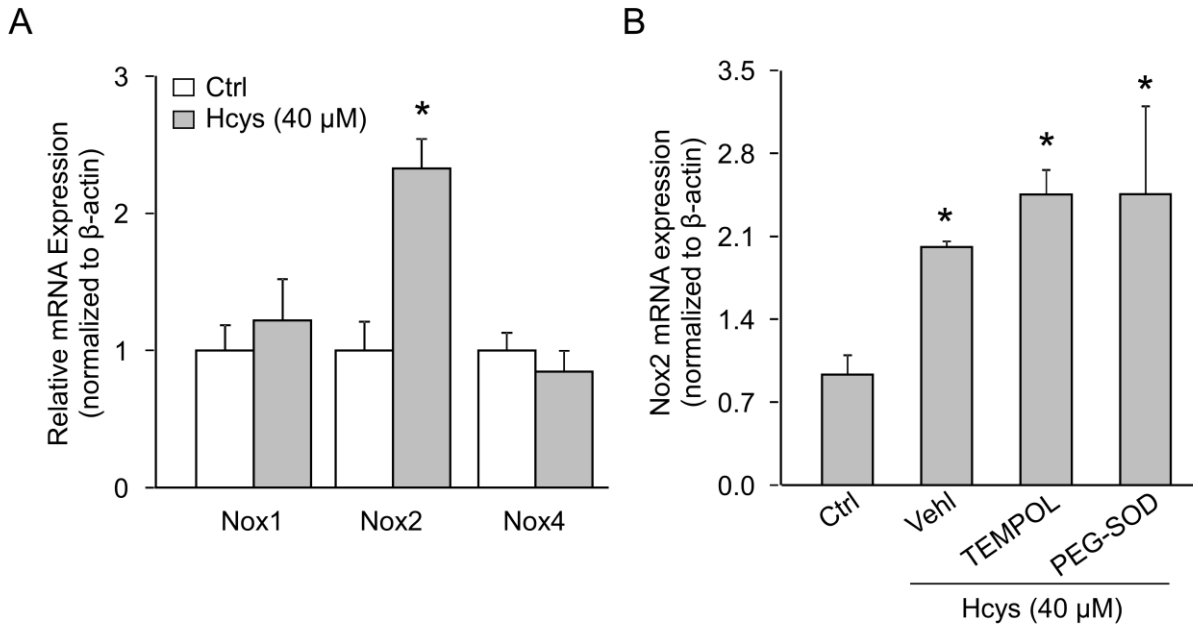


**Figure 15. Hcys specifically induced Nox2 mRNA expression.** A. As detected by real-time RT-PCR, 24 hr treatment of podocytes with 40 μM Hcys caused significant upregulation of Nox2, but not Nox1 or Nox4 (n=3). B. Scavenging of $O_2^{\bullet-}$ by TEMPOL and PEG-SOD had no effect on Hcys-induced Nox2 mRNA upregulation (n=3). * $P$<0.05 vs. Ctrl.

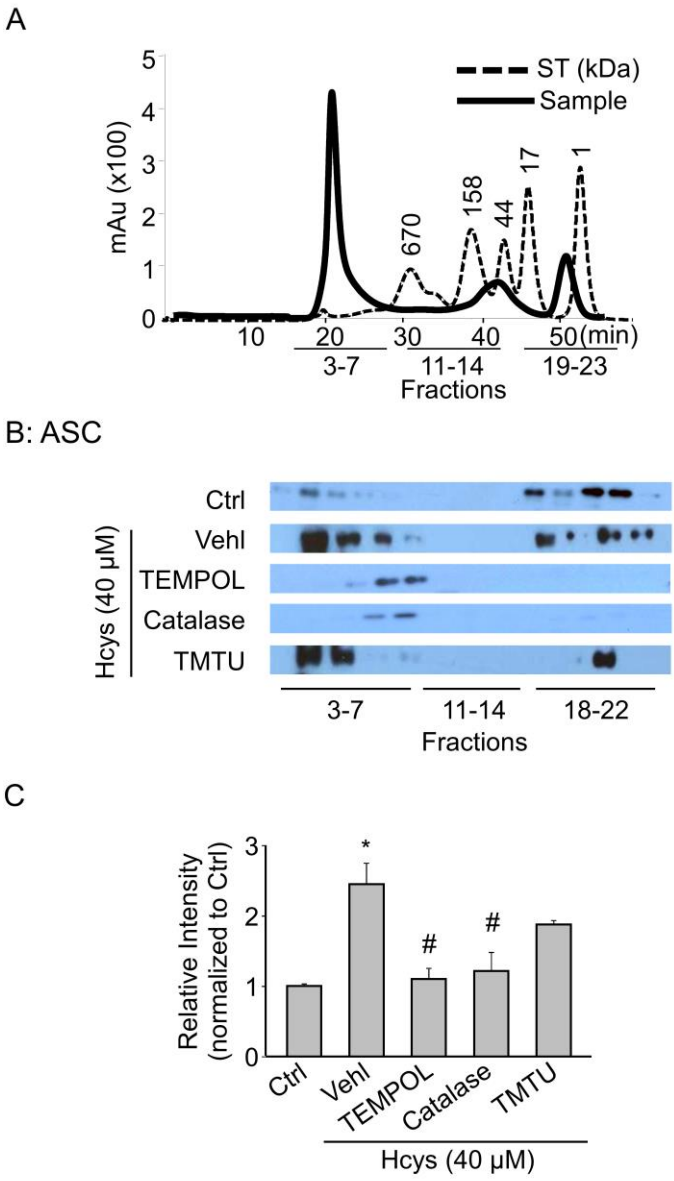


**Figure 16. Size-exclusion chromatography demonstrated inhibition of Hcys-induced ASC protein redistribution after $O_2^{\bullet-}$ and $H_2O_2$ scavenging.** A. Representative chromatogram illustrating the elution profile of proteins from both a standard and podocyte sample taken from an absorbance of 280 nm. Elution of a gel filtration standard allowed for the determination of the molecular mass of the samples. B. Western blot was performed on selected FPLC protein fractions and probed with an anti-ASC antibody. C. Summarized data determined from the ASC band intensities of the inflammasome complex fractions (3-7) (n=4-6). Ctrl: Control; Vehl: Vehicle; TMTU: tetramethylthiourea. * $P$<0.05 vs. Control; # $P$<0.05 vs. Hcys.

### 4.2.2 TEMPOL and catalase, but not TMTU or ebselen, blocked activation of NLRP3 inflammasomes in podocytes

Aside from measures of NLRP3 inflammasome formation, previous studies have indicated that caspase-1 activation and IL-1β production reflect the activation of NLRP3 inflammasomes [169, 183]. In the present study, we tested whether TEMPOL and catalase abolish Hcys-induced NLRP3 inflammasome activation. As shown in **Figures 17A and 17B**, Hcys treatment significantly increased caspase-1 activity and IL-1β production compared to control cells. However, pretreatment of podocytes with either TEMPOL or catalase significantly attenuated Hcys-induced increases in caspase-1 activity and IL-1β secretion, indicating that $O_2^{\bullet-}$ and $H_2O_2$ are necessary for the functionality of inflammasomes in response to Hcys. In addition, we also tested the role of another SOD mimetic MnTMPyP as well as cell permeable PEG-SOD in podocytes with or without Hcys stimulation. We found that pretreatment with either MnTMPyP or PEG-SOD significantly attenuated the Hcys-induced caspase-1 activity and IL-1β production (**Figures 17C and 17D**). We demonstrated that scavenging of $^{\bullet}OH$ by TMTU or $ONOO^-$ by ebselen did not have effects on Hcys-induced NLRP3 inflammasome formation and activation in podocytes. In the following *in vivo* studies, therefore, six groups of experiments are presented that include mice on the normal or FF diet with or without TEMPOL and catalase.

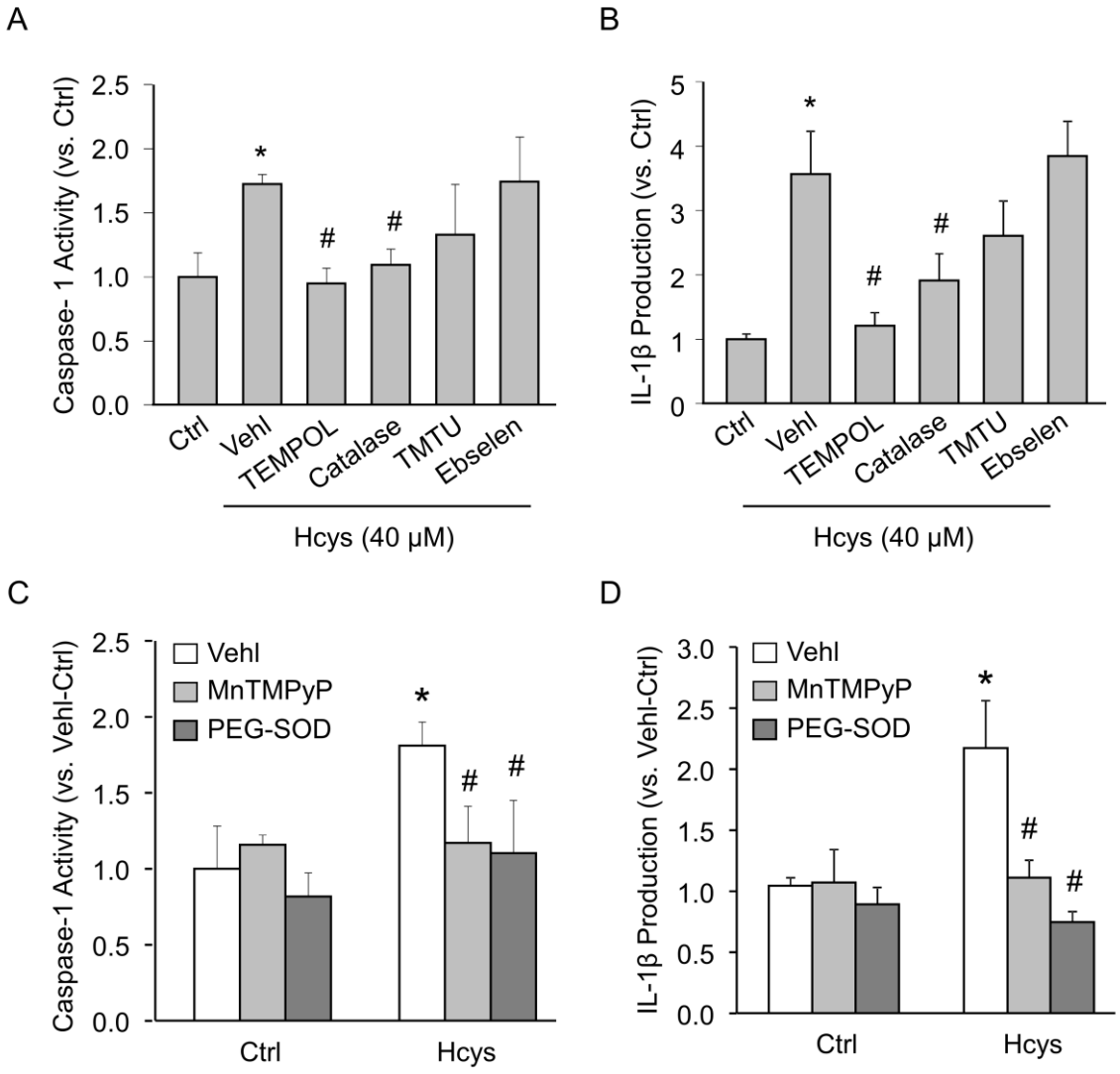


**Figure 17. Effects of ROS scavenging on caspase-1 activity and IL-1β secretion in the presence of Hcys.** A. Caspase-1 activity, shown as folds versus Ctrl, measured in podocytes treated with Hcys in the presence of various ROS scavengers (n=6-8). B. IL-1β production measured in the supernatant of podocytes treated with Hcys in the presence of various ROS scavengers (n=6-8). C. Inhibition of $O_2^{\bullet -}$ by MnTMPyP and PEG-SOD significantly inhibited Hcys-induced caspase-1 activation (n=3-4). D. Treatment of podocytes with either MnTMPyP or PEG-SOD prevented Hcys-induced maturation of IL-1β (n=4-5).Ctrl: Control; Vehl: Vehicle; TMTU: tetramethylthiourea. * $P$<0.05 vs. Control; # $P$<0.05 vs. Hcys.

### 4.2.3 Inhibition of NLRP3 inflammasome formation and activation in the glomeruli of hyperhomocysteinemic mice by TEMPOL and catalase

To further determine whether $O_2^{\bullet-}$ and $H_2O_2$ are implicated in inflammasome formation and activation *in vivo*, C57BL/6J wild type mice were treated with TEMPOL or catalase and fed a normal diet (ND) or FF diet for 4 weeks. HPLC analysis revealed that folate free (FF) diet treatment significantly increased the plasma total Hcys levels in uninephrectomized C57BL/6J mice compared with ND fed mice. Neither uninephrectomy nor the treatment of TEMPOL or catalase altered the Hcys levels on either diet, indicating that any observed effects were not due to a reduction in plasma Hcys (**Figure 18**). As shown in **Figure 19**, the glomeruli of mice maintained on the FF diet had increased colocalization of NLRP3 with ASC or NLRP3 with caspase-1 compared to ND fed mice, suggesting the enhanced formation of NLRP3 inflammasomes in glomeruli of hHcys mice. hHcys, known to cause podocyte injury, significantly decreased the amount of podocin staining in the glomeruli, thus resulting in minimal colocalization with inflammasome protein NLRP3 (**Figure 20**). However, the formation of hHcys-induced NLRP3 inflammasomes mainly occurred in podocytes within glomeruli, evidenced by the increased colocalization of NLRP3 with podocyte damage marker desmin (**Figure 20**). This colocalization of NLRP3 was not evident with either VE-cadherin or α-SMA, respective markers of glomerular endothelial and mesangial cells (data not shown). hHcys also resulted in podocyte injury, demonstrated by the increase in protein expression of podocyte damage marker desmin. Correspondingly, caspase-1 activity and IL-1β production were significantly enhanced in hHcys mice compared to normal diet fed mice, further confirming NLRP3 inflammasome activation (**Figures 21A and 21B**). Concurrent with this inflammasome activation, SOD-sensitive $O_2^{\bullet-}$ production was 2.1 fold greater in mice fed the FF diet than those

on the ND (**Figure 21C**). All of these hHcys-induced effects on parameters of inflammasome formation and activation were abolished by administration of either SOD mimetic TEMPOL or $H_2O_2$ decomposer catalase. Taken together, these data suggest that both $O_2^{\bullet-}$ and $H_2O_2$ play a pivotal role in hHcys-induced NLRP3 inflammasome formation and activation in glomeruli of hHcys mice.

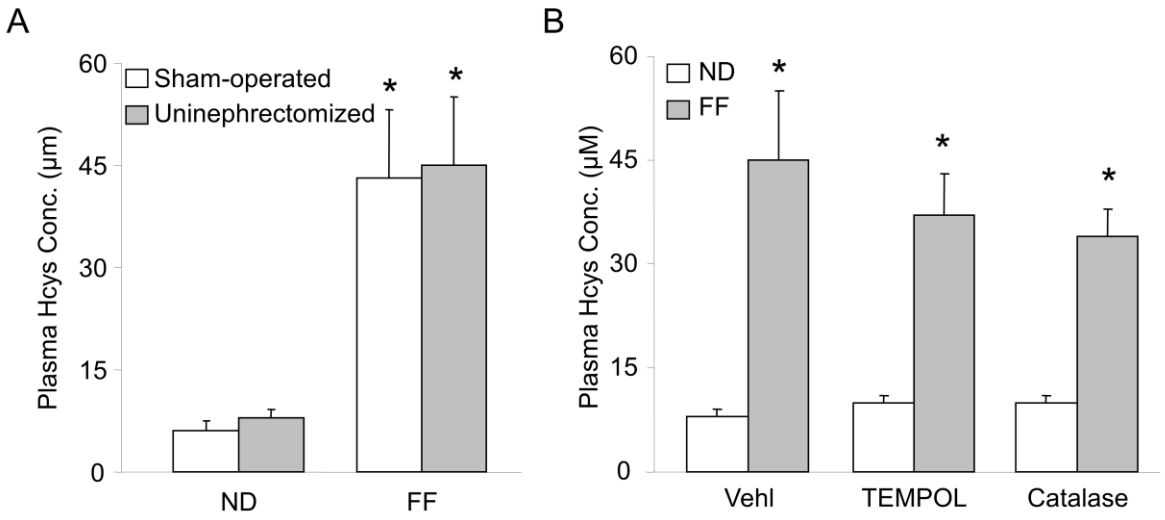


**Figure 18. Effects of uninephrectomy or *in vivo* TEMPOL and catalase administration on FF diet-induced plasma Hcys levels.** A. Measured by HPLC, uninephrectomy had no effect on plasma Hcys levels in mice receiving either ND or FF diet (n=4-6). B. Mice maintained on the FF diet for 4 weeks displayed significantly elevated plasma Hcys concentrations compared to those on the ND. TEMPOL and catalase did not alter these levels either in the normal or FF diet mice (n=4-6). * $P$<0.05 vs. ND.

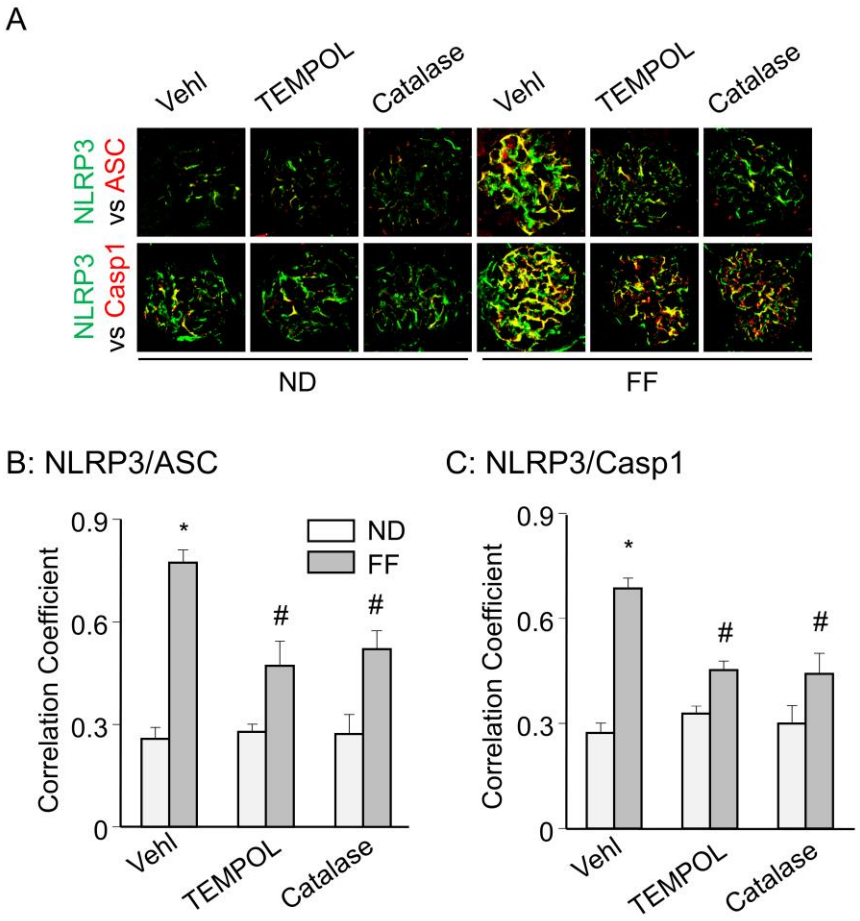


**Figure 19. *In vivo* effect of $O_2^{\bullet-}$ and $H_2O_2$ inhibition on hHcys-induced inflammasome formation in glomeruli of hyperhomocysteinemic mice.** A. Colocalization of NLRP3 (green) with ASC or caspase-1 (red) in the mouse glomeruli of vehicle, TEMPOL, or catalase-treated mice fed a normal or FF diet. B-C. Summarized data showing the correlation coefficient between NLRP3 with ASC or caspase-1 (n=6). Casp1: caspase-1, Vehl: Vehicle, ND: Normal diet, FF: Folate-free diet. **P*<0.05 vs. Vehl on ND; # *P*<0.05 vs. Vehl on FF Diet.

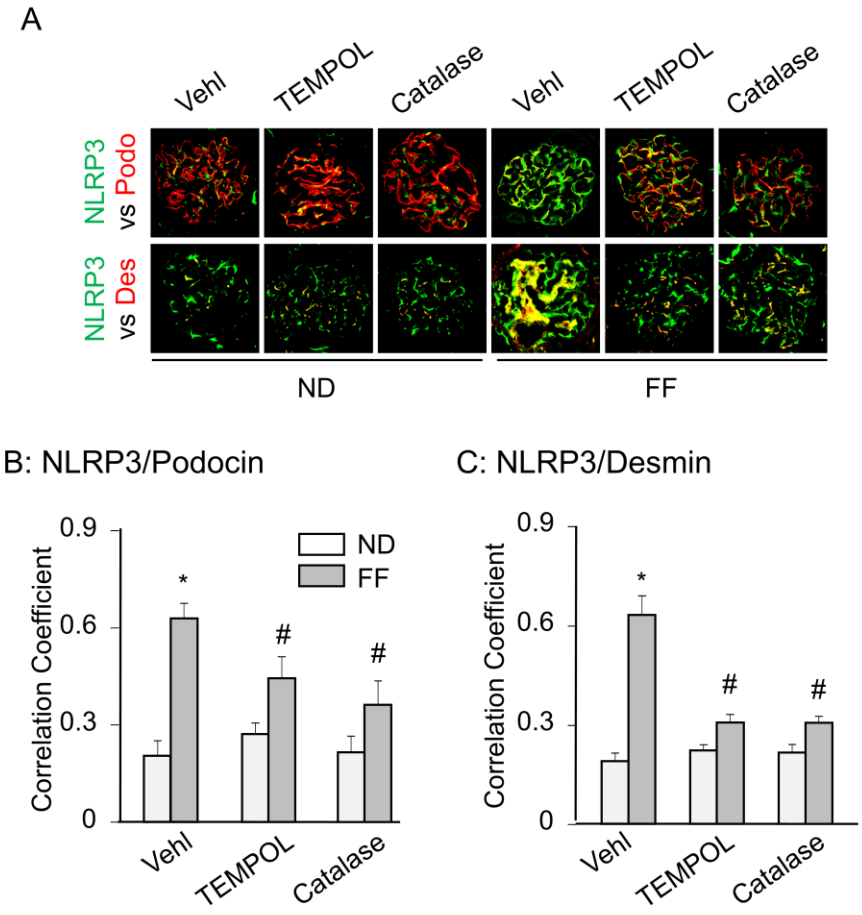


**Figure 20. hHcys-induced inflammasome formation occurred primarily in podocytes of hyperhomocysteinemic mice.** A. Colocalization of NLRP3 (green) with podocyte markers podocin or desmin (red) in the mouse glomeruli of vehicle, TEMPOL, or catalase-treated mice fed a normal or FF diet. B-C. Summarized data showing the correlation coefficient between NLRP3 with podocin or desmin (n=6). Podo: Podocin; Des: Desmin, Vehl: Vehicle, ND: Normal diet, FF: Folate-free diet. **P*<0.05 vs. Vehl on ND; # *P*<0.05 vs. Vehl on FF Diet.

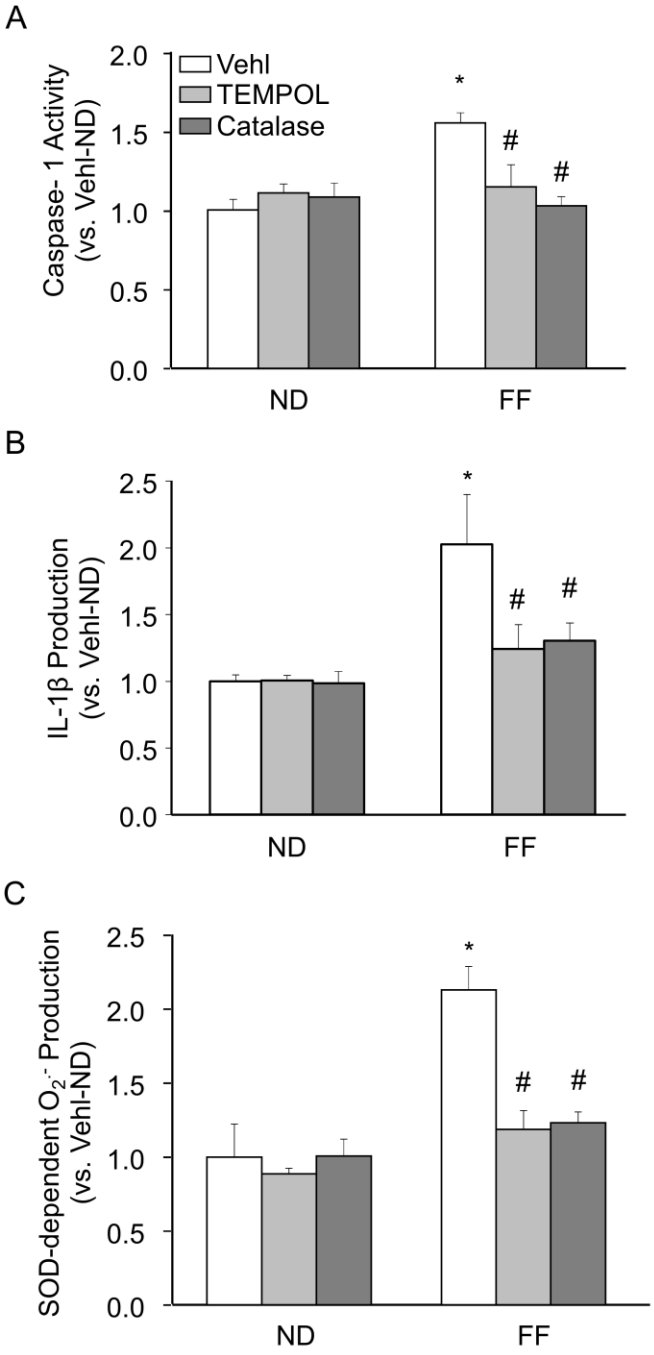


**Figure 21. *In vivo* administration of TEMPOL and catalase prevented caspase-1 activation, IL-1β production, and $O_2^{\bullet-}$ production.** A. Caspase-1 activity in Vehl, TEMPOL, or catalase-treated mice with hHcys induced by the FF diet (n=7). B. TEMPOL and catalase administration prevented hHcys-induced IL-1β production (n=6-7). C. $O_2^{\bullet-}$ production induced by hHcys was inhibited in mice treated with TEMPOL or catalase (n=6). Vehl: Vehicle, ND: Normal diet, FF: Folate-free diet. *$P$<0.05 vs. Vehl on ND; # $P$<0.05 vs. Vehl on FF Diet.

### 4.2.4 *In vivo* TEMPOL and catalase administration protected mouse glomeruli from hHcys-induced dysfunction and injury

As shown in **Figure 22**, FF diet-induced hHcys resulted in significantly elevated urinary protein excretion as well as marked pathological changes in glomerular morphology, compared to mice on the ND. However, hHcys-induced proteinuria and glomerular injury were not evident in hyperhomocysteinemic mice treated with TEMPOL or catalase. Dismutation of $O_2^{\bullet -}$ and decomposition of $H_2O_2$ was able to prevent hHcys-induced renal dysfunction and glomerular damage, signifying the importance of $O_2^{\bullet -}$ and $H_2O_2$ in the mechanism of hHcys-induced injury.

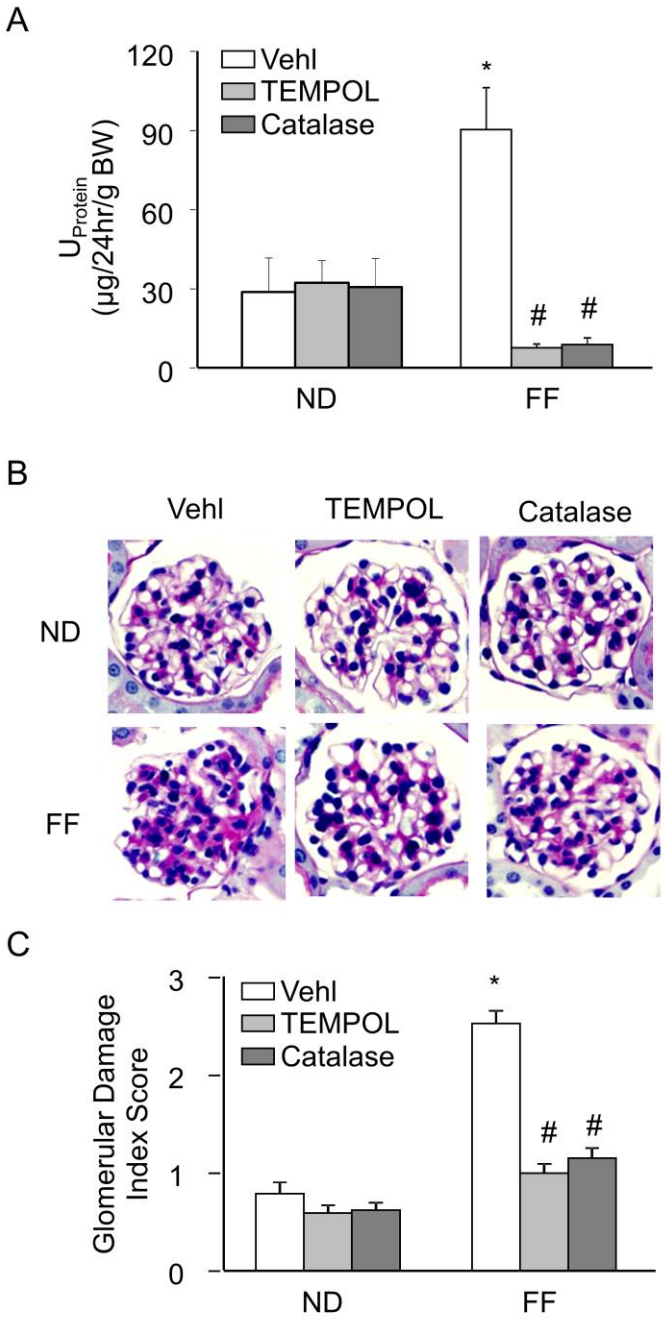


**Figure 22. Renal protective effects of $O_2^{\bullet-}$ and $H_2O_2$ inhibition on hHcys-induced glomerular injury.** A. hHcys-induced proteinuria was attenuated in mice receiving TEMPOL or catalase treatment (n=6). B. Microscopic observation of glomeruli in PAS stained kidney sections demonstrated TEMPOL and catalase prevented hHcys-induced changes in glomerular morphological structure by preventing capillary collapse, fibrosis, cellular proliferation and mesangial cell expansion (n=4-6). C. Extent of glomerular sclerosis was assessed semiquantitatively and expressed as the Glomerular damage index (GDI). Vehl: Vehicle, ND: Normal diet, FF: Folate-free diet. *$P$<0.05 vs. Vehl on ND; # $P$<0.05 vs. Vehl on FF Diet.

## 4.3 Summary

In summary, this series of studies demonstrated that reducing $O_2^{\bullet-}$ and $H_2O_2$ inhibited NLRP3 inflammasome formation and consequent processing of IL-1β, suggesting that both species are importantly implicated in the instigation of Hcys-induced NLRP3 inflammasome activation in cultured podocytes. Similar effects were seen *in vivo* in glomerular podocytes of hyperhomocysteinemic mice, where dismutation of $O_2^{\bullet-}$ by TEMPOL and decomposition of $H_2O_2$ by catalase not only prevented glomerular NLRP3 inflammasome formation and activation, but also importantly protected against hHcys-induced glomerular injury and dysfunction. Together, these results indicate that $O_2^{\bullet-}$ and $H_2O_2$ contribute to inflammasome triggering and consequent podocyte injury, ultimately leading to the potential progression toward glomerular sclerosis and ESRD during hHcys.

# CHAPTER FIVE

# NLRP3 inflammasome activation and podocyte injury via thioredoxin-interacting protein during hyperhomocysteinemia

## 5.1 Rationale and Hypothesis

Thus far, this hHcys-induced NLRP3 inflammasome activating process was shown to depend on NADPH oxidase and the reactive oxygen species (ROS) derived from its activation, specifically $O_2^{\bullet-}$ and $H_2O_2$, where inhibition of the $gp91^{phox}$ subunit of NADPH oxidase or scavenging of $O_2^{\bullet-}$ and $H_2O_2$ suppressed NLRP3 inflammasome activation and furthermore ameliorated subsequent glomerular dysfunction [169-170]. However, the exact mechanism of how the NADPH oxidase-derived ROS are sensed by podocytes to form and activate the NLRP3 inflammasome and thereby lead to its activation in glomerular podocytes is still largely unknown. In this regard, the work done by Zhou et al provided strong evidence of thioredoxin-interacting protein (TXNIP) as a binding partner to NLRP3, where association between these two proteins was necessary for downstream inflammasome activation [126]. TXNIP, the negative regulator of the antioxidant thioredoxin (TRX), may time-dependently dissociate from TRX to bind with NLRP3 leading to inflammasome formation and activation. In this series of studies, we attempted to investigate the role of TXNIP during hHcys and to explore its potential effects on NLRP3 inflammasome activation and consequent podocyte injury and glomerular sclerosis (**Figure 23**). We first characterized the feature of TXNIP binding to NLRP3 and its related role in the formation and activation of NLRP3 inflammasomes using cultured podocytes. Then, we determined the pathological role of TXNIP-mediated activation of NLRP3 inflammasomes in mice with hHcys. These studies together elucidate the key role of TXNIP in bridging redox

signals with activation of NLRP3 inflammasomes leading to podocyte injury and ultimate glomerular sclerosis.

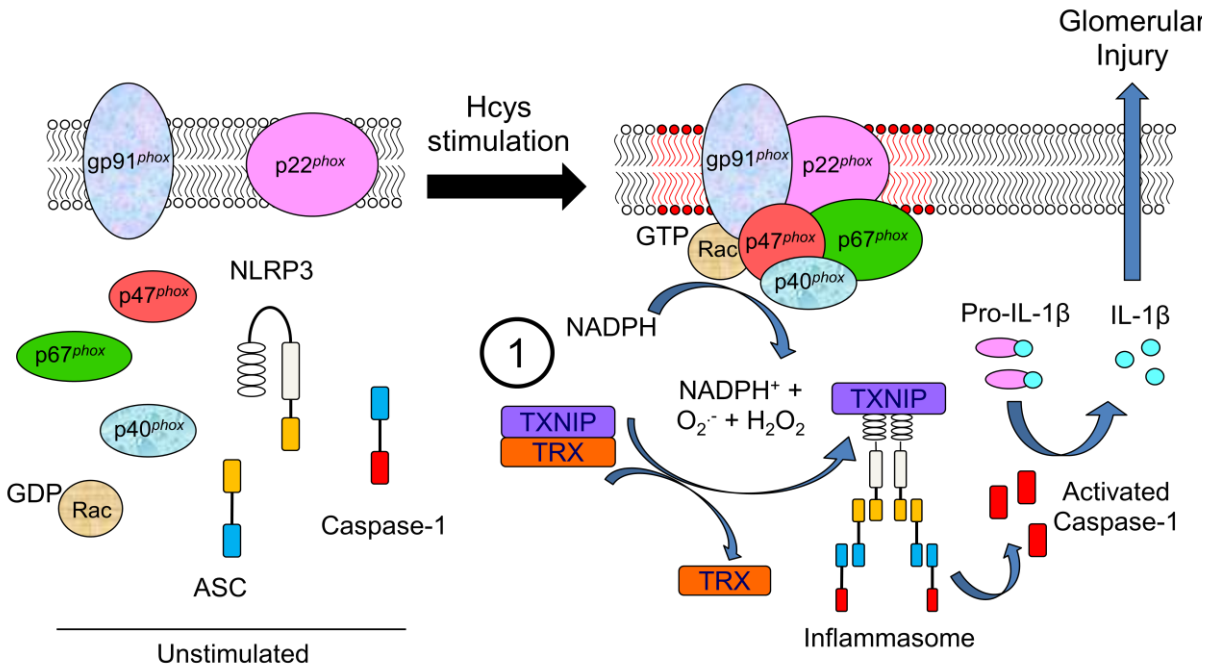


**Figure 23. Diagram showing the potential TXNIP involvement in Aim 1.** Further studies in Aim 1 will elucidate the potential role of TXNIP-NLRP3 binding in this mechanism of hHcys-induced NLRP3 inflammasome activation and subsequent glomerular injury.

## 5.2 Results

### 5.2.1 TXNIP inhibition prevented TXNIP protein recruitment to NLRP3 inflammasome fractions

In the chromatogram illustrating a typical standard and sample elution profile, the elution of inflammasome proteins in earlier fractions signifies the aggregation of inflammasome proteins to higher molecular weight complexes and the formation of inflammasomes (**Figure 24A**). Demonstrated by SEC in previous studies, Hcys stimulation of podocytes resulted in increased NLRP3 inflammasome formation [49, 169]. The present study further validated this concept as shown by the increased expression of NLRP3 protein in fractions 4-7, termed the inflammasome fractions in Hcys-treated podocytes (**Figure 24B**). In these podocytes stimulated by Hcys, we observed increased expression of TXNIP as well as the recruitment of TXNIP to the inflammasome fractions, suggesting TXNIP aggregation to the NLRP3 inflammasome complex. To further elucidate the role of TXNIP, we pretreated Hcys-stimulated podocytes with siRNA or verapamil to inhibit its expression and found that inhibition of TXNIP not only prevented its own shift to the inflammasome fractions, but also blocked the formation of NLRP3 complex in podocytes in response to Hcys stimulations. The relative band intensities at fractions 4-7 were quantified and summarized in **Figure 24C**. These SEC results provided strong evidence for a possible role of TXNIP and its aggregation with the inflammasome complex in Hcys-induced NLRP3 inflammasome formation.

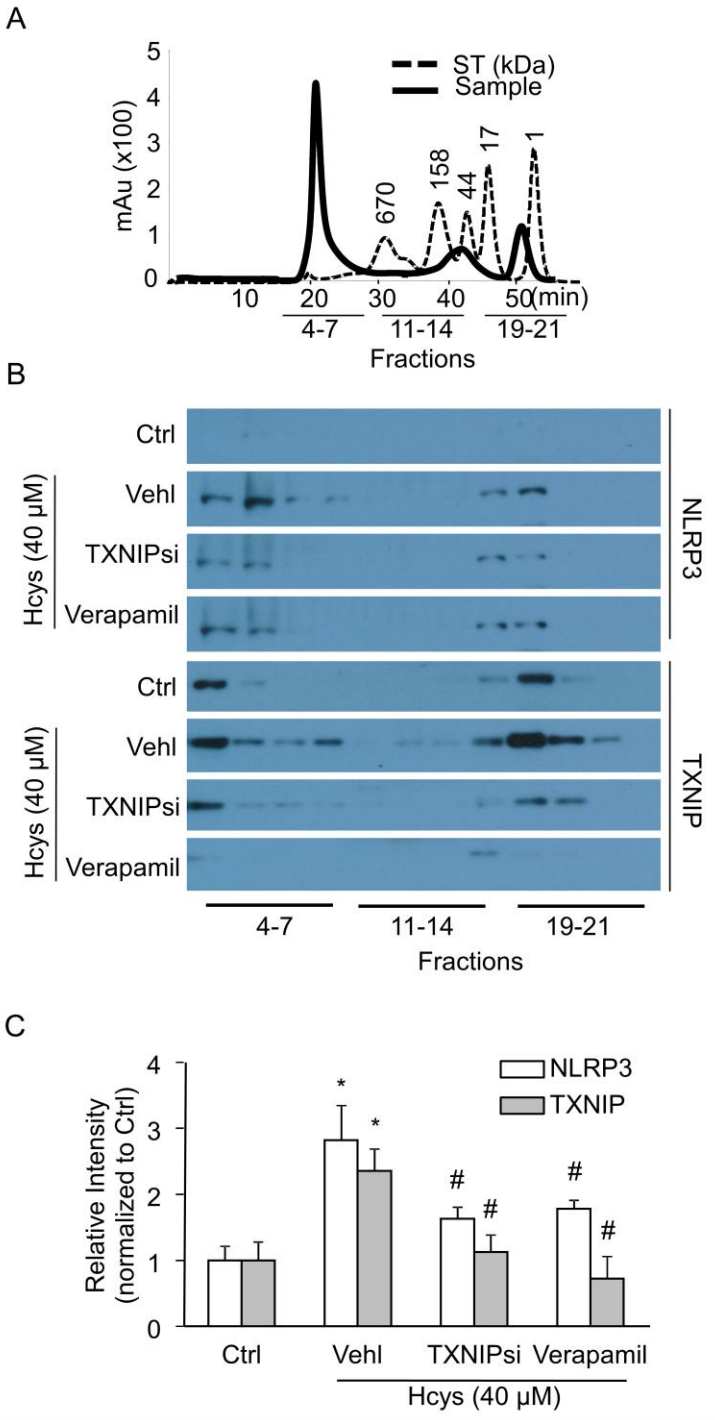


**Figure 24. TXNIP and NLRP3 recruitment to the high molecular weight inflammasome fractions upon stimulation with Hcys.** A. SEC chromatogram illustrating the elution curves of a typical standard and podocyte protein sample. B. Representative Western blot gel documents depicting the shift of NLRP3 and TXNIP protein during Hcys treatment, which was prevented during TXNIP inhibition. C. Summarized quantification of either NLRP3 or TXNIP protein residing in the inflammasome fractions (n=4). Ctrl: Control, Vehl: Vehicle, TXNIPsi: TXNIP siRNA. * $P<0.05$ *vs.* Ctrl, # $P<0.05$ *vs.* Hcys.

### 5.2.2 Inhibition of Hcys-induced TXNIP-NLRP3 binding and NLRP3 inflammasome formation upon TXNIP blockade

As an additional method for detection of NLRP3 inflammasome formation, confocal microscopy was used to observe the colocalization of inflammasome proteins in podocytes. Shown in **Figure 25A**, Hcys increased the colocalization of NLRP3 (green) and ASC (red) compared to control cells, suggesting the formation of NLRP3 inflammasomes in podocytes. Furthermore, Hcys stimulation also increased the colocalization of NLRP3 (green) with TXNIP (red), suggesting that Hcys induces the aggregation of TXNIP together with NLRP3. However, prior treatment with TXNIP siRNA or verapamil significantly attenuated the colocalization of NLRP3 with either ASC or TXNIP. This reveals that TXNIP expression and its binding to NLRP3 are necessary for NLRP3 inflammasome formation in Hcys-treated podocytes. The colocalization of NLRP3 with ASC and NLRP3 with TXNIP was quantified and summarized in **Figures 25B and 25C**.

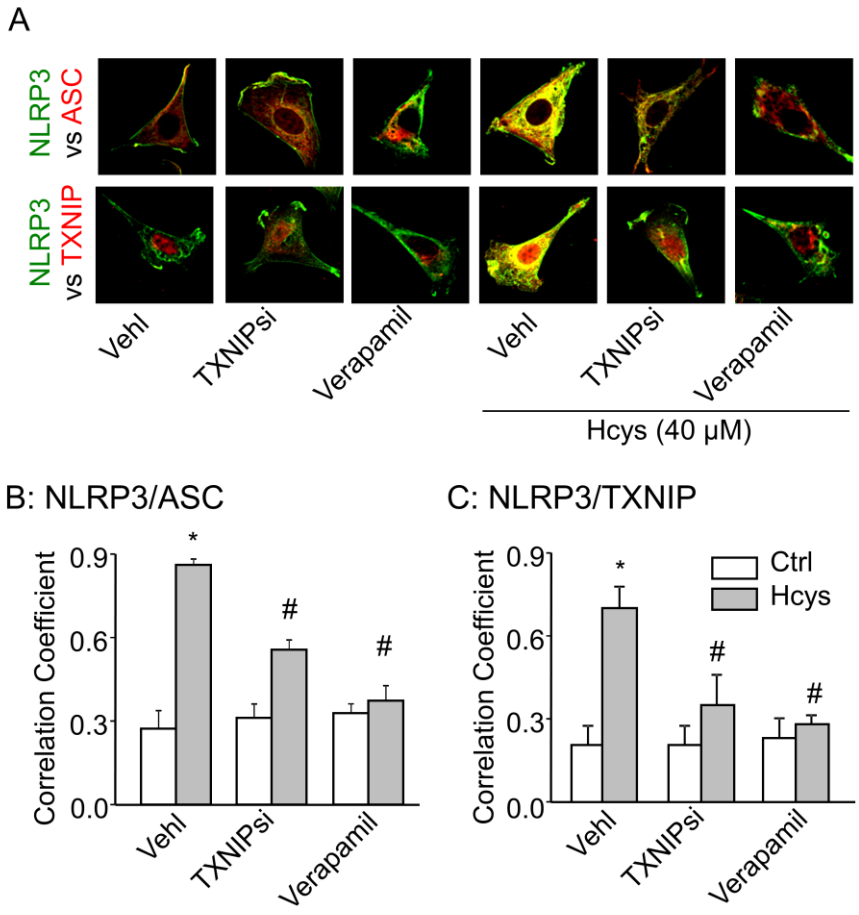


**Figure 25. TXNIP inhibition prevented Hcys-induced NLRP3 inflammasome formation.** A. Confocal microscopic detection of NLRP3 (green) with ASC (red) and NLRP3 (green) with TXNIP (red) and their colocalization together (yellow), indicative of the inflammasome formation. B-C. Summarized data showing the quantification of the extent of colocalization between NLRP3 with ASC and NLRP3 with TXNIP (n=4-6). Ctrl: Control, Vehl: Vehicle, TXNIPsi: TXNIP siRNA. * $P<0.05$ *vs.* Vehl-Ctrl, # $P<0.05$ *vs.* Vehl-Hcys.

### 5.2.3 Blocking TXNIP abrogated Hcys-induced increases in caspase-1 activity and IL-1β secretion

It is known that the formation of NLRP3 inflammasomes results in downstream caspase-1 activation and subsequent IL-1β maturation. These effects reflect the functionality of the formed inflammasomes and thus were used to determine the effect of TXNIP inhibition on Hcys-induced inflammasome activation in the current study. Hcys treatment significantly increased caspase-1 activity and IL-1β production in podocytes compared to control cells, suggesting activation of NLRP3 inflammasomes (**Figures 26A and 26B**). Both TXNIP siRNA transfection and pretreatment with verapamil significantly attenuated Hcys-induced caspase-1 activity and IL-1B production.

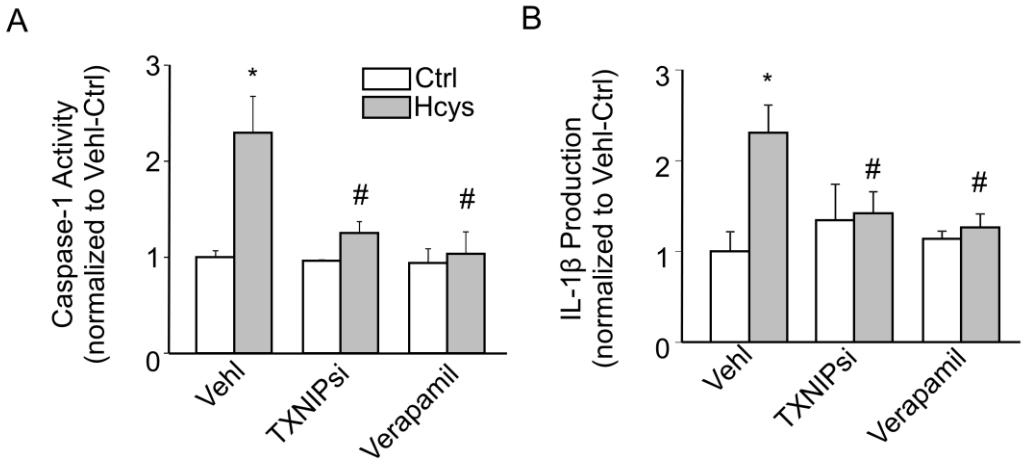


**Figure 26. Attenuation of Hcys-induced NLRP3 inflammasome activation by TXNIP blockade.** A. Effect of TXNIPsi and verapamil on Hcys-induced NLRP3 inflammasome activation, shown as the fold change of caspase-1 activation versus Vehl-Ctrl (n=7-8). B. Measured in the supernatant of cultured podocytes, TXNIP inhibition suppressed Hcys-induced IL-1β production (n=8). Ctrl: Control, Vehl: Vehicle, TXNIPsi: TXNIP siRNA. * $P<0.05$ *vs*. Vehl-Ctrl, # $P<0.05$ *vs*. Vehl-Hcys.

### 5.2.4 Protection from Hcys-induced podocyte damage by TXNIP inhibition

To assess the extent of podocyte damage, the protein expression of slit diaphragm molecules like podocin and desmin was monitored. Podocin, a podocyte-specific marker, decreases in expression during injury, while podocyte damage marker desmin increases during injury [184-185]. Immunofluorescence analysis demonstrated that Hcys-treated podocytes displayed a dramatic decrease in podocin staining and increase in desmin staining, signifying podocyte damage (**Figure 27A**). However, TXNIP inhibition resulted in the reversal of these podocyte damages as shown by restoration of podocin and desmin protein expression to control levels. Quantification of fluorescence was summarized in **Figure 27B**. Moreover, the ability of podocytes to secrete VEGF is considered to be an additional measure of podocyte functionality [186]. Hcys-injured podocytes displayed impaired secretion of VEGF, which was precluded in TXNIP siRNA or verapamil treated cells (**Figure 27C**). Together, these data suggest that TXNIP mediates Hcys-induced podocyte dysfunction and that inhibition of TXNIP ameliorates the deleterious effects of Hcys or inflammation activation on podocytes.

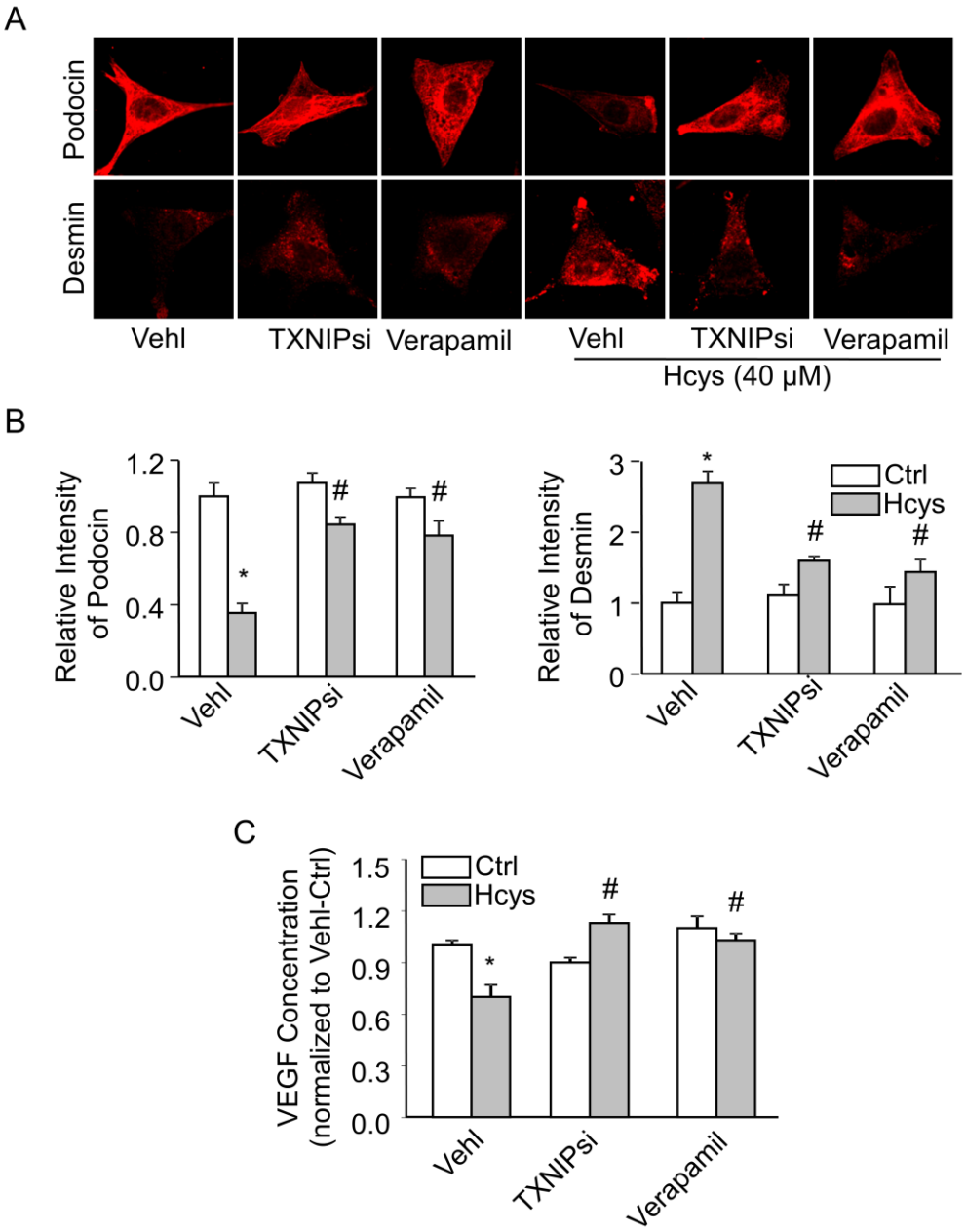


**Figure 27. Inhibition of TXNIP preserved podocyte integrity.** A. Immunofluorescence staining of podocyte-specific marker podocin and podocyte injury marker desmin, where Hcys-induced decrease in podocin and increase in desmin expression were attenuated by TXNIPsi and verapamil. B. Summarized data showing the relative intensity of podocin and desmin staining (n=6). C. VEGF was measured in the supernatant of podocytes and used as an indicator of podocyte functionality, where Hcys-damaged podocytes suppressed VEGF secretion, which was restored upon TXNIP inhibition (n=6). Ctrl: Control, Vehl: Vehicle, TXNIPsi: TXNIP siRNA. * $P<0.05$ *vs.* Vehl-Ctrl, # $P<0.05$ *vs.* Vehl-Hcys.

### 5.2.5 Local *in vivo* TXNIP shRNA transfection inhibited TXNIP mRNA and protein expression in mouse kidneys

To further determine the role of TXNIP in NLRP3 inflammasome activation and glomerular injury in mice, we transfected TXNIP shRNA into the kidney via the renal artery to locally silence the TXNIP gene. Our previous reports have demonstrated that introduction of plasmids locally into mouse kidneys by the ultrasound-microbubble technique displayed stable expression of transfected gene for at least 4 weeks [187]. In order to monitor plasmid transfection efficiency, a plasmid with a luciferase expression vector was cotransfected together with the targeting TXNIP shRNA plasmid to act as a reporter. **Figure 28A** represents *in vivo* imaging of gene expression in mouse kidneys monitored 3, 7, and 14 days post-transfection by an IVIS rodent animal imaging system. In a semidissected kidney 4 days after transfection, a strong luciferase signal was detected in the renal cortex, where the observed signal represents efficient transfection and gene expression (**Figure 28B**). It was demonstrated that efficient transfection of plasmids and gene expression were maintained throughout experiments and such *in vivo* imaging of gene expression was used to determine whether mice can continue for further functional studies. After transfected mice were maintained on either a normal or FF diet for 4 weeks, the TXNIP mRNA levels in the kidney were assessed by real time RT-PCR to validate the efficiency of plasmid transfection and gene expression. As shown in **Figure 28C**, TXNIP shRNA transfection significantly decreased TXNIP mRNA expression in mice on the ND when compared to those transfected only with luciferase plasmids. Although TXNIP mRNA expression increased in luciferase-transfected mice maintained on the FF diet, TXNIP shRNA-transfected mice exhibited substantially reduced TXNIP mRNA expression. These findings were translated to the protein level, demonstrated by immunofluorescent staining of TXNIP in the

glomeruli of transfected mice (**Figure 28D**). Together, we concluded that TXNIP shRNA is efficiently delivered locally to the mouse kidney and successfully being expressed, as evidenced by the markedly reduced TXNIP expression in glomeruli of mice.

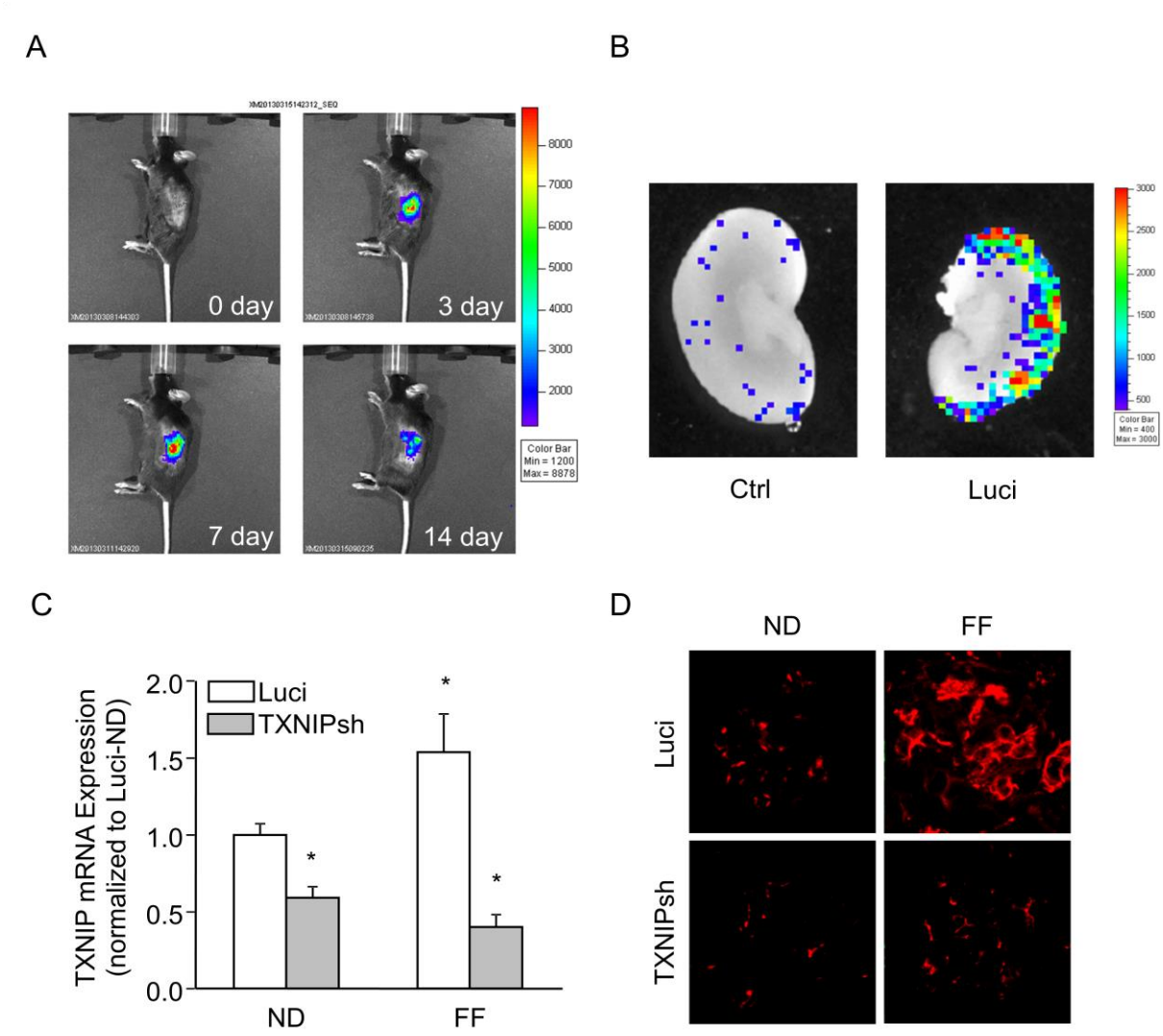


**Figure 28. Efficiency of local *in vivo* transfection of TXNIP shRNA into the renal cortex by the ultrasound-microbubble technique.** A. Images taken 3, 7, and 14 days post-transfection by an *in vivo* imaging system daily confirmed transfection efficiency. B. *Ex vivo* image 4 days after transfection of semidissected kidney demonstrated successful localized gene expression. C. Real time RT-PCR data quantifying mRNA silencing efficiency of the plasmid after 4 weeks of maintenance on either a ND or FF diet (n=6). D. Immunofluorescent staining of TXNIP in the glomeruli of transfected mice. ND: Normal diet, FF: Folate-free diet, Luci: Luciferase, TXNIPsh: TXNIP shRNA. * $P<0.05$ *vs.* Luci-ND.

### 5.2.6 Effect of *in vivo* TXNIP inhibition on hHcys-induced TXNIP-NLRP3 binding and NLRP3 inflammasome formation in glomeruli

After 4 weeks of uninephrectomized mice receiving the FF diet regiment, mice developed hHcys which resulted in NLRP3 inflammasome formation in their glomeruli, mainly in podocytes as shown in our previous studies [49, 170]. Illustrated in **Figure 29A**, confocal microscopic analysis demonstrated that FF diet-fed mice increased colocalization of NLRP3 with ASC (increased yellow staining) in glomeruli of luciferase transfected mice compared to ND fed mice, suggesting glomerular NLRP3 inflammasome formation during hHcys. This was further accompanied with an increase in TXNIP expression, which colocalized significantly with NLRP3, and possible binding to the NLRP3-ASC-caspase-1 inflammasome complex. However, TXNIP inhibition (either by verapamil or TXNIP shRNA transfection) substantially suppressed colocalization of NLRP3 with either ASC or TXNIP (**Figure 29A**). This colocalization was quantified and summarized in **Figure 29B and 29C**. Further exemplified by co-immunoprecipitation studies, hyperhomocysteinemic mice displayed robust amounts of TXNIP protein pulled down together with NLRP3 compared to ND fed mice, suggesting that NLRP3-TXNIP binding was enhanced during hHcys (**Figure 29D**). However, this enhanced NLRP3-TXNIP binding was not observed in glomeruli of TXNIP shRNA transfected or verapamil treated mice.

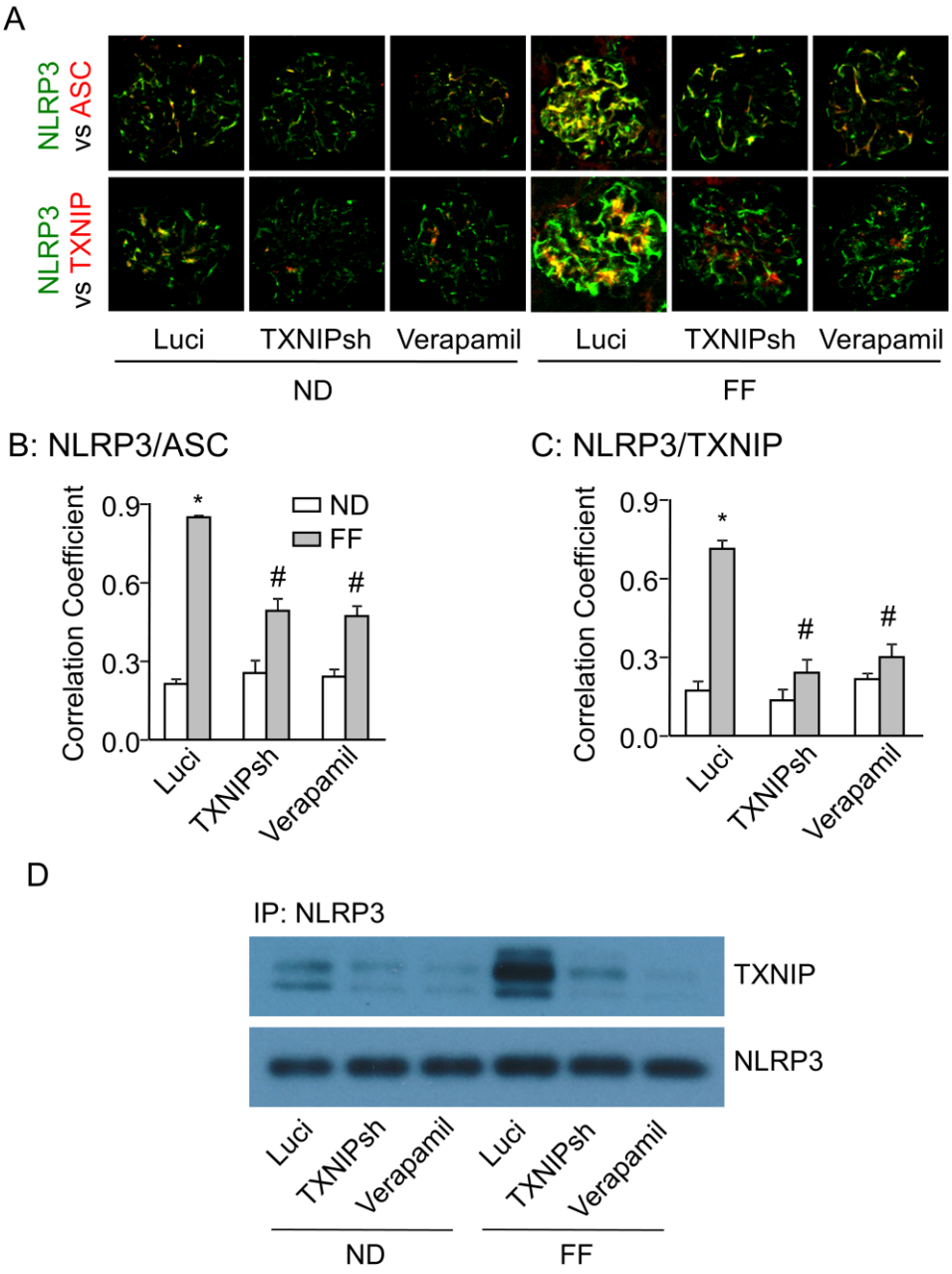


**Figure 29. *In vivo* inhibition of TXNIP and its effect on NLRP3 inflammasome formation.** A. Confocal microscopy demonstrated the colocalization between NLRP3 (green) with ASC (red) and NLRP3 (green) with TXNIP (red) in the glomeruli of Luci, TXNIPsh, and verapamil treated mice maintained on either a ND or FF diet. B-C. Summarized data showing the quantification of the extent of colocalization between NLRP3 with ASC and NLRP3 with TXNIP (n=6). D. Co-immunoprecipitation studies demonstrated robust *in vivo* TXNIP-NLRP3 binding in mice with hHcys, which was not evident after TXNIP inhibition (n=5). ND: Normal diet, FF: Folate-free diet, Luci: Luciferase, TXNIPsh: TXNIP shRNA. * $P<0.05$ *vs.* Luci-ND, # $P<0.05$ *vs.* Luci-FF.

### 5.2.7 TXNIP inhibition diminished renal caspase-1 activation and IL-1β secretion induced by hHcys

Caspase-1 activity and IL-1β production was measured to evaluate the effects of *in vivo* TXNIP inhibition on hHcys-induced NLRP3 inflammasome activation (**Figure 30A and 30B**). Mice with hHcys induced by the FF diet displayed increased caspase-1 activation and IL-1β production compared to those on the ND, suggesting increased NLRP3 inflammasome activity in the cortical tissue. This activation was not apparent in the mice where TXNIP was inhibited by either shRNA transfection or verapamil treatment.

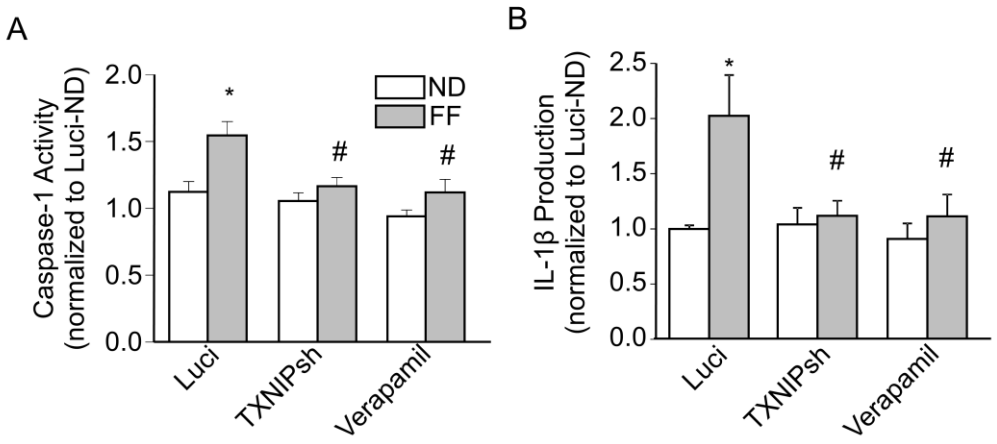


**Figure 30. *In vivo* TXNIP shRNA transfection and verapamil treatment blocked caspase-1 activation and IL-1β production.** A. Caspase-1 activity, shown as fold change versus Luci-ND, in Luci, TXNIPsh, and verapamil-treated mice with FF diet-induced hHcys (n=5-6). B. *In vivo* TXNIP inhibition prevented hHcys-induced IL-1β production (n=6). ND: Normal diet, FF: Folate-free diet, Luci: Luciferase, TXNIPsh: TXNIP shRNA. * $P<0.05$ *vs.* Luci-ND, # $P<0.05$ *vs.* Luci-FF.

### 5.2.8 Attenuation of hHcys-induced glomerular dysfunction by TXNIP inhibition

As shown above and documented by many of our previous studies, the hyperhomocysteinemic mouse model successfully induced significant glomerular dysfunction and ultimate sclerosis [48, 169, 179]. Demonstrated in **Figures 31A and 31B**, luciferase transfected mice on the FF diet also exhibited severe urinary protein and albumin excretion compared to control mice on the ND, suggesting glomerular injury or dysfunction. Furthermore, mice with hHcys displayed aberrant glomerular morphology, characterized by a shrunken phenotype with extracellular matrix and collagen deposition, capillary collapse, and mesangial cell expansion (**Figure 31C**). Decreased expression of podocyte specific marker, podocin and increase in podocyte damage marker, desmin, both hallmarks of podocyte injury, were also observed in the glomeruli of mice on the FF diet (**Figures 31E and 31F**). *In vivo* TXNIP inhibition by shRNA transfection or verapamil treatment was able to prevent all of the aforementioned destructive changes induced by hHcys as shown by the reduction of proteinuria, albuminuria, glomerular pathological changes, and restored expression of podocin and desmin. It should be noted that all of these observed effects occurred independently of changes to blood pressure, as there was no measurable difference in mean arterial pressure between all groups of mice (data not shown). These data provided solid evidence that TXNIP plays a detrimental role in hHcys-induced podocyte and glomerular damage, which is due to its ability to mediate NLRP3 inflammasome activation.

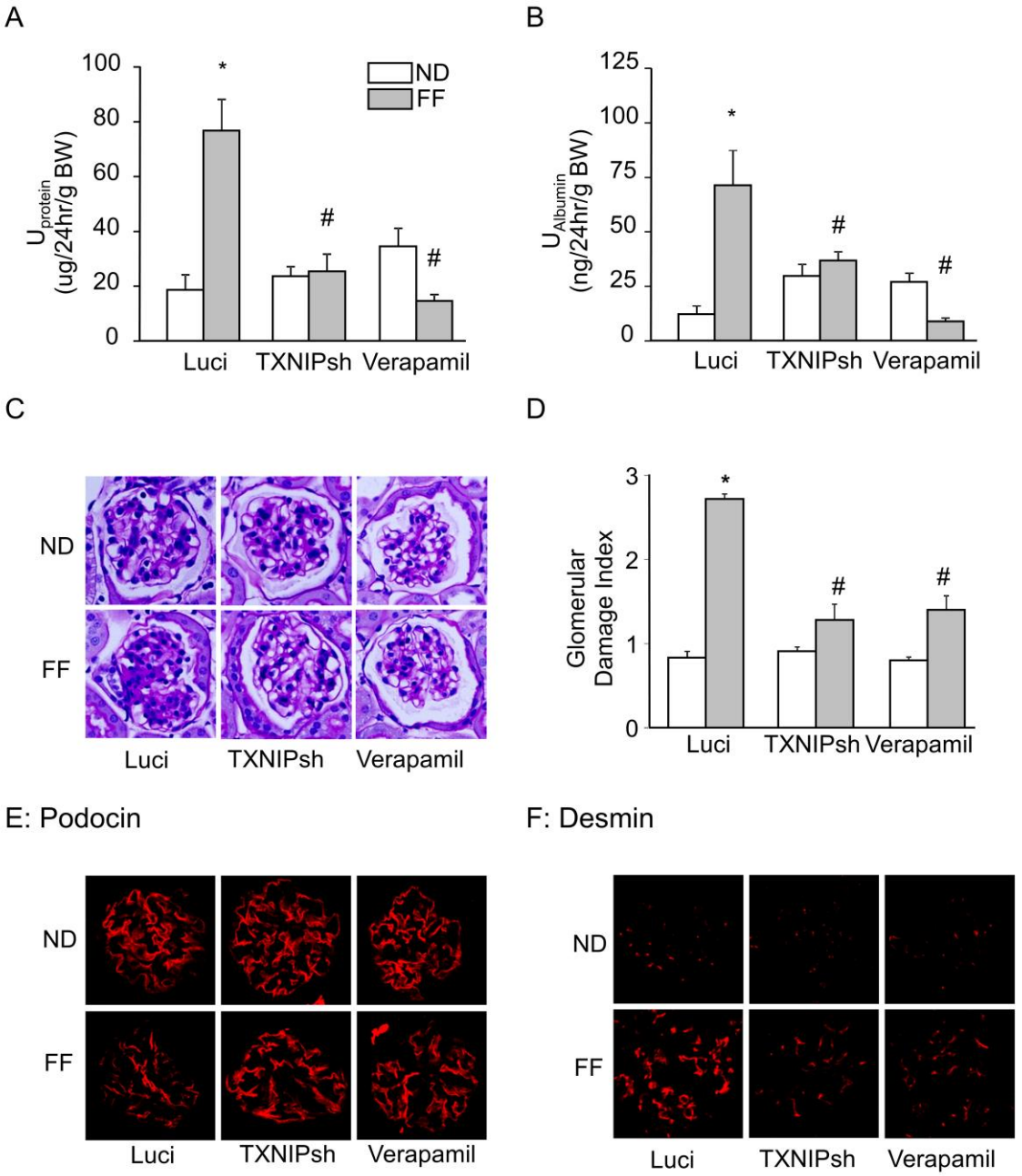


**Figure 31. Amelioration of hHcys-induced glomerular damage by *in vivo* TXNIP inhibition.** A-B. hHcys-induced increases in proteinuria and albuminuria were diminished by TXNIPsh transfection and verapamil administration (n=6-8). C. Observation of glomerular morphology in PAS stained slides revealed severe pathological changes in the glomeruli of Luci-FF mice, which were prevented in TXNIP inhibited mice. D. Pathological changes in the glomeruli were semiquantitatively scored and summarized as the glomerular damage index (GDI) (n=5). E-F. *In vivo* immunofluorescent staining of podocin and desmin to assess glomerular podocyte condition (n=6). ND: Normal diet, FF: Folate-free diet, Luci: Luciferase, TXNIPsh: TXNIP shRNA. * $P<0.05$ *vs*. Luci-ND, # $P<0.05$ *vs.* Luci-FF.

## 5.3 Summary

Taken together, we provided direct evidence that inhibition of TXNIP and diminished TXNIP-NLRP3 binding reduced NLRP3 inflammasome formation and activation, even in the continued presence of elevated Hcys or during hHcys in mice. This reduction in TXNIP–mediated inflammasome activation protected podocytes from the early deleterious effects of Hcys that, if left unattended, may ultimately progress to glomerular sclerosis and potential ESRD.

# CHAPTER SIX

## Contribution of guanine nucleotide exchange factor Vav2 to hyperhomocysteinemia-induced NLRP3 inflammasome activation

### 6.1 Rationale and Hypothesis

Our evidence thus far demonstrated that NADPH oxidase-derived reactive oxygen species (ROS) mediate the activation of podocyte NLRP3 inflammasomes in response to elevated levels of Hcys or *in vivo* during hHcys. Our laboratory has also previously provided evidence that the guanine nucleotide exchange factor Vav2 exhibits high specificity to Rac1-mediated NADPH oxidase activation by elevated Hcys [44]. Vav2 overexpression alone and its subsequent NADPH oxidase activation were able to cause glomerular injury, even without the presence of hHcys. However, it remains unknown whether NADPH oxidase activator, Vav2, is involved in NLRP3 inflammasome activation. Therefore, this last series of studies was designed to further validate the central role of NADPH oxidase by testing whether its molecular activator, Vav2 contributes to hHcys-induced NLRP3 inflammasome activation. In order to test this hypothesis, which is schematically represented in **Figure 32**, podocytes were transfected with either a scramble, constitutively active form of Vav2 (oncoVav2) or Vav2 shRNA plasmid directly to the nucleus via nucleofection. Mice were also locally transfected with either the oncoVav2 or Vav2sh plasmid into the renal cortex, maintained on the normal or FF diet to induce hHcys, and then assessed for NLRP3 inflammasome formation and activation after 4 weeks of treatment.

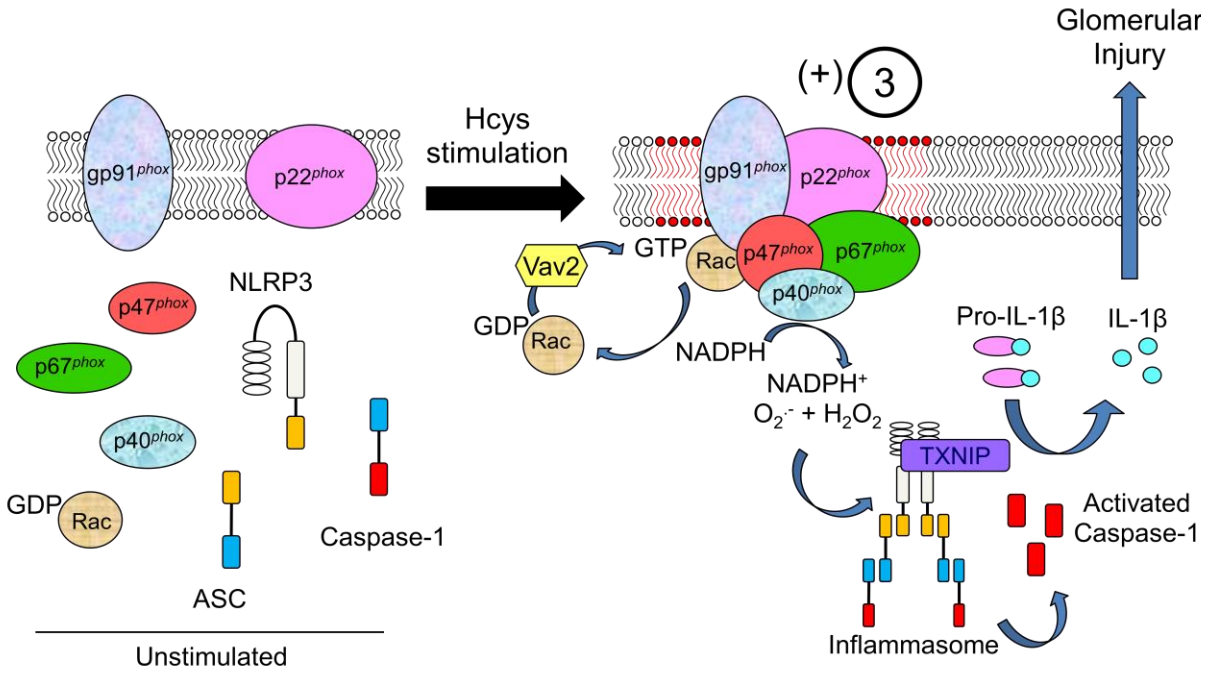


**Figure 32. Diagram showing the participation of Vav2 in NLRP3 inflammasome activation.** Aim 3 tested whether enhanced NADPH oxidase activity via Vav2 overexpression, both *in vitro* and *in vivo*, is sufficient to cause NLRP3 inflammasome activation. Additionally, Aim 3 further confirmed the central role of NADPH oxidase by looking at the effect of Vav2 inhibition.

## 6.2 Results

### 6.2.1 OncoVav2 induced NLRP3 inflammasome activation and podocyte injury

As demonstrated earlier, Hcys treatment of podocytes significantly increased NLRP3 inflammasome activation measured through caspase-1 activation and IL-1β production (**Figures 33A and 33B**). We now found that the inhibition of Vav2 attenuated both of these measures of inflammasome activation. Additionally, overexpression of Vav2 by nucleofection of the oncoVav2 plasmid resulted in increased caspase-1 activity and IL-1β secretion even in the absence of Hcys, importantly suggesting that NADPH oxidase activation alone is sufficient to stimulate NLRP3 inflammasome activation. Hcys treatment or oncoVav2 nucleofection also caused podocyte dysfunction, seen in the impaired ability of these podocytes to secrete VEGF

(**Figure 33C**). Inhibition of Vav2, however, protected podocytes from this injury and restored VEGF secretion levels. Altogether, these *in vitro* results demonstrate an essential role for Vav2 in Hcys-induced NLRP3 inflammasome activation and podocyte injury.

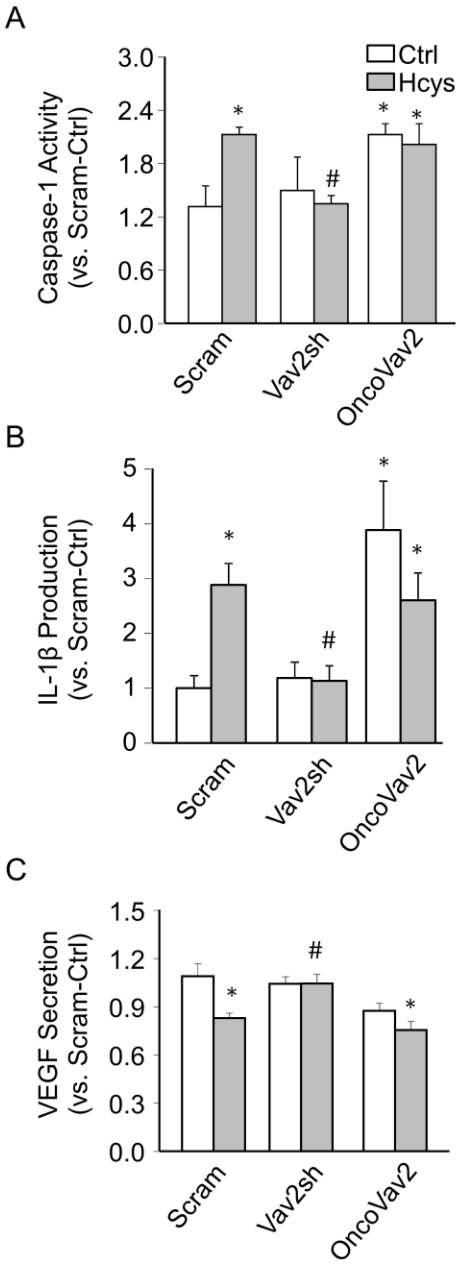


**Figure 33. Overexpression of Vav2 induced NLRP3 inflammasome activation and podocyte injury.** A-B. Hcys treatment of podocytes, as well as oncoVav2 nucleofection alone, increased caspase-1 activation and IL-1β production, which was inhibited upon Vav2sh nucleofection. (n=4-5). C. Inhibition of Vav2 protected podocytes from Hcys-induced dysfunction, seen in restored levels of VEGF secretion (n=5). Ctrl: Control, Scram: Scramble, Vav2sh: Vav2 shRNA. * $P<0.05$ *vs.* Scram-Ctrl, # $P<0.05$ *vs.* Scram-Hcys.

### 6.2.2 *In vivo* inhibition of Vav2 prevented glomerular NLRP3 inflammasome formation and activation

Through confocal microscopy observation, mice maintained on the FF diet exhibited glomerular NLRP3 inflammasome formation and increased colocalization between NLRP3 with ASC and NLRP3 with caspase-1 (**Figure 34A**). Mice locally transfected with oncoVav2 plasmid displayed a similar pattern of NLRP3 inflammasome formation despite not being hyperhomocysteinemic, suggesting that Vav2 overexpression-induced activation of NADPH oxidase is adequate to form NLRP3 inflammasomes regardless of elevated homocysteine. However, inhibition of Vav2 hindered hHcys-induced NLRP3 inflammasome formation, seen by reduced colocalization of NLRP3 with ASC or caspase-1, depicting an important role of Vav2 and NADPH oxidase in the aggregation of inflammasome proteins in the glomeruli of hyperhomocysteinemic mice. This same pattern was observed for hHcys-induced NLRP3 inflammasome activation and measurement of caspase-1 activation (**Figure 34B**). Finally, hHcys as well as oncoVav2 transfection induced glomerular dysfunction and albuminuria, which was diminished in Vav2sh-transfected mice (**Figure 34C**). Although our laboratory has already implicated an important role for Vav2 in hHcys-induced glomerular dysfunction [44], these data newly implicate a critical role for Vav2 in hHcys-induced glomerular NLRP3 inflammasome formation and activation. Additionally, *in vivo* NADPH oxidase activation via Vav2 overexpression was sufficient to activate NLRP3 inflammasomes, signifying that these mechanisms can occur independently of elevated Hcys.

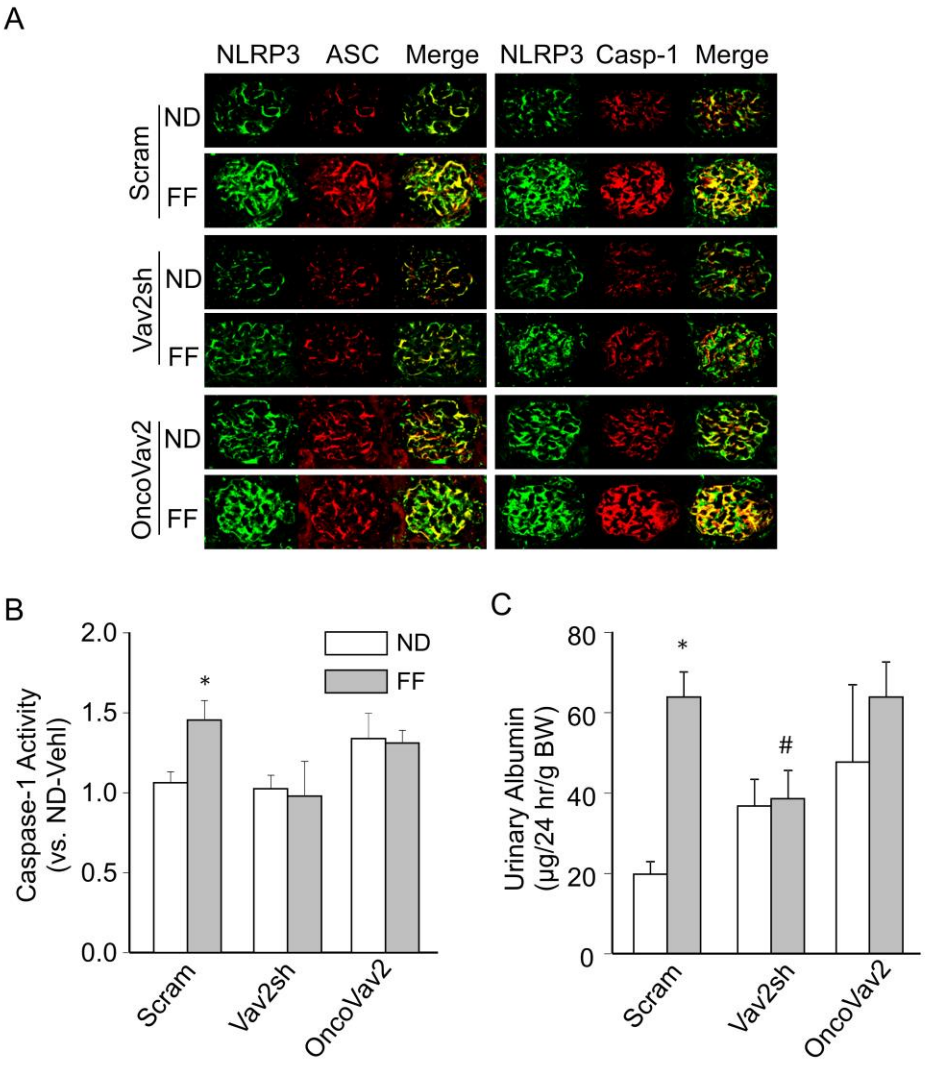


**Figure 34. *In vivo* inhibition of Vav2 prevented glomerular NLRP3 inflammasome formation and activation.** A-B. Mice with hHcys and those transfected with oncoVav2 plasmid demonstrated increased NLRP3 inflammasome formation and activation, seen by increased colocalization (yellow staining) between inflammasome proteins NLRP3 with ASC and NLRP3 with caspase-1, as well as increased caspase-1 activation. These effects were inhibited upon Vav2sh transfection (n=4). C. hHcys-induced increases in albuminuria were diminished by Vav2sh transfection (n=4). ND: Normal diet, FF: Folate-free diet, Scram: Scramble, Vav2sh: Vav2 shRNA.

## 6.3 Summary

Together, these preliminary results indicate a necessary role for Vav2 in the activation of hHcys-induced NLRP3 inflammasomes via its activating action on NADPH oxidase, where inhibition of Vav2 can prevent its activation as well as the deleterious effects of Hcys on the glomeruli. These studies further validate the central role of NADPH oxidase activation in this mechanism of podocyte NLRP3 inflammasome activation. Importantly, experiments using oncoVav2 demonstrate that NADPH oxidase activation occurring independently of hHcys can also result in NLRP3 inflammasome formation and activation, suggesting that this redox activating mechanism of NLRP3 inflammasomes is not necessarily specific to Hcys alone, but perhaps to any activators of NADPH oxidase.

# CHAPTER SEVEN

# DISCUSSION

## 7.1 Role of NADPH oxidase in mediating NLRP3 inflammasome formation and activation in podocytes in response to elevated Hcys levels

The primary goal of our first series of studies was to reveal whether NADPH oxidase-mediated redox signaling contributes to Hcys-induced inflammasome formation or activation and consequent glomerular injury. *In vitro* studies using cultured podocytes and an *in vivo* animal model of hHcys demonstrated that NADPH oxidase is necessary for the formation and activation of NLRP3 inflammasomes in podocytes upon Hcys stimulation, thereby leading to podocyte dysfunction, glomerular immune cell recruitment, and ultimately glomerular injury and sclerosis. These results for the first time demonstrate Hcys-induced redox activation of podocyte NLRP3 inflammasomes as an early mechanism switching on local inflammatory responses in glomeruli.

hHcys has been known to directly cause deleterious effects in the kidney, promoting a vicious cycle responsible for chronic renal disease, where hHcys decreases renal function and leads to further increased plasma Hcys levels due to decreases in Hcys excretion in the kidney [18]. Our most recent work demonstrated through concentration and time dependent studies that in an *in vitro* setting, a 40 μM treatment for 24 hours in cultured podocytes is sufficient to activate an inflammasome-stimulating response, verifying the effect we have seen *in vivo* [49]. Indeed, the present study showed significant glomerular damage observed in gp91$^{phox+/+}$ mice fed a FF diet for 4 weeks. Coinciding with this glomerular damage characterized by our laboratory and others to include mesangial cell expansion, overall cell proliferation, and capillary collapse

[48, 188], hHcys caused a significant increase in proteinuria and albuminuria, indicative of an impaired glomerular filtration membrane. In previous studies, these damaging effects of hHcys have been well correlated with its ability to stimulate the inflammatory response. Proinflammatory mediators, like MCP-1, NF-kB, interleukin-8, and adhesion molecules VCAM-1 and E-selectin, have been demonstrated to be upregulated during hHcys [189-190]. Furthermore, it has been shown that hHcys results in the recruitment of lymphocytes [191]. However, it remains unknown how hHcys or Hcys *in vitro* activates this response of the innate immune system in glomeruli. We have recently reported that Hcys can activate NLRP3 inflammasomes in podocytes, an intracellular molecular switch of inflammation [49]. Inflammasome activation has also been implicated in a number of inflammatory and metabolic diseases, including obesity, gout, hypersensitivity, silicosis, and diabetes, where inhibition of the inflammasome proteins NLRP3, ASC, or caspase-1 significantly attenuates the downstream inflammatory reaction produced under these conditions [118, 120, 126-127]. Similarly, our report showed that inhibition of either ASC or caspase-1 could prevent podocyte and glomerular damage induced by hHcys, improving renal structural and functional integrity [49], suggesting an important role for inflammasome activation in mediating the deleterious effects of hHcys.

We further explored the mechanism by which NLRP3 inflammasomes are activated in podocytes *in vitro* by Hcys and *in vivo* by experimental hHcys. It has been reported that many endogenous and exogenous danger signals activate the inflammasome, and it has been of great interest as to how all of these very diverse signals can activate the same molecular machinery to turn on inflammation. Of the proposed models of inflammasome activation, the ROS model provides a unifying link, utilizing the common aspect that all these danger signals produce

changes in oxidative stress, making NLRP3 a more general sensor detecting these changes in oxidative stress [149]. Interestingly, our laboratory and others have found the damaging effects of hHcys to be strongly associated with increased local oxidative stress, chiefly through NADPH oxidase [47, 64-65]. With reports of gp91$^{phox}$/Nox2 being the predominant isoform found in podocytes, our laboratory has also demonstrated that this NADPH oxidase isoform and its activity are essential for hHcys to induce glomerular injury, since knockout of the gp91$^{phox}$ gene in mice protected podocytes and glomeruli from hHcys-induced glomerular sclerosis [48]. Therefore, we hypothesized that redox signaling associated with NADPH oxidase in podocytes may be critical in triggering NLRP3 inflammasome formation and activation upon Hcys stimulation. Although there are reports that NLRP3 inflammasomes can be activated by ROS in different cells or tissues [126, 149, 181], to our knowledge, our results for the first time link NADPH oxidase to the formation and activation of these inflammasomes in podocytes, where Hcys-induced NADPH oxidase activation produces $O_2^{\bullet-}$ to conduct redox signaling that triggers the formation of NLRP3 inflammasomes and production of inflammatory cytokines like IL-1β.

Next, we tested the *in vivo* triggering action of NADPH oxidase activation in the formation of NLRP3 inflammasomes using mice lacking the gp91$^{phox}$ gene and in mice treated with NADPH oxidase inhibitory peptide, gp91*ds-tat.* Although the strategies used to genetically and pharmacologically inhibit NADPH oxidase in mice were not podocyte-specific, confocal results demonstrated that this inhibition prevented hHcys-induced NLRP3 inflammasome formation as shown by less colocalization of NLRP3 with ASC and NLRP3 with caspase-1, which mainly occurred in podocytes given the increased colocalization of NLRP3 molecules with podocin and desmin within glomeruli. Correspondingly, both interventions also inhibited hHcys-induced

activation of NLRP3 inflammasomes, confirmed by decreased caspase-1 activity and IL-1β production. The inflammatory response in glomeruli during hHcys, indicated by recruitment of macrophages and T-cells, was also significantly suppressed by both RNA interference and pharmacological inhibition of NADPH oxidase. These results from *in vivo* animal experiments further support the view that NADPH oxidase-mediated redox signaling promotes the formation and activation of NLRP3 inflammasomes in podocytes during hHcys. Again, to our knowledge, these findings represent the first *in vivo* experimental evidence that triggering of NLRP3 inflammasomes is attributed to NADPH oxidase-mediated redox signaling, which results in local inflammation in glomeruli during hHcys.

We also performed *in vitro* and *in vivo* experiments to address the functional relevance of NADPH oxidase-mediated triggering of NLRP3 inflammasomes on Hcys-stimulated podocyte and glomerular injury. Podocytes, the epithelial cells lining the outermost layer of the glomeruli, are essential for proper filtration, and the injury to podocytes is indicative of impaired glomerular filtration and proteinuria, ultimately leading to glomerular sclerosis [192-193]. Foot process effacement, considered as the hallmark sign of podocyte injury, is usually accompanied by the destruction of the actin cytoskeleton, increased expression of slit diaphragm molecule and podocyte injury factor desmin, and reduction of the slit diaphragm molecule podocin, an important marker for cell polarity and survival. Although such protection of podocytes observed in *in vivo* experiments may be due to a suppressed inflammatory response, it is interesting to note that in *in vitro* experiments the direct effects of suppressed inflammasome or NADPH oxidase also protect the functional and structural integrity of podocytes, even before a typical inflammatory response is instigated. This non-inflammatory effect or direct action on podocytes

has been reported to be associated with IL-1β-induced podocyte dysfunction, which is beyond inflammation [194]. In addition to the detrimental actions of hHcys-induced inflammatory response, the early effect of activated inflammasome products, like IL-1β, directly on podocytes may also importantly contribute to podocyte injury. If triggering of such inflammasomes by NADPH oxidase-derived ROS is blocked, both direct and indirect effects of inflammasome activation in the induction of podocytes injury may be blocked, as shown in our results.

Corresponding to protection of podocytes from Hcys-induced injury, inhibition of inflammasome activation by deletion of $gp91^{phox}$ gene or inhibition of NADPH oxidase activity significantly ameliorated hHcys-induced glomerular injury in mice, which may be due to decreased podocyte injury as well as suppressed local glomerular inflammatory response. Together, this NADPH oxidase-derived ROS may act as redox signaling messengers to activate the NLRP3 inflammasome, which serves as the bridging and amplifying mechanism leading to an eventual robust inflammatory response which promotes the progression to glomerular sclerosis.

### 7.2 Redox activation of NLRP3 inflammasomes in response to elevated Hcys or during hHcys depends on both $O_2^{\bullet-}$ and $H_2O_2$

The goal for this portion of the study was to dissect which endogenously produced ROS in response to increased Hcys in podocytes *in vitro* and *in vivo* contributes to hHcys-induced NLRP3 inflammasome formation and activation. Studies using cultured podocytes revealed that reduction of intracellular $O_2^{\bullet-}$ and $H_2O_2$ levels attenuated Hcys-induced NLRP3 inflammasome formation and suppressed downstream caspase-1 activation and IL-1β production. *In vivo,*

dismutation of $O_2^{\bullet-}$ and decomposition of $H_2O_2$ in hyperhomocysteinemic mice not only prevented NLRP3 inflammasome formation in glomeruli, but also protected mice with hHcys from renal dysfunction and glomerular sclerosis. To our knowledge, this study is the first effort to dissect endogenously produced ROS in NLRP3 inflammasome activation in podocytes and glomeruli during exposure to high Hcys levels or hHcys.

Many studies provided increasing evidence for the central role of ROS in NLRP3 inflammasome activation [126, 195-196]. Additional studies have demonstrated that IL-1β production in response to even more diverse stimuli could be prevented through the use of either NADPH oxidase inhibitors or general ROS scavengers such as diphenylene iodonium (DPI) and N-acetyl-cysteine (NAC) [151, 197-199]. However, by using these general ROS scavengers, it remains largely unexplored as to exactly which species of ROS is being sensed and is indeed contributing to NLRP3 inflammasome activation. Aside from $O_2^{\bullet-}$, other species derived from NADPH oxidase include $H_2O_2$, peroxynitrite ($ONOO^-$), and $^{\bullet}OH$ [200]. A small subset of reports has attempted the use of ROS scavengers, but to our knowledge, the present study is the first to dissect the action of these common endogenously produced ROS to elucidate their role in hHcys-induced NLRP3 inflammasome activation.

TEMPOL, used for its antioxidant properties, has been widely demonstrated to have protective effects against many disease models including diabetes, cardiovascular complications, heart failure, angiogenesis, ischemia-reperfusion injury, cancer, and glomerular injury [201-203]. Catalase is responsible for the enzymatic decomposition of $H_2O_2$ down to $H_2O$ and $O_2$ [204-205], and TMTU has been used as a specific $^{\bullet}OH$ scavenger [203]. These pharmacologic tools enabled

the dissection of the ROS participating in Hcys-induced NLRP3 inflammasome formation and activation. However, the use of TEMPOL is fairly limited in that its selectivity for $O_2^{\bullet-}$ is quite restricted due to a number of nonspecific targets, hence our use of PEG-SOD as well as an additional SOD mimetic, MnTMPyP, in *in vitro* experiments to further verify our results. But, similar to our findings in podocytes or glomeruli, a recent report provided evidence that scavenging of extracellular $O_2^{\bullet-}$ by SOD mimetic Mn(III)tetrakis(N-ethylpyridinium-2-yl) porphyrin (MnTE-2-PyP) could prevent NLRP3 inflammasome activation in a model of hypoxia-induced pulmonary hypertension [183]. In addition, Zhou et al demonstrated the ability of exogenous $H_2O_2$ to directly activate NLRP3 inflammasomes to produce IL-1β [126]. Taken together, these data suggest the requirement of $O_2^{\bullet-}$ dismutation to $H_2O_2$ in ROS-stimulated inflammasomes, which proposes an important role for $H_2O_2$ not only in Hcys-induced NLRP3 inflammasome formation, but also in inflammasome formation in response to other stimuli that increase $H_2O_2$ production.

The $^{\bullet}OH$ scavenger TMTU did not significantly inhibit any measure of Hcys-induced NLRP3 inflammasome formation or activation, suggesting that in comparison to $O_2^{\bullet-}$ and $H_2O_2$, $^{\bullet}OH$ does not play a crucial role to inflammasome stimulation. Although TMTU did not produce inhibitory effects that were of statistical significance, caspase-1 activity and IL-1β production appeared lower when TMTU was used. This effect may be due to some non-specific action of TMTU because thiourea compounds, although commonly used as potent scavengers of $^{\bullet}OH$, are also able to scavenge $O_2^{\bullet-}$ and $H_2O_2$ at higher doses [206-207].

An important role for $ONOO^-$ in many disease processes is supported throughout the literature, including Hcys-induced cardiovascular and renal injury where $ONOO^-$ participates in detrimental events such as endothelial dysfunction and renal ischemia-reperfusion injury [208-209]. Therefore, we examined the role of $ONOO^-$ scavenging on Hcys-induced NLRP3 inflammasome formation and activation in podocytes. It was found that ebselen, a specific $ONOO^-$ scavenger, failed to decrease the formation and activation of NLRP3 inflammasomes in podocytes treated with Hcys, suggesting that $ONOO^-$ may not play a critical role in this particular pathological process in podocytes.

With respect to the models of NLRP3 inflammasome activation, there is debate whether pro- or antioxidant events contribute to this phenomenon. Our study, along with many of the aforementioned studies, provided supportive evidence for a ROS-dependent mechanism that can be hindered when these species are scavenged. This concept, however, has been challenged with evidence demonstrating that ROS inhibition prevents the priming, but not activation of inflammasomes [156]. Furthermore, monocytes and macrophages isolated from patients with chronic granulomatous disease and NADPH oxidase-deficient mice exhibited typical IL-1β secretion [119, 157], which was different from our results in podocytes [169]. It is possible that different cell types may have altered sensitivity to redox regulation of NLRP3 inflammasomes or to different danger signals. Activation of NLRP3 or other inflammasomes in macrophages *in vitro* may require a priming process, a step that perhaps is not necessary in other cell types [49, 210]. In addition, since NLRP3 inflammasome activation only requires a low level of intracellular $O_2^{\bullet-}$ or $H_2O_2$ as a signaling mechanism rather than a injurious event, monocytes and macrophages isolated from patients with chronic granulomatous disease and NADPH oxidase-

deficient mice may still potentially generate enough ROS to stimulate NLRP3 inflammasome activation and IL-1β production. Perhaps other ROS-producing pathways in these sick cells may also exert compensatory redox regulation to NLRP3 inflammasome activation. Additional studies are needed to further explore such potential for the redox regulation of NLRP3 inflammasomes in different cell types.

These findings importantly implicate a specific role for both $O_2^{\bullet-}$ and $H_2O_2$ in the instigation of NLRP3 inflammasome activation in cultured podocytes and in glomeruli of mice with hHcys. $O_2^{\bullet-}$ and $H_2O_2$ may be the redox signaling messengers linking NADPH oxidase activation to the stimulation of the innate immune system through NLRP3 inflammasome activation, where initiation of the inflammatory response may lead to more extensive oxidative stress that is responsible for hHcys-induced detrimental and pathological glomerular changes.

### 7.3 TXNIP senses redox signals to activate NLRP3 inflammasomes in response to increased Hcys *in vitro* or during hHcys *in vivo*

Additional experiments in this study were designed to address the role of TXNIP in hHcys-induced NLRP3 inflammasome activation and associated podocyte injury and glomerular sclerosis. It was found that Hcys treatment of podocytes upregulated protein expression of TXNIP, which resulted in increased binding of TXNIP with inflammasome protein NLRP3. Both *in vitro* and *in vivo* inhibition of TXNIP by its inhibitor verapamil or RNA interference blocked TXNIP expression and prevented TXNIP-NLRP3 binding and subsequent NLRP3 inflammasome activation in response to Hcys. These findings demonstrate the critical role of

TXNIP binding in the activation of NLRP3 inflammasomes and subsequent podocyte injury and glomerular dysfunction or sclerosis.

Despite studies that have demonstrated an important role for ROS in inflammasome activation, it remains unclear how NLRP3 is able to sense redox changes in a variety of cells, in particular, in podocytes during hHcys. Through a yeast two hybrid screen, it has been shown that thioredoxin-interacting protein (TXNIP), a ROS sensor and an endogenous inhibitor of the antioxidant thioredoxin, is a binding partner of NLRP3. TXNIP, also known as vitamin D3 upregulated protein 1 (VDUP-1) and thioredoxin-binding protein-2 (TBP-2), plays a critical role in growth suppression, making it particularly important in cancer progression by causing G1 cell cycle arrest. It is also a crucial regulator of lipid metabolism where overexpression of TXNIP during hyperglycemia causing β-cell death and impaired insulin secretion [211]. Zhou et al confirmed an important role for TXNIP in the pathogenesis of type 2 diabetes by showing that TXNIP binding to NLRP3 was essential for ROS-mediated inflammasome activation [126]. Additionally, in human and rat kidneys, TXNIP mRNA and protein is most abundantly expressed in the glomeruli [212], and although some studies have demonstrated its upregulation in response to high glucose [213-214], there have been no studies to date determining the effects of Hcys on TXNIP, in particular, in podocyte or glomerular injury, which was one of the goals in the current study.

Using RNA interference and pharmacologic inhibitors of TXNIP, we found that TXNIP mRNA and protein expression was significantly reduced after transfection of siRNA into cultured mouse podocytes (data not shown) and local transfection of TXNIP shRNA *in vivo* into mouse kidneys. To complement this RNA manipulation, we used pharmacologic calcium

channel blocker verapamil to inhibit TXNIP expression both *in vitro* and *in vivo*. It has been demonstrated that verapamil, when administered to mice through the drinking water at an average dose of 100 mg/kg/day, decreased diabetes-induced cardiomyocyte apoptosis, an effect specifically due to its potent inhibition of TXNIP expression [168]. Additionally, verapamil enhanced β-cell survival and function through its reduction of β-cell TXNIP expression [215], and this may be due to verapamil-induced transcriptional repression of TXNIP [216]. It was found that verapamil, at a dose of 50 μM, strongly inhibited TXNIP expression (data not shown), blocked TXNIP binding to NLRP3, and prevented Hcys-induced NLRP3 inflammasome formation and activation in podocytes. *In vivo* experiments furthermore displayed TXNIP inhibition hindering caspase-1 activation and IL-1β maturation in hyperhomocysteinemic mice. To our knowledge, this provides the first evidence showing the critical role of TXNIP-NLRP3 binding in mediating podocyte inflammasome activation in response to Hcys stimulation.

It is well known that prolonged elevation of blood homocysteine level results in hallmarks typical of glomerular sclerosis, including glomerular hypercellularity, capillary collapse, and fibrous extracellular matrix deposition [217-219]. However, inhibition of TXNIP by either genetic manipulation or by verapamil treatment prevented the Hcys-induced detrimental effects on both podocytes in culture and glomerular structure and function. Verapamil has long been demonstrated to have glomerular protective effects [220-221]; however, our study is the first to demonstrate that, at least in hHcys-induced glomerular injury, this protective effect of verapamil is associated with its inhibitory action of TXNIP.

In other studies, inhibition of TXNIP expression by verapamil has also been reported [222], but this effect has been extended to other calcium channel blockers and inhibitors such as diltiazem and $NiCl_2$, as well as with calcium chelator EGTA. This suggests that this inhibition of TXNIP function is perhaps not a direct effect of verapamil itself, but more likely due to a reduction in intracellular calcium concentrations [215]. Additionally, calcium signaling is emerging as an important component of NLRP3 inflammasome activation. Brough et al first demonstrated such role of calcium signaling when they found suppressed IL-1β maturation following pretreatment of cells with calcium chelator, BAPTA-AM [223]. This process may involve endoplasmic reticulum (ER) stress, calcium release from ER, and TXNIP binding [223-225]. Although these possible non-specific effects of calcium inhibition may not be excluded, our multifaceted approach of genetic and pharmacologic interventions give us confidence that the diminished NLRP3 inflammasome activation by verapamil is indeed due to the reduction in TXNIP expression and binding. It should be noted that the contribution of various calcium signaling pathways in the mediation or regulation of NLRP3 inflammasome activation in podocytes or other cells indeed warrants future exploration.

TXNIP binding to NLRP3 appears to be an essential mechanism involved in the regulation of NLRP3 inflammasome activation in response to elevated Hcys. TXNIP may initiate the NLRP3 cascade by endogenously sensing the altered redox status of the cell, triggering the secretion of pro-inflammatory cytokines like IL-1β to potentiate the inflammatory response. Inhibition of TXNIP not only prevented NLRP3 inflammasome activation and Hcys-induced podocyte injury in cultured cells, but also importantly preserved glomerular function and

morphology in hyperhomocysteinemic mice, suggesting a critical *in vivo* role for TXNIP in this sclerotic mechanism.

### 7.4 Activation of NADPH oxidase by Vav2 overexpression is sufficient to activate NLRP3 inflammasomes in podocytes, independent of hHcys

The further mechanistic studies on NLRP3 inflammasome activation were proposed to address the effect of NADPH oxidase activation through the overexpression of Vav2, which attempted to test whether NADPH oxidase activation by other stimuli also lead to NLRP3 inflammasome activity in podocytes. In cultured podocytes and mice, oncoVav2 transfection was found to result in NLRP3 inflammasome formation and activation as well as glomerular dysfunction, independent of elevated Hcys. However, inhibition of Vav2 by RNA interference prevented hHcys-induced caspase-1 activation and protected from albuminuria, indicating NADPH oxidase activation alone can activate NLRP3 inflammasomes and Vav2 can stimulate hHcys-induced detrimental effects.

There exists considerable controversy regarding the role of NADPH oxidase in the activation of NLRP3 inflammasomes in response to a diverse range of stimuli. There is evidence to suggest that NADPH oxidase and its $gp91^{phox}$ subunit are dispensable in terms of NLRP3 inflammasome activation. Wu et al demonstrated that mechanical ventilation causes IL-1β release in the lung; however, there was no inhibitory effect on released IL-1β in cyclic-stretched mouse alveolar macrophages isolated from $gp91^{phox-/-}$ mice [158]. Instead, it was concluded that ROS derived from mitochondria was necessary for NLRP3 inflammasome activation induced by cyclic stretch. Furthermore, some studies showed that peripheral blood mononuclear cells

isolated from chronic granulomatous disease (CGD) patients exhibit normal secretion of IL-1β and even exacerbated caspase-1 activation when compared to healthy controls [157, 226-227]. Interestingly, in human neutrophils isolated from CGD patients having mutations in the $gp91^{phox}$ subunit of NADPH oxidase displayed impaired IL-1β release but displayed no difference in the ability to activate caspase-1 when compared to neutrophils from control patients [228]. This suggested that NADPH oxidase, specifically $gp91^{phox}$, and the production of ROS are dispensable for NLRP3 inflammasome activation, but crucial for IL-1β secretion. This finding is altogether different from Bauernfield et al who found that ROS is necessary for the priming and regulation of NLRP3 inflammasome protein expression, but not needed for its activation [156]. On the other hand, NADPH oxidase and $gp91^{phox}$ are required for ATP-induced NLRP3 inflammasome activation in LPS-primed murine macrophages, where general NADPH oxidase inhibitors DPI and apocynin as well as specific $gp91^{phox}$ siRNA inhibited caspase-1 activation and IL-1β secretion [195]. Similar results have been found in response to many NLRP3 inflammasome stimulators like TNF-α and free fatty acids, where the effects of these stimulators can be blocked upon NADPH oxidase inhibition [153-154]. With all these contradicting findings, we sought to better understand the role of NADPH oxidase in Hcys-induced NLRP3 inflammasome activation in podocytes. Upon Vav2 overexpression, we found that NADPH oxidase activation alone led to caspase-1 activation and IL-1β production in cultured podocytes, indicating that NLRP3 inflammasome activation may vary with different stimuli, but if NADPH oxidase is activated, NLRP3 inflammasomes can become activated in podocytes.

Rac1, considered the major Rac GTPase isoform in nonphagocytic cells, mediates NADPH oxidase activity by switching between a GTP-bound “active” and a GDP-bound “inactive”

conformational state. In the presence of various stimuli, guanine nucleotide exchange factors (GEFs) like Vav and Tiam1 are responsible for this switching of Rac/Rho GTPases, leading to multiple downstream effects limited not only to NADPH oxidase activation, but also regulating cellular processes including proliferation, differentiation, and cytoskeletal arrangement [229]. The Vav family of GEFs, exhibiting high specificity to Rac-mediated NADPH oxidase activation, consists of three members – Vav1, Vav2, and Vav3, with reports of Vav2 being importantly expressed in podocytes [230]. It has been demonstrated by Inoue et al that Rac1 inhibitor NSC23766 suppressed ATP-induced ROS production and IL-1β secretion in bone marrow macrophages [231]. Additionally, macrophages isolated from NLRP3$^{-/-}$ and ASC$^{-/-}$ mice demonstrated no changes in Rac or Vav expression or ROS production, strongly suggesting these molecules to be upstream of the NLRP3 inflammasome. Our results coincide with these recent findings, supporting the manipulation of GEF Vav2 as an effective approach in modulating NADPH oxidase activity. Indeed, we found that inhibition of Vav2 reduced NADPH oxidase-derived $O_2^{\bullet-}$, attenuated caspase-1 activation and IL-1β production, and protected podocytes and mouse glomeruli from hHcys-induced injury.

Collectively, through specific activation of NADPH oxidase by overexpression of Vav2, our studies provided strong evidence for a central and crucial role for NADPH oxidase in hHcys-induced NLRP3 inflammasome activation. This stimulation of NADPH oxidase, independent of Hcys, importantly demonstrated that regardless of upstream stimulation, the activation of NADPH oxidase and the production of ROS are sufficient to stimulate aggregation and activation of NLRP3 inflammasomes. Therefore, these mechanisms may not be limited to only elevated Hcys, but to any stimulator of NADPH oxidase.

## 7.5 Summary and conclusions

The major findings of the present study are summarized below, and represented in **Figure 35**.

1. As previously demonstrated, we showed that hHcys-induced glomerular injury occured in an NLRP3 inflammasome-dependent mechanism. However, blockade of NADPH oxidase through the inhibition of its gp91$^{phox}$ subunit attenuated Hcys-induced NLRP3 inflammasome activation in cultured podocytes as well as preserved podocyte function and integrity. In hyperhomocysteinemic mice, gp91$^{phox-/-}$ as well as mice receiving a gp91*ds-tat* peptide displayed diminished NADPH oxidase activation, as exhibited through reduced $O_2^{\bullet-}$ levels, which contributed to the reduction in NLRP3 inflammasome formation and activation *in vivo*. Together, these results reveal an essential role for NADPH oxidase activation and the production of local oxidative stress in the triggering of NLRP3 inflammasomes in response to hHcys.

2. Dismutation of $O_2^{\bullet-}$ by TEMPOL and decomposition of $H_2O_2$ by catalase prevented the colocalization of NLRP3 inflammasome proteins, and reduced caspase-1 activity and IL-1β production both in cultured podocytes and in glomeruli of hyperhomocysteinemic mice. Specific ROS scavenging studies revealed that $O_2^{\bullet-}$ and $H_2O_2$, but not $^{\bullet}OH$ or $ONOO^-$, distinctly contribute to NLRP3 inflammasome formation and activation during elevated Hcys.

3. Through size-exclusion chromatography experiments, Hcys-treated podocytes exhibited both increased expression and recruitment of TXNIP to high molecular weight fractions,

indicative of TXNIP aggregation to the NLRP3 inflammasome. Confirmed by co-immunoprecipitation studies, robust increases in TXNIP-NLRP3 binding were found in cultured podocytes with Hcys exposure and in renal cortical tissue from hyperhomocysteinemic mice. Inhibition of TXNIP either by shRNA transfection or by verapamil administration blocked TXNIP-NLRP3 binding and interfered with NLRP3 inflammasome activation, demonstrating the crucial role of TXNIP in hHcys-induced NLRP3 inflammasome activation.

4. TXNIP expression was upregulated in podocytes in response to elevated Hcys, and *in vivo* TXNIP inhibition significantly preserved glomerular morphology and function during hHcys. FF diet-maintained mice receiving either TXNIP shRNA transfection or verapamil exhibited drastically reduced proteinuria and albuminuria, as well as protection from hHcys-induced glomerular sclerotic changes. To our knowledge, this is the first study elucidating that TXNIP inhibition is glomerular protective against hHcys-induced insult.

5. The inhibition of guanine nucleotide exchange factor Vav2 prevented hHcys-induced NLRP3 inflammasome formation and activation in both cultured podocytes and hyperhomocysteinemic mice, further verifying the important role of functional NADPH oxidase in this mechanism. However, overexpression of Vav2 and consequent activation of NADPH oxidase, independent of elevated Hcys, were also able to produce these inflammasome-activating effects, suggesting that NADPH oxidase activation alone via Vav2 is sufficient to initiate the cascade that leads to NLRP3 inflammasome activation and downstream glomerular injury.

In conclusion, evidenced by gp91$^{phox}$ and Vav2 inhibition, NADPH oxidase is demonstrated to be critical in mediating NLRP3 inflammasome formation, with $O_2^{\bullet -}$ and $H_2O_2$ being important signaling messengers. TXNIP may be the unique key that is responsible for sensing these changes in these signaling ROS and initiating the cascade of NLRP3 inflammasome activation, eventually progressing to the pathogenesis of glomerular sclerosis during hHcys. Activation of NADPH oxidase via overexpression of Vav2 was sufficient to stimulate aggregation and activation of NLRP3 inflammasomes, suggesting these mechanisms may not be limited to only elevated Hcys, but other potential pathogenic processes involving NADPH oxidase activation.

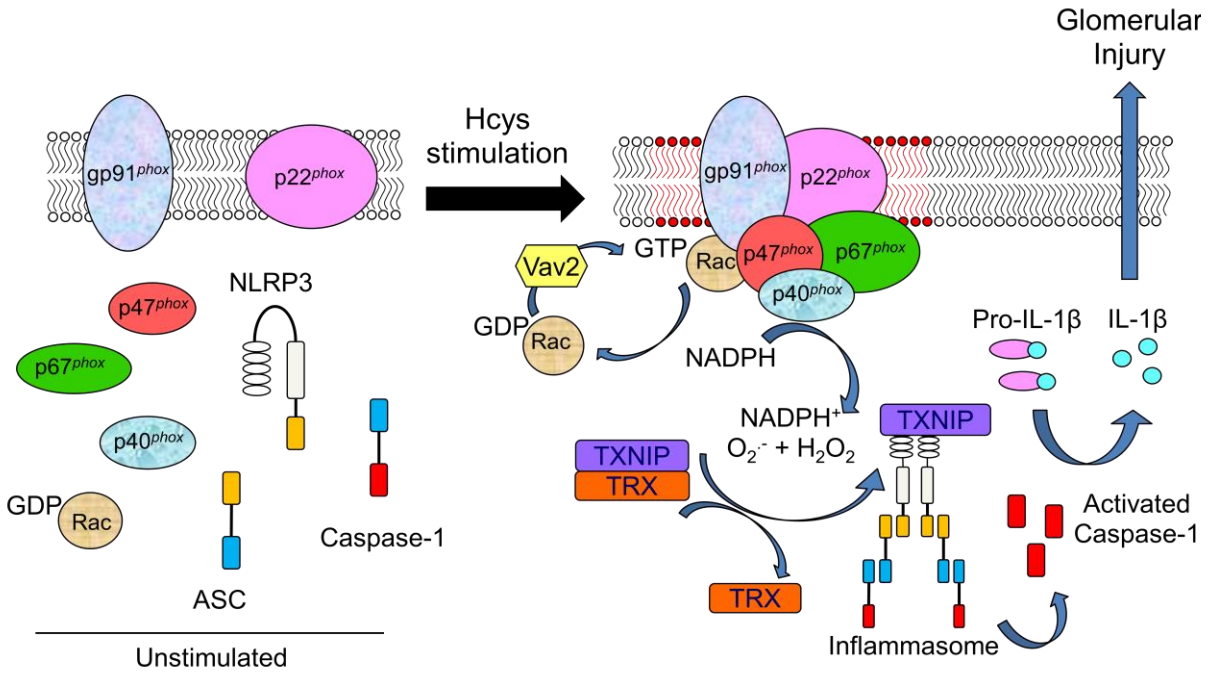


**Figure 35. Summary Diagram.**

## 7.6 Significance and perspectives

hHcys is widely recognized as an important, independent risk factor for the progression of various sclerotic diseases, including glomerular sclerosis and ESRD. However, the therapeutic value of Hcys-lowering interventions is marginal, and this may be attributed to Hcys-induced irreversible detrimental effects on glomerular structure and function, on which Hcys-lowering therapies would have negligible effects. Thus, our focus has been centered on identifying the initiating and promoting mechanisms that occur during early stages of hHcys. In our search of early biomarkers, the NLRP3 inflammasome became an attractive target since its major functional role is to proteolytically cleave caspases leading to the maturation of pro-inflammatory cytokines and initiate the innate immune response from the single cell level. The presence of activated NLRP3 inflammasomes, perhaps in the urine, may be an early biomarker, useful in the diagnosis of early damage and the prevention of more serious glomerular sclerosis. Importantly, sustained NLRP3 inflammasome activation may be a perpetual cellular trigger responsible for initiating both inflammatory and non-inflammatory-related injury of podocytes, ultimately resulting in progressive glomerular disease leading to ESRD. The findings in the present study indicate the essential role of NADPH oxidase and the production of ROS, specifically $O_2^{\bullet -}$ and $H_2O_2$, in hHcys-induced NLRP3 inflammasome formation and activation, which may be a target to terminate inflammasome activation. TXNIP is also critical in this NLRP3 inflammasome-activating mechanism because it is a ROS sensor linking NADPH oxidase-derived ROS to NLRP3 inflammasome stimulation. Together, these findings provide the first evidence that targeting either NLRP3 inflammasomes directly or their activating mechanisms may be an effective therapeutic strategy for the prevention, detection, and early treatment of glomerular sclerosis and other end-stage organ damage resulted from hHcys.

## REFERENCES


[1] Gonzalez, S.; Huerta, J. M.; Fernandez, S.; Patterson, A. M.; Lasheras, C. Homocysteine increases the risk of mortality in elderly individuals. *Br J Nutr* **97:**1138-1143; 2007.

[2] Herrmann, W.; Obeid, R. Homocysteine: a biomarker in neurodegenerative diseases. *Clin Chem Lab Med* **49:**435-441; 2011.

[3] McCully, K. S. Vascular pathology of homocysteinemia: implications for the pathogenesis of arteriosclerosis. *Am J Pathol* **56:**111-128; 1969.

[4] Refsum, H.; Smith, A. D.; Ueland, P. M.; Nexo, E.; Clarke, R.; McPartlin, J.; Johnston, C.; Engbaek, F.; Schneede, J.; McPartlin, C.; Scott, J. M. Facts and recommendations about total homocysteine determinations: an expert opinion. *Clin Chem* **50:**3-32; 2004.

[5] Walker, W. G. Hypertension-related renal injury: a major contributor to end-stage renal disease. *Am J Kidney Dis* **22:**164-173; 1993.

[6] Zhuo, J. M.; Pratico, D. Normalization of hyperhomocysteinemia improves cognitive deficits and ameliorates brain amyloidosis of a transgenic mouse model of Alzheimer's disease. *FASEB J* **24:**3895-3902; 2010.

[7] Zhang, C.; Yi, F.; Xia, M.; Boini, K. M.; Zhu, Q.; Laperle, L. A.; Abais, J. M.; Brimson, C. A.; Li, P. L. NMDA receptor-mediated activation of NADPH oxidase and glomerulosclerosis in hyperhomocysteinemic rats. *Antioxid Redox Signal* **13:**975-986; 2010.

[8] Hwang, S. Y.; Siow, Y. L.; Au-Yeung, K. K.; House, J.; O, K. Folic acid supplementation inhibits NADPH oxidase-mediated superoxide anion production in the kidney. *Am J Physiol Renal Physiol* **300:**F189-198; 2011.

[9] Wu, C. C.; Zheng, C. M.; Lin, Y. F.; Lo, L.; Liao, M. T.; Lu, K. C. Role of homocysteine in end-stage renal disease. *Clin Biochem* **45:**1286-1294; 2012.

[10] de Koning, L.; Hu, F. B. Homocysteine lowering in end-stage renal disease: is there any cardiovascular benefit? *Circulation* **121:**1379-1381; 2010.

[11] Perla-Kajan, J.; Jakubowski, H. Paraoxonase 1 and homocysteine metabolism. *Amino Acids* **43:**1405-1417; 2012.

[12] Cavalca, V.; Cighetti, G.; Bamonti, F.; Loaldi, A.; Bortone, L.; Novembrino, C.; De Franceschi, M.; Belardinelli, R.; Guazzi, M. D. Oxidative stress and homocysteine in coronary artery disease. *Clin Chem* **47:**887-892; 2001.

[13] Bialecka, M.; Kurzawski, M.; Roszmann, A.; Robowski, P.; Sitek, E. J.; Honczarenko, K.; Gorzkowska, A.; Budrewicz, S.; Mak, M.; Jarosz, M.; Golab-Janowska, M.; Koziorowska-Gawron, E.; Drozdzik, M.; Slawek, J. Association of COMT, MTHFR, and SLC19A1(RFC-1) polymorphisms with homocysteine blood levels and cognitive impairment in Parkinson's disease. *Pharmacogenet Genomics* **22:**716-724; 2012.

[14] Schalinske, K. L.; Smazal, A. L. Homocysteine imbalance: a pathological metabolic marker. *Adv Nutr* **3:**755-762; 2012.

[15] Yu, M.; Sturgill-Short, G.; Ganapathy, P.; Tawfik, A.; Peachey, N. S.; Smith, S. B. Age-related changes in visual function in cystathionine-beta-synthase mutant mice, a model of hyperhomocysteinemia. *Exp Eye Res* **96:**124-131; 2012.

[16] McLean, R. R.; Jacques, P. F.; Selhub, J.; Tucker, K. L.; Samelson, E. J.; Broe, K. E.; Hannan, M. T.; Cupples, L. A.; Kiel, D. P. Homocysteine as a predictive factor for hip fracture in older persons. *N Engl J Med* **350:**2042-2049; 2004.

[17] Schafer, S. A.; Mussig, K.; Stefan, N.; Haring, H. U.; Fritsche, A.; Balletshofer, B. M. Plasma homocysteine concentrations in young individuals at increased risk of type 2 diabetes are associated with subtle differences in glomerular filtration rate but not with insulin resistance. *Exp Clin Endocrinol Diabetes* **114:**306-309; 2006.

[18] Yi, F.; Li, P. L. Mechanisms of homocysteine-induced glomerular injury and sclerosis. *Am J Nephrol* **28:**254-264; 2008.

[19] Brosnan, J. T.; Jacobs, R. L.; Stead, L. M.; Brosnan, M. E. Methylation demand: a key determinant of homocysteine metabolism. *Acta Biochim Pol* **51:**405-413; 2004.

[20] Guttormsen, A. B.; Ueland, P. M.; Svarstad, E.; Refsum, H. Kinetic basis of hyperhomocysteinemia in patients with chronic renal failure. *Kidney Int* **52:**495-502; 1997.

[21] Bostom, A.; Brosnan, J. T.; Hall, B.; Nadeau, M. R.; Selhub, J. Net uptake of plasma homocysteine by the rat kidney in vivo. *Atherosclerosis* **116:**59-62; 1995.

[22] Finkelstein, J. D. The metabolism of homocysteine: pathways and regulation. *Eur J Pediatr* **157 Suppl 2:**S40-44; 1998.

[23] Selhub, J.; Jacques, P. F.; Wilson, P. W.; Rush, D.; Rosenberg, I. H. Vitamin status and intake as primary determinants of homocysteinemia in an elderly population. *JAMA* **270:**2693-2698; 1993.

[24] Pastore, A.; De Angelis, S.; Casciani, S.; Ruggia, R.; Di Giovamberardino, G.; Noce, A.; Splendiani, G.; Cortese, C.; Federici, G.; Dessi, M. Effects of folic acid before and after vitamin B12 on plasma homocysteine concentrations in hemodialysis patients with known MTHFR genotypes. *Clin Chem* **52:**145-148; 2006.

[25] Bailey, L. B.; Gregory, J. F., 3rd. Polymorphisms of methylenetetrahydrofolate reductase and other enzymes: metabolic significance, risks and impact on folate requirement. *J Nutr* **129:**919-922; 1999.

[26] Brattstrom, L.; Lindgren, A.; Israelsson, B.; Malinow, M. R.; Norrving, B.; Upson, B.; Hamfelt, A. Hyperhomocysteinaemia in stroke: prevalence, cause, and relationships to type of stroke and stroke risk factors. *Eur J Clin Invest* **22:**214-221; 1992.

[27] Malinow, M. R.; Kang, S. S.; Taylor, L. M.; Wong, P. W.; Coull, B.; Inahara, T.; Mukerjee, D.; Sexton, G.; Upson, B. Prevalence of hyperhomocyst(e)inemia in patients with peripheral arterial occlusive disease. *Circulation* **79:**1180-1188; 1989.

[28] Malinow, M. R.; Levenson, J.; Giral, P.; Nieto, F. J.; Razavian, M.; Segond, P.; Simon, A. Role of blood pressure, uric acid, and hemorheological parameters on plasma homocyst(e)ine concentration. *Atherosclerosis* **114:**175-183; 1995.

[29] Nygard, O.; Vollset, S. E.; Refsum, H.; Stensvold, I.; Tverdal, A.; Nordrehaug, J. E.; Ueland, M.; Kvale, G. Total plasma homocysteine and cardiovascular risk profile. The Hordaland Homocysteine Study. *JAMA* **274:**1526-1533; 1995.

[30] Perry, I. J. Homocysteine, hypertension and stroke. *J Hum Hypertens* **13:**289-293; 1999.

[31] Brattstrom, L.; Wilcken, D. E. Homocysteine and cardiovascular disease: cause or effect? *Am J Clin Nutr* **72:**315-323; 2000.

[32] Wilcken, D. E.; Gupta, V. J.; Reddy, S. G. Accumulation of sulphur-containing amino acids including cysteine-homocysteine in patients on maintenance haemodialysis. *Clin Sci (Lond)* **58:**427-430; 1980.

[33] Arnadottir, M.; Hultberg, B.; Nilsson-Ehle, P.; Thysell, H. The effect of reduced glomerular filtration rate on plasma total homocysteine concentration. *Scand J Clin Lab Invest* **56:**41-46; 1996.

[34] Bostom, A. G.; Lathrop, L. Hyperhomocysteinemia in end-stage renal disease: prevalence, etiology, and potential relationship to arteriosclerotic outcomes. *Kidney Int* **52:**10-20; 1997.

[35] Kundu, S.; Tyagi, N.; Sen, U.; Tyagi, S. C. Matrix imbalance by inducing expression of metalloproteinase and oxidative stress in cochlea of hyperhomocysteinemic mice. *Mol Cell Biochem* **332:**215-224; 2009.

[36] Solini, A.; Santini, E.; Nannipieri, M.; Ferrannini, E. High glucose and homocysteine synergistically affect the metalloproteinases-tissue inhibitors of metalloproteinases pattern, but not TGFB expression, in human fibroblasts. *Diabetologia* **49:**2499-2506; 2006.

[37] Steed, M. M.; Tyagi, N.; Sen, U.; Schuschke, D. A.; Joshua, I. G.; Tyagi, S. C. Functional consequences of the collagen/elastin switch in vascular remodeling in hyperhomocysteinemic wild-type, eNOS-/-, and iNOS-/- mice. *Am J Physiol Lung Cell Mol Physiol* **299:**L301-311; 2010.

[38] Yi, F.; Xia, M.; Li, N.; Zhang, C.; Tang, L.; Li, P. L. Contribution of guanine nucleotide exchange factor Vav2 to hyperhomocysteinemic glomerulosclerosis in rats. *Hypertension* **53:**90-96; 2009.

[39] Gill, P. S.; Wilcox, C. S. NADPH oxidases in the kidney. *Antioxid Redox Signal* **8:**1597-1607; 2006.

[40] Jiang, F. NADPH oxidase in the kidney: a Janus in determining cell fate. *Kidney Int* **75:**135-137; 2009.

[41] McCully, K. S. Chemical pathology of homocysteine. IV. Excitotoxicity, oxidative stress, endothelial dysfunction, and inflammation. *Ann Clin Lab Sci* **39:**219-232; 2009.

[42] Upchurch, G. R., Jr.; Welch, G. N.; Fabian, A. J.; Freedman, J. E.; Johnson, J. L.; Keaney, J. F., Jr.; Loscalzo, J. Homocyst(e)ine decreases bioavailable nitric oxide by a mechanism involving glutathione peroxidase. *J Biol Chem* **272:**17012-17017; 1997.

[43] Upchurch, G. R., Jr.; Welch, G. N.; Fabian, A. J.; Pigazzi, A.; Keaney, J. F., Jr.; Loscalzo, J. Stimulation of endothelial nitric oxide production by homocyst(e)ine. *Atherosclerosis* **132:**177-185; 1997.

[44] Yi, F.; Chen, Q. Z.; Jin, S.; Li, P. L. Mechanism of homocysteine-induced Rac1/NADPH oxidase activation in mesangial cells: role of guanine nucleotide exchange factor Vav2. *Cell Physiol Biochem* **20:**909-918; 2007.

[45] Yi, F.; Jin, S.; Zhang, F.; Xia, M.; Bao, J. X.; Hu, J.; Poklis, J. L.; Li, P. L. Formation of lipid raft redox signalling platforms in glomerular endothelial cells: an early event of homocysteine-induced glomerular injury. *J Cell Mol Med* **13:**3303-3314; 2009.

[46] Zhang, C.; Hu, J. J.; Xia, M.; Boini, K. M.; Brimson, C.; Li, P. L. Redox signaling via lipid raft clustering in homocysteine-induced injury of podocytes. *Biochim Biophys Acta* **1803:**482-491; 2010.

[47] Edirimanne, V. E.; Woo, C. W.; Siow, Y. L.; Pierce, G. N.; Xie, J. Y.; O, K. Homocysteine stimulates NADPH oxidase-mediated superoxide production leading to endothelial dysfunction in rats. *Can J Physiol Pharmacol* **85:**1236-1247; 2007.

[48] Zhang, C.; Hu, J. J.; Xia, M.; Boini, K. M.; Brimson, C. A.; Laperle, L. A.; Li, P. L. Protection of podocytes from hyperhomocysteinemia-induced injury by deletion of the gp91phox gene. *Free Radic Biol Med* **48:**1109-1117; 2010.

[49] Zhang, C.; Boini, K. M.; Xia, M.; Abais, J. M.; Li, X.; Liu, Q.; Li, P. L. Activation of Nod-like receptor protein 3 inflammasomes turns on podocyte injury and glomerular sclerosis in hyperhomocysteinemia. *Hypertension* **60:**154-162; 2012.

[50] Watanabe, M.; Osada, J.; Aratani, Y.; Kluckman, K.; Reddick, R.; Malinow, M. R.; Maeda, N. Mice deficient in cystathionine beta-synthase: animal models for mild and severe homocyst(e)inemia. *Proc Natl Acad Sci U S A* **92:**1585-1589; 1995.

[51] Mudd, S. H.; Skovby, F.; Levy, H. L.; Pettigrew, K. D.; Wilcken, B.; Pyeritz, R. E.; Andria, G.; Boers, G. H.; Bromberg, I. L.; Cerone, R.; et al. The natural history of homocystinuria due to cystathionine beta-synthase deficiency. *Am J Hum Genet* **37:**1-31; 1985.

[52] Jiang, X.; Yang, F.; Tan, H.; Liao, D.; Bryan, R. M., Jr.; Randhawa, J. K.; Rumbaut, R. E.; Durante, W.; Schafer, A. I.; Yang, X.; Wang, H. Hyperhomocystinemia impairs endothelial function and eNOS activity via PKC activation. *Arterioscler Thromb Vasc Biol* **25:**2515-2521; 2005.

[53] Schwahn, B. C.; Laryea, M. D.; Chen, Z.; Melnyk, S.; Pogribny, I.; Garrow, T.; James, S. J.; Rozen, R. Betaine rescue of an animal model with methylenetetrahydrofolate reductase deficiency. *Biochem J* **382:**831-840; 2004.

[54] Chen, Z.; Karaplis, A. C.; Ackerman, S. L.; Pogribny, I. P.; Melnyk, S.; Lussier-Cacan, S.; Chen, M. F.; Pai, A.; John, S. W.; Smith, R. S.; Bottiglieri, T.; Bagley, P.; Selhub, J.; Rudnicki, M. A.; James, S. J.; Rozen, R. Mice deficient in methylenetetrahydrofolate

reductase exhibit hyperhomocysteinemia and decreased methylation capacity, with neuropathology and aortic lipid deposition. *Hum Mol Genet* **10:**433-443; 2001.

[55] Swanson, D. A.; Liu, M. L.; Baker, P. J.; Garrett, L.; Stitzel, M.; Wu, J.; Harris, M.; Banerjee, R.; Shane, B.; Brody, L. C. Targeted disruption of the methionine synthase gene in mice. *Mol Cell Biol* **21:**1058-1065; 2001.

[56] Lentz, S. R.; Haynes, W. G. Homocysteine: is it a clinically important cardiovascular risk factor? *Cleve Clin J Med* **71:**729-734; 2004.

[57] Bylund, J.; Brown, K. L.; Movitz, C.; Dahlgren, C.; Karlsson, A. Intracellular generation of superoxide by the phagocyte NADPH oxidase: how, where, and what for? *Free Radic Biol Med* **49:**1834-1845; 2010.

[58] Lambeth, J. D. NOX enzymes and the biology of reactive oxygen. *Nat Rev Immunol* **4:**181-189; 2004.

[59] Cai, H.; Griendling, K. K.; Harrison, D. G. The vascular NAD(P)H oxidases as therapeutic targets in cardiovascular diseases. *Trends Pharmacol Sci* **24:**471-478; 2003.

[60] Griendling, K. K.; Sorescu, D.; Lassegue, B.; Ushio-Fukai, M. Modulation of protein kinase activity and gene expression by reactive oxygen species and their role in vascular physiology and pathophysiology. *Arterioscler Thromb Vasc Biol* **20:**2175-2183; 2000.

[61] Bayraktutan, U.; Blayney, L.; Shah, A. M. Molecular characterization and localization of the NAD(P)H oxidase components gp91-phox and p22-phox in endothelial cells. *Arterioscler Thromb Vasc Biol* **20:**1903-1911; 2000.

[62] Zou, A. P.; Cowley, A. W., Jr. Reactive oxygen species and molecular regulation of renal oxygenation. *Acta Physiol Scand* **179:**233-241; 2003.

[63] Lee, H. B.; Yu, M. R.; Yang, Y.; Jiang, Z.; Ha, H. Reactive oxygen species-regulated signaling pathways in diabetic nephropathy. *J Am Soc Nephrol* **14:**S241-245; 2003.

[64] Malinowska, J.; Olas, B. Effect of resveratrol on hemostatic properties of human fibrinogen and plasma during model of hyperhomocysteinemia. *Thromb Res* **126:**e379-382; 2010.

[65] Yi, F.; Zhang, A. Y.; Janscha, J. L.; Li, P. L.; Zou, A. P. Homocysteine activates NADH/NADPH oxidase through ceramide-stimulated Rac GTPase activity in rat mesangial cells. *Kidney Int* **66:**1977-1987; 2004.

[66] Takeya, R.; Sumimoto, H. Regulation of novel superoxide-producing NAD(P)H oxidases. *Antioxid Redox Signal* **8:**1523-1532; 2006.

[67] Bokoch, G. M.; Diebold, B. A. Current molecular models for NADPH oxidase regulation by Rac GTPase. *Blood* **100:**2692-2696; 2002.

[68] Hordijk, P. L. Regulation of NADPH oxidases: the role of Rac proteins. *Circ Res* **98:**453-462; 2006.

[69] Evers, E. E.; Zondag, G. C.; Malliri, A.; Price, L. S.; ten Klooster, J. P.; van der Kammen, R. A.; Collard, J. G. Rho family proteins in cell adhesion and cell migration. *Eur J Cancer* **36:**1269-1274; 2000.

[70] Etienne-Manneville, S.; Hall, A. Rho GTPases in cell biology. *Nature* **420:**629-635; 2002.

[71] Ippagunta, S. K.; Malireddi, R. K.; Shaw, P. J.; Neale, G. A.; Vande Walle, L.; Green, D. R.; Fukui, Y.; Lamkanfi, M.; Kanneganti, T. D. The inflammasome adaptor ASC regulates the function of adaptive immune cells by controlling Dock2-mediated Rac activation and actin polymerization. *Nat Immunol* **12:**1010-1016; 2011.

[72] Abo, A.; Pick, E.; Hall, A.; Totty, N.; Teahan, C. G.; Segal, A. W. Activation of the NADPH oxidase involves the small GTP-binding protein p21rac1. *Nature* **353:**668-670; 1991.

[73] Werner, E. GTPases and reactive oxygen species: switches for killing and signaling. *J Cell Sci* **117:**143-153; 2004.

[74] Ming, W.; Li, S.; Billadeau, D. D.; Quilliam, L. A.; Dinauer, M. C. The Rac effector p67phox regulates phagocyte NADPH oxidase by stimulating Vav1 guanine nucleotide exchange activity. *Mol Cell Biol* **27:**312-323; 2007.

[75] Hornstein, I.; Alcover, A.; Katzav, S. Vav proteins, masters of the world of cytoskeleton organization. *Cell Signal* **16:**1-11; 2004.

[76] Miletic, A. V.; Graham, D. B.; Montgrain, V.; Fujikawa, K.; Kloeppel, T.; Brim, K.; Weaver, B.; Schreiber, R.; Xavier, R.; Swat, W. Vav proteins control MyD88-dependent oxidative burst. *Blood* **109:**3360-3368; 2007.

[77] Utomo, A.; Cullere, X.; Glogauer, M.; Swat, W.; Mayadas, T. N. Vav proteins in neutrophils are required for FcgammaR-mediated signaling to Rac GTPases and nicotinamide adenine dinucleotide phosphate oxidase component p40(phox). *J Immunol* **177:**6388-6397; 2006.

[78] Geiszt, M.; Kopp, J. B.; Varnai, P.; Leto, T. L. Identification of renox, an NAD(P)H oxidase in kidney. *Proc Natl Acad Sci U S A* **97:**8010-8014; 2000.

[79] Banfi, B.; Molnar, G.; Maturana, A.; Steger, K.; Hegedus, B.; Demaurex, N.; Krause, K. H. A Ca(2+)-activated NADPH oxidase in testis, spleen, and lymph nodes. *J Biol Chem* **276:**37594-37601; 2001.

[80] Sedeek, M.; Nasrallah, R.; Touyz, R. M.; Hebert, R. L. NADPH oxidases, reactive oxygen species, and the kidney: friend and foe. *J Am Soc Nephrol* **24:**1512-1518; 2013.

[81] Winiarska, K.; Grabowski, M.; Rogacki, M. K. Inhibition of renal gluconeogenesis contributes to hypoglycaemic action of NADPH oxidase inhibitor, apocynin. *Chem Biol Interact* **189:**119-126; 2011.

[82] Han, H. J.; Lee, Y. J.; Park, S. H.; Lee, J. H.; Taub, M. High glucose-induced oxidative stress inhibits Na+/glucose cotransporter activity in renal proximal tubule cells. *Am J Physiol Renal Physiol* **288:**F988-996; 2005.

[83] Liu, R.; Ren, Y.; Garvin, J. L.; Carretero, O. A. Superoxide enhances tubuloglomerular feedback by constricting the afferent arteriole. *Kidney Int* **66:**268-274; 2004.

[84] Silva, E.; Soares-da-Silva, P. Reactive oxygen species and the regulation of renal Na+-K+-ATPase in opossum kidney cells. *Am J Physiol Regul Integr Comp Physiol* **293:**R1764-1770; 2007.

[85] Silva, G. B.; Garvin, J. L. Rac1 mediates NaCl-induced superoxide generation in the thick ascending limb. *Am J Physiol Renal Physiol* **298:**F421-425; 2010.

[86] Mamenko, M.; Zaika, O.; Ilatovskaya, D. V.; Staruschenko, A.; Pochynyuk, O. Angiotensin II increases activity of the epithelial Na+ channel (ENaC) in distal nephron additively to aldosterone. *J Biol Chem* **287:**660-671; 2012.

[87] Kitiyakara, C.; Chabrashvili, T.; Chen, Y.; Blau, J.; Karber, A.; Aslam, S.; Welch, W. J.; Wilcox, C. S. Salt intake, oxidative stress, and renal expression of NADPH oxidase and superoxide dismutase. *J Am Soc Nephrol* **14:**2775-2782; 2003.

[88] Lerman, L. O.; Nath, K. A.; Rodriguez-Porcel, M.; Krier, J. D.; Schwartz, R. S.; Napoli, C.; Romero, J. C. Increased oxidative stress in experimental renovascular hypertension. *Hypertension* **37:**541-546; 2001.

[89] Fukuda, M.; Nakamura, T.; Kataoka, K.; Nako, H.; Tokutomi, Y.; Dong, Y. F.; Ogawa, H.; Kim-Mitsuyama, S. Potentiation by candesartan of protective effects of pioglitazone against type 2 diabetic cardiovascular and renal complications in obese mice. *J Hypertens* **28:**340-352; 2010.

[90] Huang, A.; Sun, D.; Kaley, G.; Koller, A. Superoxide released to high intra-arteriolar pressure reduces nitric oxide-mediated shear stress- and agonist-induced dilations. *Circ Res* **83:**960-965; 1998.

[91] Katusic, Z. S.; Vanhoutte, P. M. Superoxide anion is an endothelium-derived contracting factor. *Am J Physiol* **257:**H33-37; 1989.

[92] Zou, A. P.; Li, N.; Cowley, A. W., Jr. Production and actions of superoxide in the renal medulla. *Hypertension* **37:**547-553; 2001.

[93] O'Connor, W., Jr.; Harton, J. A.; Zhu, X.; Linhoff, M. W.; Ting, J. P. Cutting edge: CIAS1/cryopyrin/PYPAF1/NALP3/CATERPILLER 1.1 is an inducible inflammatory mediator with NF-kappa B suppressive properties. *J Immunol* **171:**6329-6333; 2003.

[94] Martinon, F.; Agostini, L.; Meylan, E.; Tschopp, J. Identification of bacterial muramyl dipeptide as activator of the NALP3/cryopyrin inflammasome. *Curr Biol* **14:**1929-1934; 2004.

[95] Petrilli, V.; Martinon, F. The inflammasome, autoinflammatory diseases, and gout. *Joint Bone Spine* **74:**571-576; 2007.

[96] Yin, Y.; Pastrana, J. L.; Li, X.; Huang, X.; Mallilankaraman, K.; Choi, E. T.; Madesh, M.; Wang, H.; Yang, X. F. Inflammasomes: sensors of metabolic stresses for vascular inflammation. *Front Biosci (Landmark Ed)* **18:**638-649; 2013.

[97] Bakker, P. J.; Butter, L. M.; Kors, L.; Teske, G. J.; Aten, J.; Sutterwala, F. S.; Florquin, S.; Leemans, J. C. Nlrp3 is a key modulator of diet-induced nephropathy and renal cholesterol accumulation. *Kidney Int*; 2013.

[98] Martinon, F.; Tschopp, J. NLRs join TLRs as innate sensors of pathogens. *Trends Immunol* **26:**447-454; 2005.

[99] Sutterwala, F. S.; Ogura, Y.; Flavell, R. A. The inflammasome in pathogen recognition and inflammation. *J Leukoc Biol* **82:**259-264; 2007.

[100] Yang, F.; Wang, Z.; Wei, X.; Han, H.; Meng, X.; Zhang, Y.; Shi, W.; Li, F.; Xin, T.; Pang, Q.; Yi, F. NLRP3 deficiency ameliorates neurovascular damage in experimental ischemic stroke. *J Cereb Blood Flow Metab*; 2014.

[101] Masters, S. L. Specific inflammasomes in complex diseases. *Clin Immunol* **147:**223-228; 2013.

[102] Martinon, F.; Burns, K.; Tschopp, J. The inflammasome: a molecular platform triggering activation of inflammatory caspases and processing of proIL-beta. *Mol Cell* **10:**417-426; 2002.

[103] Bauernfeind, F.; Ablasser, A.; Bartok, E.; Kim, S.; Schmid-Burgk, J.; Cavlar, T.; Hornung, V. Inflammasomes: current understanding and open questions. *Cell Mol Life Sci* **68:**765-783; 2011.

[104] Dinarello, C. A. Immunological and inflammatory functions of the interleukin-1 family. *Annu Rev Immunol* **27:**519-550; 2009.

[105] Faustin, B.; Lartigue, L.; Bruey, J. M.; Luciano, F.; Sergienko, E.; Bailly-Maitre, B.; Volkmann, N.; Hanein, D.; Rouiller, I.; Reed, J. C. Reconstituted NALP1 inflammasome reveals two-step mechanism of caspase-1 activation. *Mol Cell* **25:**713-724; 2007.

[106] Boyden, E. D.; Dietrich, W. F. Nalp1b controls mouse macrophage susceptibility to anthrax lethal toxin. *Nat Genet* **38:**240-244; 2006.

[107] Kofoed, E. M.; Vance, R. E. Innate immune recognition of bacterial ligands by NAIPs determines inflammasome specificity. *Nature* **477:**592-595; 2011.

[108] Miao, E. A.; Mao, D. P.; Yudkovsky, N.; Bonneau, R.; Lorang, C. G.; Warren, S. E.; Leaf, I. A.; Aderem, A. Innate immune detection of the type III secretion apparatus through the NLRC4 inflammasome. *Proc Natl Acad Sci U S A* **107:**3076-3080; 2010.

[109] Zhao, Y.; Yang, J.; Shi, J.; Gong, Y. N.; Lu, Q.; Xu, H.; Liu, L.; Shao, F. The NLRC4 inflammasome receptors for bacterial flagellin and type III secretion apparatus. *Nature* **477:**596-600; 2011.

[110] Hornung, V.; Ablasser, A.; Charrel-Dennis, M.; Bauernfeind, F.; Horvath, G.; Caffrey, D. R.; Latz, E.; Fitzgerald, K. A. AIM2 recognizes cytosolic dsDNA and forms a caspase-1-activating inflammasome with ASC. *Nature* **458:**514-518; 2009.

[111] Cassel, S. L.; Sutterwala, F. S. Sterile inflammatory responses mediated by the NLRP3 inflammasome. *Eur J Immunol* **40:**607-611; 2010.

[112] Ichinohe, T.; Lee, H. K.; Ogura, Y.; Flavell, R.; Iwasaki, A. Inflammasome recognition of influenza virus is essential for adaptive immune responses. *J Exp Med* **206:**79-87; 2009.

[113] Thomas, P. G.; Dash, P.; Aldridge, J. R., Jr.; Ellebedy, A. H.; Reynolds, C.; Funk, A. J.; Martin, W. J.; Lamkanfi, M.; Webby, R. J.; Boyd, K. L.; Doherty, P. C.; Kanneganti, T. D. The intracellular sensor NLRP3 mediates key innate and healing responses to influenza A virus via the regulation of caspase-1. *Immunity* **30:**566-575; 2009.

[114] Muruve, D. A.; Petrilli, V.; Zaiss, A. K.; White, L. R.; Clark, S. A.; Ross, P. J.; Parks, R. J.; Tschopp, J. The inflammasome recognizes cytosolic microbial and host DNA and triggers an innate immune response. *Nature* **452:**103-107; 2008.

[115] Mariathasan, S.; Weiss, D. S.; Newton, K.; McBride, J.; O'Rourke, K.; Roose-Girma, M.; Lee, W. P.; Weinrauch, Y.; Monack, D. M.; Dixit, V. M. Cryopyrin activates the inflammasome in response to toxins and ATP. *Nature* **440:**228-232; 2006.

[116] Duncan, J. A.; Gao, X.; Huang, M. T.; O'Connor, B. P.; Thomas, C. E.; Willingham, S. B.; Bergstralh, D. T.; Jarvis, G. A.; Sparling, P. F.; Ting, J. P. Neisseria gonorrhoeae activates the proteinase cathepsin B to mediate the signaling activities of the NLRP3 and ASC-containing inflammasome. *J Immunol* **182:**6460-6469; 2009.

[117] Joly, S.; Ma, N.; Sadler, J. J.; Soll, D. R.; Cassel, S. L.; Sutterwala, F. S. Cutting edge: Candida albicans hyphae formation triggers activation of the Nlrp3 inflammasome. *J Immunol* **183:**3578-3581; 2009.

[118] Martinon, F.; Petrilli, V.; Mayor, A.; Tardivel, A.; Tschopp, J. Gout-associated uric acid crystals activate the NALP3 inflammasome. *Nature* **440:**237-241; 2006.

[119] Hornung, V.; Bauernfeind, F.; Halle, A.; Samstad, E. O.; Kono, H.; Rock, K. L.; Fitzgerald, K. A.; Latz, E. Silica crystals and aluminum salts activate the NALP3 inflammasome through phagosomal destabilization. *Nat Immunol* **9:**847-856; 2008.

[120] Dostert, C.; Petrilli, V.; Van Bruggen, R.; Steele, C.; Mossman, B. T.; Tschopp, J. Innate immune activation through Nalp3 inflammasome sensing of asbestos and silica. *Science* **320:**674-677; 2008.

[121] Pelegrin, P.; Surprenant, A. Pannexin-1 mediates large pore formation and interleukin-1beta release by the ATP-gated P2X7 receptor. *EMBO J* **25:**5071-5082; 2006.

[122] Halle, A.; Hornung, V.; Petzold, G. C.; Stewart, C. R.; Monks, B. G.; Reinheckel, T.; Fitzgerald, K. A.; Latz, E.; Moore, K. J.; Golenbock, D. T. The NALP3 inflammasome is involved in the innate immune response to amyloid-beta. *Nat Immunol* **9:**857-865; 2008.

[123] Griffin, W. S.; Stanley, L. C.; Ling, C.; White, L.; MacLeod, V.; Perrot, L. J.; White, C. L., 3rd; Araoz, C. Brain interleukin 1 and S-100 immunoreactivity are elevated in Down syndrome and Alzheimer disease. *Proc Natl Acad Sci U S A* **86:**7611-7615; 1989.

[124] Duewell, P.; Kono, H.; Rayner, K. J.; Sirois, C. M.; Vladimer, G.; Bauernfeind, F. G.; Abela, G. S.; Franchi, L.; Nunez, G.; Schnurr, M.; Espevik, T.; Lien, E.; Fitzgerald, K. A.; Rock, K. L.; Moore, K. J.; Wright, S. D.; Hornung, V.; Latz, E. NLRP3 inflammasomes are required for atherogenesis and activated by cholesterol crystals. *Nature* **464:**1357-1361; 2010.

[125] Yamasaki, K.; Muto, J.; Taylor, K. R.; Cogen, A. L.; Audish, D.; Bertin, J.; Grant, E. P.; Coyle, A. J.; Misaghi, A.; Hoffman, H. M.; Gallo, R. L. NLRP3/cryopyrin is necessary for interleukin-1beta (IL-1beta) release in response to hyaluronan, an endogenous trigger of inflammation in response to injury. *J Biol Chem* **284:**12762-12771; 2009.

[126] Zhou, R.; Tardivel, A.; Thorens, B.; Choi, I.; Tschopp, J. Thioredoxin-interacting protein links oxidative stress to inflammasome activation. *Nat Immunol* **11:**136-140; 2010.

[127] Watanabe, H.; Gaide, O.; Petrilli, V.; Martinon, F.; Contassot, E.; Roques, S.; Kummer, J. A.; Tschopp, J.; French, L. E. Activation of the IL-1beta-processing inflammasome is involved in contact hypersensitivity. *J Invest Dermatol* **127:**1956-1963; 2007.

[128] Nishi, Y.; Satoh, M.; Nagasu, H.; Kadoya, H.; Ihoriya, C.; Kidokoro, K.; Sasaki, T.; Kashihara, N. Selective estrogen receptor modulation attenuates proteinuria-induced renal tubular damage by modulating mitochondrial oxidative status. *Kidney Int* **83:**662-673; 2013.

[129] Wang, C.; Pan, Y.; Zhang, Q. Y.; Wang, F. M.; Kong, L. D. Quercetin and allopurinol ameliorate kidney injury in STZ-treated rats with regulation of renal NLRP3 inflammasome activation and lipid accumulation. *PLoS One* **7:**e38285; 2012.

[130] Wang, W.; Wang, X.; Chun, J.; Vilaysane, A.; Clark, S.; French, G.; Bracey, N. A.; Trpkov, K.; Bonni, S.; Duff, H. J.; Beck, P. L.; Muruve, D. A. Inflammasome-independent NLRP3 augments TGF-beta signaling in kidney epithelium. *J Immunol* **190:**1239-1249; 2013.

[131] Spranger, J.; Kroke, A.; Mohlig, M.; Hoffmann, K.; Bergmann, M. M.; Ristow, M.; Boeing, H.; Pfeiffer, A. F. Inflammatory cytokines and the risk to develop type 2 diabetes: results of the prospective population-based European Prospective Investigation into Cancer and Nutrition (EPIC)-Potsdam Study. *Diabetes* **52:**812-817; 2003.

[132] Larsen, C. M.; Faulenbach, M.; Vaag, A.; Volund, A.; Ehses, J. A.; Seifert, B.; Mandrup-Poulsen, T.; Donath, M. Y. Interleukin-1-receptor antagonist in type 2 diabetes mellitus. *N Engl J Med* **356:**1517-1526; 2007.

[133] Stienstra, R.; Joosten, L. A.; Koenen, T.; van Tits, B.; van Diepen, J. A.; van den Berg, S. A.; Rensen, P. C.; Voshol, P. J.; Fantuzzi, G.; Hijmans, A.; Kersten, S.; Muller, M.; van den Berg, W. B.; van Rooijen, N.; Wabitsch, M.; Kullberg, B. J.; van der Meer, J. W.; Kanneganti, T.; Tack, C. J.; Netea, M. G. The inflammasome-mediated caspase-1 activation controls adipocyte differentiation and insulin sensitivity. *Cell Metab* **12:**593-605; 2010.

[134] Vandanmagsar, B.; Youm, Y. H.; Ravussin, A.; Galgani, J. E.; Stadler, K.; Mynatt, R. L.; Ravussin, E.; Stephens, J. M.; Dixit, V. D. The NLRP3 inflammasome instigates obesity-induced inflammation and insulin resistance. *Nat Med* **17:**179-188; 2011.

[135] Frantz, S.; Ducharme, A.; Sawyer, D.; Rohde, L. E.; Kobzik, L.; Fukazawa, R.; Tracey, D.; Allen, H.; Lee, R. T.; Kelly, R. A. Targeted deletion of caspase-1 reduces early mortality and left ventricular dilatation following myocardial infarction. *J Mol Cell Cardiol* **35:**685-694; 2003.

[136] Syed, F. M.; Hahn, H. S.; Odley, A.; Guo, Y.; Vallejo, J. G.; Lynch, R. A.; Mann, D. L.; Bolli, R.; Dorn, G. W., 2nd. Proapoptotic effects of caspase-1/interleukin-converting enzyme dominate in myocardial ischemia. *Circ Res* **96:**1103-1109; 2005.

[137] Kawaguchi, M.; Takahashi, M.; Hata, T.; Kashima, Y.; Usui, F.; Morimoto, H.; Izawa, A.; Takahashi, Y.; Masumoto, J.; Koyama, J.; Hongo, M.; Noda, T.; Nakayama, J.; Sagara, J.; Taniguchi, S.; Ikeda, U. Inflammasome activation of cardiac fibroblasts is essential for myocardial ischemia/reperfusion injury. *Circulation* **123:**594-604; 2011.

[138] Iyer, S. S.; Pulskens, W. P.; Sadler, J. J.; Butter, L. M.; Teske, G. J.; Ulland, T. K.; Eisenbarth, S. C.; Florquin, S.; Flavell, R. A.; Leemans, J. C.; Sutterwala, F. S. Necrotic cells trigger a sterile inflammatory response through the Nlrp3 inflammasome. *Proc Natl Acad Sci U S A* **106:**20388-20393; 2009.

[139] Vilaysane, A.; Chun, J.; Seamone, M. E.; Wang, W.; Chin, R.; Hirota, S.; Li, Y.; Clark, S. A.; Tschopp, J.; Trpkov, K.; Hemmelgarn, B. R.; Beck, P. L.; Muruve, D. A. The NLRP3 inflammasome promotes renal inflammation and contributes to CKD. *J Am Soc Nephrol* **21:**1732-1744; 2010.

[140] Matsumoto, K.; Kanmatsuse, K. Elevated interleukin-18 levels in the urine of nephrotic patients. *Nephron* **88:**334-339; 2001.

[141] Sassy-Prigent, C.; Heudes, D.; Mandet, C.; Belair, M. F.; Michel, O.; Perdereau, B.; Bariety, J.; Bruneval, P. Early glomerular macrophage recruitment in streptozotocin-induced diabetic rats. *Diabetes* **49:**466-475; 2000.

[142] Niemir, Z. I.; Stein, H.; Dworacki, G.; Mundel, P.; Koehl, N.; Koch, B.; Autschbach, F.; Andrassy, K.; Ritz, E.; Waldherr, R.; Otto, H. F. Podocytes are the major source of IL-1 alpha and IL-1 beta in human glomerulonephritides. *Kidney Int* **52:**393-403; 1997.

[143] Benko, S.; Philpott, D. J.; Girardin, S. E. The microbial and danger signals that activate Nod-like receptors. *Cytokine* **43:**368-373; 2008.

[144] Henao-Mejia, J.; Elinav, E.; Jin, C.; Hao, L.; Mehal, W. Z.; Strowig, T.; Thaiss, C. A.; Kau, A. L.; Eisenbarth, S. C.; Jurczak, M. J.; Camporez, J. P.; Shulman, G. I.; Gordon, J. I.; Hoffman, H. M.; Flavell, R. A. Inflammasome-mediated dysbiosis regulates progression of NAFLD and obesity. *Nature* **482:**179-185; 2012.

[145] Overley-Adamson, B.; Artlett, C. M.; Stephens, C.; Sassi-Gaha, S.; Weis, R. D.; Thacker, J. D. Targeting the unfolded protein response, XBP1, and the NLRP3 inflammasome in fibrosis and cancer. *Cancer Biol Ther* **15**; 2014.

[146] Mariathasan, S. ASC, Ipaf and Cryopyrin/Nalp3: bona fide intracellular adapters of the caspase-1 inflammasome. *Microbes Infect* **9:**664-671; 2007.

[147] Bauernfeind, F. G.; Horvath, G.; Stutz, A.; Alnemri, E. S.; MacDonald, K.; Speert, D.; Fernandes-Alnemri, T.; Wu, J.; Monks, B. G.; Fitzgerald, K. A.; Hornung, V.; Latz, E. Cutting edge: NF-kappaB activating pattern recognition and cytokine receptors license NLRP3 inflammasome activation by regulating NLRP3 expression. *J Immunol* **183:**787-791; 2009.

[148] Surprenant, A.; Rassendren, F.; Kawashima, E.; North, R. A.; Buell, G. The cytolytic P2Z receptor for extracellular ATP identified as a P2X receptor (P2X7). *Science* **272:**735-738; 1996.

[149] Tschopp, J.; Schroder, K. NLRP3 inflammasome activation: The convergence of multiple signalling pathways on ROS production? *Nat Rev Immunol* **10:**210-215; 2010.

[150] Bae, J. Y.; Park, H. H. Crystal structure of NALP3 protein pyrin domain (PYD) and its implications in inflammasome assembly. *J Biol Chem* **286:**39528-39536; 2011.

[151] Cruz, C. M.; Rinna, A.; Forman, H. J.; Ventura, A. L.; Persechini, P. M.; Ojcius, D. M. ATP activates a reactive oxygen species-dependent oxidative stress response and secretion of proinflammatory cytokines in macrophages. *J Biol Chem* **282:**2871-2879; 2007.

[152] Hewinson, J.; Moore, S. F.; Glover, C.; Watts, A. G.; MacKenzie, A. B. A key role for redox signaling in rapid P2X7 receptor-induced IL-1 beta processing in human monocytes. *J Immunol* **180:**8410-8420; 2008.

[153] Wen, H.; Gris, D.; Lei, Y.; Jha, S.; Zhang, L.; Huang, M. T.; Brickey, W. J.; Ting, J. P. Fatty acid-induced NLRP3-ASC inflammasome activation interferes with insulin signaling. *Nat Immunol* **12:**408-415; 2011.

[154] Alvarez, S.; Munoz-Fernandez, M. A. TNF-Alpha may mediate inflammasome activation in the absence of bacterial infection in more than one way. *PLoS One* **8:**e71477; 2013.

[155] Xiao, H.; Lu, M.; Lin, T. Y.; Chen, Z.; Chen, G.; Wang, W. C.; Marin, T.; Shentu, T. P.; Wen, L.; Gongol, B.; Sun, W.; Liang, X.; Chen, J.; Huang, H. D.; Pedra, J. H.; Johnson, D. A.; Shyy, J. Y. Sterol regulatory element binding protein 2 activation of NLRP3 inflammasome in endothelium mediates hemodynamic-induced atherosclerosis susceptibility. *Circulation* **128:**632-642; 2013.

[156] Bauernfeind, F.; Bartok, E.; Rieger, A.; Franchi, L.; Nunez, G.; Hornung, V. Cutting edge: reactive oxygen species inhibitors block priming, but not activation, of the NLRP3 inflammasome. *J Immunol* **187:**613-617; 2011.

[157] van Bruggen, R.; Koker, M. Y.; Jansen, M.; van Houdt, M.; Roos, D.; Kuijpers, T. W.; van den Berg, T. K. Human NLRP3 inflammasome activation is Nox1-4 independent. *Blood* **115:**5398-5400; 2010.

[158] Wu, J.; Yan, Z.; Schwartz, D. E.; Yu, J.; Malik, A. B.; Hu, G. Activation of NLRP3 inflammasome in alveolar macrophages contributes to mechanical stretch-induced lung inflammation and injury. *J Immunol* **190:**3590-3599; 2013.

[159] Zhou, R.; Yazdi, A. S.; Menu, P.; Tschopp, J. A role for mitochondria in NLRP3 inflammasome activation. *Nature* **469:**221-225; 2011.

[160] Bulua, A. C.; Simon, A.; Maddipati, R.; Pelletier, M.; Park, H.; Kim, K. Y.; Sack, M. N.; Kastner, D. L.; Siegel, R. M. Mitochondrial reactive oxygen species promote production of proinflammatory cytokines and are elevated in TNFR1-associated periodic syndrome (TRAPS). *J Exp Med* **208:**519-533; 2011.

[161] Liu, B. P.; Burridge, K. Vav2 activates Rac1, Cdc42, and RhoA downstream from growth factor receptors but not beta1 integrins. *Mol Cell Biol* **20:**7160-7169; 2000.

[162] Yi, F.; Zhang, A. Y.; Li, N.; Muh, R. W.; Fillet, M.; Renert, A. F.; Li, P. L. Inhibition of ceramide-redox signaling pathway blocks glomerular injury in hyperhomocysteinemic rats. *Kidney Int* **70:**88-96; 2006.

[163] Neuman, J. C.; Albright, K. A.; Schalinske, K. L. Exercise prevents hyperhomocysteinemia in a dietary folate-restricted mouse model. *Nutr Res* **33:**487-493; 2013.

[164] Jackson, E. K.; Gillespie, D. G.; Zhu, C.; Ren, J.; Zacharia, L. C.; Mi, Z. Alpha2-adrenoceptors enhance angiotensin II-induced renal vasoconstriction: role for NADPH oxidase and RhoA. *Hypertension* **51:**719-726; 2008.

[165] Rey, F. E.; Cifuentes, M. E.; Kiarash, A.; Quinn, M. T.; Pagano, P. J. Novel competitive inhibitor of NAD(P)H oxidase assembly attenuates vascular O(2)(-) and systolic blood pressure in mice. *Circ Res* **89:**408-414; 2001.

[166] Nishiyama, A.; Yoshizumi, M.; Hitomi, H.; Kagami, S.; Kondo, S.; Miyatake, A.; Fukunaga, M.; Tamaki, T.; Kiyomoto, H.; Kohno, M.; Shokoji, T.; Kimura, S.; Abe, Y.

The SOD mimetic tempol ameliorates glomerular injury and reduces mitogen-activated protein kinase activity in Dahl salt-sensitive rats. *J Am Soc Nephrol* **15:**306-315; 2004.

[167] Sousa, T.; Oliveira, S.; Afonso, J.; Morato, M.; Patinha, D.; Fraga, S.; Carvalho, F.; Albino-Teixeira, A. Role of H(2)O(2) in hypertension, renin-angiotensin system activation and renal medullary disfunction caused by angiotensin II. *Br J Pharmacol* **166:**2386-2401; 2012.

[168] Chen, J.; Cha-Molstad, H.; Szabo, A.; Shalev, A. Diabetes induces and calcium channel blockers prevent cardiac expression of proapoptotic thioredoxin-interacting protein. *Am J Physiol Endocrinol Metab* **296:**E1133-1139; 2009.

[169] Abais, J. M.; Zhang, C.; Xia, M.; Liu, Q.; Gehr, T. W.; Boini, K. M.; Li, P. L. NADPH oxidase-mediated triggering of inflammasome activation in mouse podocytes and glomeruli during hyperhomocysteinemia. *Antioxid Redox Signal* **18:**1537-1548; 2013.

[170] Abais, J. M.; Xia, M.; Li, G.; Gehr, T. W.; Boini, K. M.; Li, P. L. Contribution of endogenously produced reactive oxygen species to the activation of podocyte NLRP3 inflammasomes in hyperhomocysteinemia. *Free Radic Biol Med* **67:**211-220; 2014.

[171] Boini, K. M.; Xia, M.; Li, C.; Zhang, C.; Payne, L. P.; Abais, J. M.; Poklis, J. L.; Hylemon, P. B.; Li, P. L. Acid sphingomyelinase gene deficiency ameliorates the hyperhomocysteinemia-induced glomerular injury in mice. *Am J Pathol* **179:**2210-2219; 2011.

[172] Zhang, C.; Xia, M.; Boini, K. M.; Li, C. X.; Abais, J. M.; Li, X. X.; Laperle, L. A.; Li, P. L. Epithelial-to-mesenchymal transition in podocytes mediated by activation of NADPH oxidase in hyperhomocysteinemia. *Pflugers Arch* **462:**455-467; 2011.

[173] Yang, L.; Zheng, S.; Epstein, P. N. Metallothionein over-expression in podocytes reduces adriamycin nephrotoxicity. *Free Radic Res* **43:**174-182; 2009.

[174] De Miguel, C.; Guo, C.; Lund, H.; Feng, D.; Mattson, D. L. Infiltrating T lymphocytes in the kidney increase oxidative stress and participate in the development of hypertension and renal disease. *Am J Physiol Renal Physiol* **300:**F734-742; 2011.

[175] Li, N.; Yi, F.; dos Santos, E. A.; Donley, D. K.; Li, P. L. Role of renal medullary heme oxygenase in the regulation of pressure natriuresis and arterial blood pressure. *Hypertension* **49:**148-154; 2007.

[176] Boini, K. M.; Xia, M.; Xiong, J.; Li, C.; Payne, L. P.; Li, P. L. Implication of CD38 gene in podocyte epithelial-to-mesenchymal transition and glomerular sclerosis. *J Cell Mol Med* **16:**1674-1685; 2012.

[177] Raij, L.; Azar, S.; Keane, W. Mesangial immune injury, hypertension, and progressive glomerular damage in Dahl rats. *Kidney Int* **26:**137-143; 1984.

[178] Chen, Y. F.; Li, P. L.; Zou, A. P. Effect of hyperhomocysteinemia on plasma or tissue adenosine levels and renal function. *Circulation* **106:**1275-1281; 2002.

[179] Boini, K. M.; Xia, M.; Abais, J. M.; Xu, M.; Li, C. X.; Li, P. L. Acid sphingomyelinase gene knockout ameliorates hyperhomocysteinemic glomerular injury in mice lacking cystathionine-beta-synthase. *PLoS One* **7:**e45020; 2012.

[180] Koshikawa, M.; Mukoyama, M.; Mori, K.; Suganami, T.; Sawai, K.; Yoshioka, T.; Nagae, T.; Yokoi, H.; Kawachi, H.; Shimizu, F.; Sugawara, A.; Nakao, K. Role of p38 mitogen-activated protein kinase activation in podocyte injury and proteinuria in experimental nephrotic syndrome. *J Am Soc Nephrol* **16:**2690-2701; 2005.

[181] Jin, C.; Flavell, R. A. Inflammasome activation. The missing link: how the inflammasome senses oxidative stress. *Immunol Cell Biol* **88:**510-512; 2010.

[182] Gross, O.; Thomas, C. J.; Guarda, G.; Tschopp, J. The inflammasome: an integrated view. *Immunol Rev* **243:**136-151; 2011.

[183] Villegas, L. R.; Kluck, D.; Field, C.; Oberley-Deegan, R. E.; Woods, C.; Yeager, M. E.; El Kasmi, K. C.; Savani, R. C.; Bowler, R. P.; Nozik-Grayck, E. Superoxide dismutase mimetic, MnTE-2-PyP, attenuates chronic hypoxia-induced pulmonary hypertension, pulmonary vascular remodeling, and activation of the NALP3 inflammasome. *Antioxid Redox Signal* **18:**1753-1764; 2013.

[184] Floege, J.; Alpers, C. E.; Sage, E. H.; Pritzl, P.; Gordon, K.; Johnson, R. J.; Couser, W. G. Markers of complement-dependent and complement-independent glomerular visceral epithelial cell injury in vivo. Expression of antiadhesive proteins and cytoskeletal changes. *Lab Invest* **67:**486-497; 1992.

[185] Kawachi, H.; Miyauchi, N.; Suzuki, K.; Han, G. D.; Orikasa, M.; Shimizu, F. Role of podocyte slit diaphragm as a filtration barrier. *Nephrology (Carlton)* **11:**274-281; 2006.

[186] Kang, D. H.; Johnson, R. J. Vascular endothelial growth factor: a new player in the pathogenesis of renal fibrosis. *Curr Opin Nephrol Hypertens* **12:**43-49; 2003.

[187] Boini, K. M.; Xia, M.; Abais, J. M.; Li, G.; Pitzer, A. L.; Gehr, T. W.; Zhang, Y.; Li, P. L. Activation of inflammasomes in podocyte injury of mice on the high fat diet: Effects of ASC gene deletion and silencing. *Biochim Biophys Acta* **1843:**836-845; 2014.

[188] Henegar, J. R.; Bigler, S. A.; Henegar, L. K.; Tyagi, S. C.; Hall, J. E. Functional and structural changes in the kidney in the early stages of obesity. *J Am Soc Nephrol* **12:**1211-1217; 2001.

[189] Dai, J.; Wang, X. Immunoregulatory effects of homocysteine on cardiovascular diseases. *Sheng Li Xue Bao* **59:**585-592; 2007.

[190] Wang, G.; Woo, C. W.; Sung, F. L.; Siow, Y. L.; O, K. Increased monocyte adhesion to aortic endothelium in rats with hyperhomocysteinemia: role of chemokine and adhesion molecules. *Arterioscler Thromb Vasc Biol* **22:**1777-1783; 2002.

[191] Postea, O.; Koenen, R. R.; Hristov, M.; Weber, C.; Ludwig, A. Homocysteine up-regulates vascular transmembrane chemokine CXCL16 and induces CXCR6+ lymphocyte recruitment in vitro and in vivo. *J Cell Mol Med* **12:**1700-1709; 2008.

[192] Kriz, W. Podocyte is the major culprit accounting for the progression of chronic renal disease. *Microsc Res Tech* **57:**189-195; 2002.

[193] Marshall, C. B.; Pippin, J. W.; Krofft, R. D.; Shankland, S. J. Puromycin aminonucleoside induces oxidant-dependent DNA damage in podocytes in vitro and in vivo. *Kidney Int* **70:**1962-1973; 2006.

[194] Takano, Y.; Yamauchi, K.; Hayakawa, K.; Hiramatsu, N.; Kasai, A.; Okamura, M.; Yokouchi, M.; Shitamura, A.; Yao, J.; Kitamura, M. Transcriptional suppression of nephrin in podocytes by macrophages: roles of inflammatory cytokines and involvement of the PI3K/Akt pathway. *FEBS Lett* **581:**421-426; 2007.

[195] Liao, P. C.; Chao, L. K.; Chou, J. C.; Dong, W. C.; Lin, C. N.; Lin, C. Y.; Chen, A.; Ka, S. M.; Ho, C. L.; Hua, K. F. Lipopolysaccharide/adenosine triphosphate-mediated signal transduction in the regulation of NLRP3 protein expression and caspase-1-mediated interleukin-1beta secretion. *Inflamm Res* **62:**89-96; 2013.

[196] Varga, A.; Budai, M. M.; Milesz, S.; Bacsi, A.; Tozser, J.; Benko, S. Ragweed pollen extract intensifies lipopolysaccharide-induced priming of NLRP3 inflammasome in human macrophages. *Immunology* **138:**392-401; 2013.

[197] Cassel, S. L.; Eisenbarth, S. C.; Iyer, S. S.; Sadler, J. J.; Colegio, O. R.; Tephly, L. A.; Carter, A. B.; Rothman, P. B.; Flavell, R. A.; Sutterwala, F. S. The Nalp3 inflammasome is essential for the development of silicosis. *Proc Natl Acad Sci U S A* **105:**9035-9040; 2008.

[198] Pelegrin, P.; Surprenant, A. Dynamics of macrophage polarization reveal new mechanism to inhibit IL-1beta release through pyrophosphates. *EMBO J* **28:**2114-2127; 2009.

[199] Lindauer, M.; Wong, J.; Magun, B. Ricin Toxin Activates the NALP3 Inflammasome. *Toxins (Basel)* **2:**1500-1514; 2010.

[200] Tojo, A.; Asaba, K.; Onozato, M. L. Suppressing renal NADPH oxidase to treat diabetic nephropathy. *Expert Opin Ther Targets* **11:**1011-1018; 2007.

[201] Wilcox, C. S. Effects of tempol and redox-cycling nitroxides in models of oxidative stress. *Pharmacol Ther* **126:**119-145; 2010.

[202] Peixoto, E. B.; Papadimitriou, A.; Lopes de Faria, J. M.; Lopes de Faria, J. B. Tempol reduces podocyte apoptosis via PARP signaling pathway in experimental diabetes mellitus. *Nephron Exp Nephrol* **120:**e81-90; 2012.

[203] Yang, Z. Z.; Zhang, A. Y.; Yi, F. X.; Li, P. L.; Zou, A. P. Redox regulation of HIF-1alpha levels and HO-1 expression in renal medullary interstitial cells. *Am J Physiol Renal Physiol* **284:**F1207-1215; 2003.

[204] Beaman, M.; Birtwistle, R.; Howie, A. J.; Michael, J.; Adu, D. The role of superoxide anion and hydrogen peroxide in glomerular injury induced by puromycin aminonucleoside in rats. *Clin Sci (Lond)* **73:**329-332; 1987.

[205] Birtwistle, R. J.; Michael, J.; Howie, A. J.; Adu, D. Reactive oxygen products in heterologous anti-glomerular basement membrane nephritis in rats. *Br J Exp Pathol* **70:**207-213; 1989.

[206] Kelner, M. J.; Bagnell, R.; Welch, K. J. Thioureas react with superoxide radicals to yield a sulfhydryl compound. Explanation for protective effect against paraquat. *J Biol Chem* **265:**1306-1311; 1990.

[207] Wasil, M.; Halliwell, B.; Grootveld, M.; Moorhouse, C. P.; Hutchison, D. C.; Baum, H. The specificity of thiourea, dimethylthiourea and dimethyl sulphoxide as scavengers of hydroxyl radicals. Their protection of alpha 1-antiproteinase against inactivation by hypochlorous acid. *Biochem J* **243:**867-870; 1987.

[208] Cheng, Z.; Jiang, X.; Kruger, W. D.; Pratico, D.; Gupta, S.; Mallilankaraman, K.; Madesh, M.; Schafer, A. I.; Durante, W.; Yang, X.; Wang, H. Hyperhomocysteinemia impairs endothelium-derived hyperpolarizing factor-mediated vasorelaxation in transgenic cystathionine beta synthase-deficient mice. *Blood* **118:**1998-2006; 2011.

[209] Prathapasinghe, G. A.; Siow, Y. L.; O, K. Detrimental role of homocysteine in renal ischemia-reperfusion injury. *Am J Physiol Renal Physiol* **292:**F1354-1363; 2007.

[210] Savage, C. D.; Lopez-Castejon, G.; Denes, A.; Brough, D. NLRP3-Inflammasome Activating DAMPs Stimulate an Inflammatory Response in Glia in the Absence of Priming Which Contributes to Brain Inflammation after Injury. *Front Immunol* **3:**288; 2012.

[211] Minn, A. H.; Pise-Masison, C. A.; Radonovich, M.; Brady, J. N.; Wang, P.; Kendziorski, C.; Shalev, A. Gene expression profiling in INS-1 cells overexpressing thioredoxin-interacting protein. *Biochem Biophys Res Commun* **336:**770-778; 2005.

[212] Advani, A.; Gilbert, R. E.; Thai, K.; Gow, R. M.; Langham, R. G.; Cox, A. J.; Connelly, K. A.; Zhang, Y.; Herzenberg, A. M.; Christensen, P. K.; Pollock, C. A.; Qi, W.; Tan, S. M.; Parving, H. H.; Kelly, D. J. Expression, localization, and function of the thioredoxin system in diabetic nephropathy. *J Am Soc Nephrol* **20:**730-741; 2009.

[213] Li, X.; Rong, Y.; Zhang, M.; Wang, X. L.; LeMaire, S. A.; Coselli, J. S.; Zhang, Y.; Shen, Y. H. Up-regulation of thioredoxin interacting protein (Txnip) by p38 MAPK and FOXO1 contributes to the impaired thioredoxin activity and increased ROS in glucose-treated endothelial cells. *Biochem Biophys Res Commun* **381:**660-665; 2009.

[214] Shah, A.; Xia, L.; Goldberg, H.; Lee, K. W.; Quaggin, S. E.; Fantus, I. G. Thioredoxin-interacting protein mediates high glucose-induced reactive oxygen species generation by mitochondria and the NADPH oxidase, Nox4, in mesangial cells. *J Biol Chem* **288:**6835-6848; 2013.

[215] Xu, G.; Chen, J.; Jing, G.; Shalev, A. Preventing beta-cell loss and diabetes with calcium channel blockers. *Diabetes* **61:**848-856; 2012.

[216] Cha-Molstad, H.; Xu, G.; Chen, J.; Jing, G.; Young, M. E.; Chatham, J. C.; Shalev, A. Calcium channel blockers act through nuclear factor Y to control transcription of key cardiac genes. *Mol Pharmacol* **82:**541-549; 2012.

[217] Li, N.; Chen, Y. F.; Zou, A. P. Implications of hyperhomocysteinemia in glomerular sclerosis in hypertension. *Hypertension* **39:**443-448; 2002.

[218] Sen, U.; Munjal, C.; Qipshidze, N.; Abe, O.; Gargoum, R.; Tyagi, S. C. Hydrogen sulfide regulates homocysteine-mediated glomerulosclerosis. *Am J Nephrol* **31:**442-455; 2010.

[219] Cao, L.; Lou, X.; Zou, Z.; Mou, N.; Wu, W.; Huang, X.; Tan, H. Folic acid attenuates hyperhomocysteinemia-induced glomerular damage in rats. *Microvasc Res* **89:**146-152; 2013.

[220] Harris, D. C.; Hammond, W. S.; Burke, T. J.; Schrier, R. W. Verapamil protects against progression of experimental chronic renal failure. *Kidney Int* **31:**41-46; 1987.

[221] Pelayo, J. C.; Harris, D. C.; Shanley, P. F.; Miller, G. J.; Schrier, R. W. Glomerular hemodynamic adaptations in remnant nephrons: effects of verapamil. *Am J Physiol* **254:**F425-431; 1988.

[222] Al-Gayyar, M. M.; Abdelsaid, M. A.; Matragoon, S.; Pillai, B. A.; El-Remessy, A. B. Thioredoxin interacting protein is a novel mediator of retinal inflammation and neurotoxicity. *Br J Pharmacol* **164:**170-180; 2011.

[223] Brough, D.; Le Feuvre, R. A.; Wheeler, R. D.; Solovyova, N.; Hilfiker, S.; Rothwell, N. J.; Verkhratsky, A. Ca2+ stores and Ca2+ entry differentially contribute to the release of IL-1 beta and IL-1 alpha from murine macrophages. *J Immunol* **170:**3029-3036; 2003.

[224] Lerner, A. G.; Upton, J. P.; Praveen, P. V.; Ghosh, R.; Nakagawa, Y.; Igbaria, A.; Shen, S.; Nguyen, V.; Backes, B. J.; Heiman, M.; Heintz, N.; Greengard, P.; Hui, S.; Tang, Q.; Trusina, A.; Oakes, S. A.; Papa, F. R. IRE1alpha induces thioredoxin-interacting protein to activate the NLRP3 inflammasome and promote programmed cell death under irremediable ER stress. *Cell Metab* **16:**250-264; 2012.

[225] Oslowski, C. M.; Hara, T.; O'Sullivan-Murphy, B.; Kanekura, K.; Lu, S.; Hara, M.; Ishigaki, S.; Zhu, L. J.; Hayashi, E.; Hui, S. T.; Greiner, D.; Kaufman, R. J.; Bortell, R.; Urano, F. Thioredoxin-interacting protein mediates ER stress-induced beta cell death through initiation of the inflammasome. *Cell Metab* **16:**265-273; 2012.

[226] van de Veerdonk, F. L.; Smeekens, S. P.; Joosten, L. A.; Kullberg, B. J.; Dinarello, C. A.; van der Meer, J. W.; Netea, M. G. Reactive oxygen species-independent activation of the IL-1beta inflammasome in cells from patients with chronic granulomatous disease. *Proc Natl Acad Sci U S A* **107:**3030-3033; 2010.

[227] Meissner, F.; Seger, R. A.; Moshous, D.; Fischer, A.; Reichenbach, J.; Zychlinsky, A. Inflammasome activation in NADPH oxidase defective mononuclear phagocytes from patients with chronic granulomatous disease. *Blood* **116:**1570-1573; 2010.

[228] Gabelloni, M. L.; Sabbione, F.; Jancic, C.; Bass, J. F.; Keitelman, I.; Iula, L.; Oleastro, M.; Geffner, J. R.; Trevani, A. S. NADPH oxidase derived reactive oxygen species are involved in human neutrophil IL-1beta secretion but not in inflammasome activation. *Eur J Immunol* **43:**3324-3335; 2013.

[229] Rossman, K. L.; Der, C. J.; Sondek, J. GEF means go: turning on RHO GTPases with guanine nucleotide-exchange factors. *Nat Rev Mol Cell Biol* **6:**167-180; 2005.

[230] Lu, T. C.; He, J. C.; Wang, Z. H.; Feng, X.; Fukumi-Tominaga, T.; Chen, N.; Xu, J.; Iyengar, R.; Klotman, P. E. HIV-1 Nef disrupts the podocyte actin cytoskeleton by interacting with diaphanous interacting protein. *J Biol Chem* **283:**8173-8182; 2008.

[231] Inoue, M.; Williams, K. L.; Oliver, T.; Vandenabeele, P.; Rajan, J. V.; Miao, E. A.; Shinohara, M. L. Interferon-beta therapy against EAE is effective only when

development of the disease depends on the NLRP3 inflammasome. *Sci Signal* **5:**ra38; 2012.

# VITA

## 1. PERSONAL INFORMATION:

1.1 Name: Justine Mangubat Abais

1.2 Home Address:
711 South Laurel Street
Richmond, VA 23220
Phone: (757) 274-4883

1.3 Office Address:
Virginia Commonwealth University
Department of Pharmacology & Toxicology
MMRB, 3rd Floor, Room 3055
1220 East Broad Street
Richmond, VA 23298-0613

Phone: 804-628-4507
Fax: 804-828-4794
E-mail: abaisjm@vcu.edu

## 2. EDUCATION:

| | |
|---|---|
| 2005-2009 | B.S., Chemistry, Summa Cum Laude<br>Virginia Commonwealth University, Richmond VA |
| 2009- | Ph.D., Pharmacology & Toxicology<br>Virginia Commonwealth University, Richmond VA |

## 3. MEMBERSHIP – SCIENTIFIC, HONORARY, AND PROFESSIONAL SOCIETIES:

| | |
|---|---|
| 2011-2012 | Virginia Academy of Science, Chair, Medical Sciences Section |
| 2011-2013 | Phi Kappa Phi |
| 2013-present | American Physiological Society |
| 2013-present | American Society for Pharmacology and Experimental Therapeutics |
| 2013-present | American Society of Nephrology |

## 4. SPECIAL AWARDS, FELLOWSHIPS AND OTHER HONORS:

4.1 Awards

| | |
|---|---|
| 2005-2009 | VCU Provost Scholarship Recipient |
| 2007 | Multicultural Academic Achievement Award |
| 2008 | VCU University Leadership Award |
| 2009 | B.S. awarded with University Honors and Summa Cum Laude |
| 2011 | VCU School of Medicine C.C. Clayton Award |

| | |
|---|---|
| 2011 | Who's Who Among Students in American Universities & Colleges |
| 2012 | APS Predoctoral Excellence in Renal Research Award Finalist |
| 2012 | VCU Department of Pharmacology & Toxicology Anthony Ambrose Best Graduate Student Award |
| 2013 | VCU Graduate School Travel Grant Recipient |
| 2013 | VAS Medical Sciences Section Oral Presentation Winner |
| 2014 | Finalist for ASPET CVP Graduate Student Competition |
| 2014 | ASPET Graduate Student Travel Award Recipient |

4.2 Grants

| | |
|---|---|
| 2012 | F31 Ruth L. Kirschstein National Research Service Award for Individual Predoctoral Fellows, NIH National Institute of Aging |

4.3 Training

| | |
|---|---|
| 2013 | NIH Clinical Center's Clinical and Translational Research Course for Ph.D. Students |

4.4 Oral Presentations

| | |
|---|---|
| 2011 | Experimental Biology, *NADPH oxidase-mediated activation of inflammasomes by increased homocysteine in mouse podocytes and glomeruli*, Washington DC |
| 2011 | 89th Annual Virginia Academy of Science, *NADPH oxidase-mediated inflammasome activation by elevated homocysteine in mouse podocytes and glomeruli*, Richmond VA |
| 2013 | 91st Annual Virginia Academy of Science, *Thioredoxin-interacting protein mediates Hcys-induced NLRP3 inflammasome activation in mouse podocytes*, Blacksburg VA |
| 2013 | Carolina Cannabinoid Collaborative Conference, *Inhibitory action of prostamide E2 on homocysteine-induced NLRP3 inflammasome activation and podocyte damage*, Richmond VA |
| 2014 | Experimental Biology, *Contribution of guanine nucleotide exchange factor Vav2 to homocysteine-induced NLRP3 inflammasome activation in mouse podocytes,* San Diego CA |

4.5 Poster Presentations

| | |
|---|---|
| 2012 | Experimental Biology, *Role of different reactive oxygen species in homocysteine-induced NALP3 inflammasome activation in mouse podocytes; Inhibition of NADPH oxidase attenuates hyperhomocysteinemia-induced NALP3 inflammasome activation in mouse glomeruli,* San Diego CA |
| 2013 | Experimental Biology, *Contribution of reactive oxygen species to NLRP3 inflammasome activation in glomeruli of mice with hyperhomocysteinemia; Thioredoxin-interacting protein mediates Hcys-induced NLRP3 inflammasome activation in mouse podocytes*, Boston MA |

2013 American Society of Nephrology, *Thioredoxin-interacting protein mediates hHcys-induced NLRP3 inflammasome activation in glomerular sclerosis*, Atlanta GA

2014 Experimental Biology, *Contribution of guanine nucleotide exchange factor Vav2 to homocysteine-induced NLRP3 inflammasome activation in mouse podocytes*; *Protective effects of docosahexaenoic acid metabolites against homocysteine-induced podocyte injury by inhibition of NLRP3 inflammasomes*, San Diego CA

## 5. BIBLIOGRAPHY:

5.1 Papers Published


1 Zhang C, Yi F, Xia M, Boini KM, Zhu Q, Laperle LA, **Abais JM**, Brimson CA, Li PL. NMDA receptor-mediated activation of NADPH oxidase and glomerulosclerosis in hyperhomocysteinemic rats. *Antioxid Redox Signal*. 2010 Oct 1;13(7):975-86. PMID: 20406136

2 Zhang C, Xia M, Boini KM, Li CX, **Abais JM**, Li XX, Laperle LA, Li PL. Epithelial-to-mesenchymal transition in podocytes mediated by activation of NADPH oxidase in hyperhomocysteinemia *Pflugers Arch - Eur J Physiol.* 2011 Sep;462(3):455-67. PMID: 21647593

3 Boini KM, Xia M, Li CX, Zhang C, Payne LP, **Abais JM**, Poklis JL, Hylemon PB, Li PL. Acid sphingomyelinase gene deficiency ameliorates the hyperhomocysteinemia-induced glomerular injury in mice. *Am J Pathol*. 2011 Nov;179(5):2210-9. PMID: 21893018

4 Zhang C, Boini KM, Xia M, **Abais JM**, Li X, Liu Q, Li PL. Activation of Nod-like receptor protein 3 inflammasomes turns on podocyte injury and glomerular sclerosis in hyperhomocysteinemia. *Hypertension*. 2012 Jul;60(1):154-62. PMID: 22647887

5 Boini KM, Xia M, **Abais JM**, Xu M, Li CX, Li PL. Acid sphingomyelinase gene knockout ameliorates hyperhomocysteinemic glomerular injury in mice lacking cystathionine-β-synthase. *PLoS One.* 7(9):e45020, 2012. PMID: 23024785

6 **Abais JM**, Zhang C, Xia M, Liu Q, Gehr T, Boini KM, Li PL. NADPH oxidase-mediated triggering of inflammasome activation in mouse podocytes and glomeruli during hyperhomocysteinemia. *Antioxid Redox Signal*. 2013 May 1;18(13):1537-48. PMID: 23088210

7 Xu M, Li X, Walsh SW, Zhang Y, **Abais JM**, Boini KM, Li PL.M, Intracellular two-phase Ca2+ release and apoptosis controlled by TRP-ML1 channel activity in coronary arterial myocytes. *Am J Physiol Cell Physiol*. 2013 Mar 1;304(5):C458-66. PMID: 23283937

8 Xiong J, Xia M, **Abais JM**, Li CX, Boini KM, Li PL. Regulation of renin release via cyclic adp-ribose-mediated signaling: evidence from mice lacking CD38 gene. *Cell Physiol Biochem.* 2013 Jan 14;31(1):44-55. PMID: 23343681

9 Wei YM, Li X, Xiong J, **Abais JM**, Xia M, Boini KM, Zhang Y, Li PL. Attenuation by statins of membrane raft-redox signaling in coronary arterial endothelium. *J Pharmacol Exp Ther*. 2013 May;345(2):170-9. PMID: 23435541

10 Li C, Xia M, **Abais JM**, Liu X, Li N, Boini KM, Li PL. Protective role of growth hormone against hyperhomocysteinemia-induced glomerular injury. *Naunyn Schmiedebergs Arch Pharmacol*. 2013 Jun;386(6):551-61. PMID: 23529346

11 Wei YM, Li X, Xu M, **Abais JM**, Chen Y, Riebling CR, Boini KM, Li PL, Zhang Y. Enhancement of autophagy by simvastatin through inhibition of Rac1-mTOR signaling pathway in coronary arterial myocytes. *Cell Physiol Biochem.* 2013;31(6):925-37. PMID: 23817226

12 Li PL, Zhang Y, **Abais JM**, Ritter JK, Zhang F. Cyclic ADP-Ribose and NAADP in Vascular Regulation and Diseases. *Messenger*. 2013; 2, 63-85. PMID: 24749015

13 Xu M, Li XX, Ritter JK, **Abais JM**, Zhang Y, Li PL. Contribution of NADPH oxidase to membrane CD38 internalization and activation in coronary arterial myocytes. PLoS One. 2013 Aug 7;8(8):e71212. PMID: 23940720

14 **Abais JM**, Xia M, Gehr T, Boini KM, Li PL. Contribution of endogenously produced reactive oxygen species to the activation of podocyte NLRP3 inflammasomes in hyperhomocysteinemia. *Free Radic Biol Med.* 2014 Feb; 67:211-20. PMID: 24140862

15 Xiong J, Xia M, Xu M, Zhang Y, **Abais JM**, Li G, Riebling CR, Ritter JK, Boini KM, Li PL. Autophagy maturation associated with CD38-mediated regulation of lysosome function in mouse glomerular podocytes. *J Cell Mol Med.* 2013 Dec; 17(12):1598-607. PMID: 24238063

16 Boini KM, Xia M, **Abais JM**, Li G, Pitzer AL, Gehr TW, Zhang Y, Li PL. Activation of inflammasomes in podocyte injury of mice on the high fat diet: Effects of ASC gene deletion and silencing. *Biochim Biophys Acta.* 2014 May; 1843(5):836-45. PMID: 24508291

17 Xia M, Boini KM, **Abais JM**, Xu M, Zhang Y, Li PL. Endothelial NLRP3 inflammasome activation and enhanced neointima formation in mice by adipokine visfatin. *Am J Pathol.* 2014 Mar 13. [Epub ahead of print] PMID: 24140862

18 Wang M, **Abais JM**, Meng N, Zhang Y, Ritter JK, Li PL, Tang WX. Upregulation of cannabinoid receptor-1 and fibrotic activation of mouse hepatic stellate cells during *Schistosoma J.* infection: role of NADPH oxidase. *Free Radic Biol Med*. 2014 Mar 18. [Epub ahead of print] PMID: 24657416

### 5.2 Papers In Preparation

19 **Abais JM**, Xia M, Boini KM, Li PL. NLRP3 inflammasome activation and podocyte injury via thioredoxin-interacting protein during hyperhomocysteinemia. *J Biol Chem.* (In Revision).

20 **Abais JM**, Zhang Y, Boini KM, Li PL. Redox Regulation of Inflammasomes: ROS as Trigger or Effector? *Antioxid Redox Signal*. (In Preparation)

### 5.3 Abstracts

21 Yi F, **Abais JM**, Jin S, Zhang F, Li N and Li PL. NMDA receptors mediates homocysteine-induced sclerotic action on rat mesangial cells. *The FASEB Journal.* 22:748.1. **2008.**

22 **Abais JM**, Zhang C, Xia M, Boini KM, Li X, Laperle LA, Thacker AM, Li PL. NADPH oxidase-mediated activation of inflammasomes by increased homocysteine in mouse podocytes and glomeruli. *The FASEB Journal*. 25:1030.5. 2011.

23 Boini KM, Xia M, Zhang C, **Abais JM**, Li CX, and Li PL. Activation of inflammasomes as a triggering mechanism of glomerular injury in mice on the high fat diet. *The FASEB Journal 25*:*1028.6*. 2011.

24 Xia M, Boini KM, **Abais JM**, Li PL. Silencing of acid sphingomyelinase gene prevented glomerular oxidative stress and sclerosis in hyperhomocysteinemic mice. *The FASEB Journal. 25*:*667.12*. 2011.

25 Xu M, Zhang F, Xia M, Li XX, **Abais JM**, Boini KM, Li PL. Lysosomal regulation of autophagy efflux via CD38-mediated signaling in mouse coronary arterial myocytes. *Hypertension*. 2011

26 Xia M, Boini KM, **Abais JM**, Li XX , Mu X, Li PL. NALP3 inflammasome activation in the coronary arterial wall of obese mice. *FASEB J. 26*:*877.7*. 2012.

27 Xia M, Xiong J, Boini KM, **Abais JM**, Li PL. Characteristics and hypertensive actions of renal medullary NALP3 inflammasomes in mice. *FASEB J. 26*:*879.4*. 2012.

28 **Abais JM**, Boini KM, Xia M, Li PL. Role of different reactive oxygen species in homocysteine-induced NALP3 inflammasome activation in mouse podocytes. *FASEB J. 26*:*691.9*. 2012.

29 **Abais JM**, Boini KM, Xia M, Li PL. Inhibition of NADPH oxidase attenuates hyperhomocysteinemia-induced NALP3 inflammasome activation in mouse glomeruli. *FASEB J. 26*:*691.10*. 2012.

30 Boini KM, Xia M, **Abais JM**, Li PL. Instigation of NALP3 inflammasome activation and glomerular injury in mice on the high fat diet: role of acid sphingomyelinase gene. *FASEB J. 26*:*690.7*. 2012.

31 Xiong J, Xia M, Xu M, Li XX, **Abais JM**, Boini KM, Li PL. Autophagy maturation controlled by CD38-lysosome signaling in glomerular podocytes of mice. *FASEB J. 26*:*690.14*. 2012.

32 **Abais JM**, Boini KM, Xia M, Li PL. Thioredoxin interacting protein mediates Hcys-induced NLRP3 inflammasome activation in mouse podocytes. *FASEB J. 27:704.7*. 2013.

33 **Abais JM**, Boini KM, Xia M, Li PL. Contribution of reactive oxygen species to NLRP3 inflammasome activation in glomeruli of mice with hyperhomocysteinemia. *FASEB J. 27:890.3*. 2013.

34 Boini KM, Xia M, **Abais JM**, Zhang Y, Li PL. Inhibition of hyperhomocysteinemia-induced inflammasome activation and glomerular sclerosis by NLRP3 gene deletion. *FASEB J. 27:704.6*. 2013.

35 Boini KM, Xia M, **Abais JM**, Zhang Y, Li PL. High fat diet failed to induce NALP3 inflammasome activation and glomerular injury in apoptosis-associated speck-like protein (ASC) knockout mice. *FASEB J. 27:889.5*. 2013.

36 Xia M, Xiong J, **Abais JM**, Boini KM, Li PL. Regulation of renal sodium excretion by medullary NLRP3 inflammasome activation beyond turning on inflammation. *FASEB J.*

*27:1115.5*. 2013.

37 Xia M, Li CX, Li C, **Abais JM**, Zhang Y, Boini KM, Li PL. Epithelial-to-mesenchymal transition induced by accumulation of autophagosomes in podocytes. *FASEB J. 27:889.7*. 2013.

38 **Abais JM**, Xia M, Boini KM, Li PL. Contribution of guanine nucleotide exchange factor Vav2 to homocysteine-induced NLRP3 inflammasome activation in mouse podocytes. *FASEB J. 28:1063.6*. 2014.

39 **Abais JM**, Xia M, Boini KM, Li PL. Protective effects of docosahexaenoic acid metabolites against homocysteine-induced podocyte injury by inhibition of NLRP3 inflammasomes. *FASEB J. 28:1134.8*. 2014.

40 Boini KM, Xia M, **Abais JM**, Li PL. Podocyte NLRP3 inflammasome activation and glomerular injury by adipokine visfatin: in vitro and in vivo evidence. *FASEB J. 28:1134.7*. 2014.

41 Boini KM, Xia M, **Abais JM**, Li G, Li PL. Enhanced dedifferentiation and injury in mouse podocytes lacking CD38 gene. *FASEB J. 28:691.4*. 2014.

42 Wang M, **Abais JM**, Meng N, Zhang Y, Ritter JK, Li PL, Tang WX. Upregulation of cannabinoid receptor-1 and fibrotic activation of mouse hepatic stellate cells during Schistosoma J. infection: role of NADPH oxidase. *FASEB J. 28:693.13*. 2014.